

Characterization of Voltage Dependent Anion Channel (VDAC) subtypes in mammalian follicles and potential physiological relevance

Inaugural Dissertation
submitted to the
Faculty of Medicine
in partial fulfillment of the requirements
for the PhD-Degree
of the Faculties of Veterinary Medicine and Medicine
of the Justus Liebig University Giessen

by

Cassará, María Carolina

of

Buenos Aires, Argentina

Giessen 2007

From the Clinic of Dermatology and Andrology
Director: Prof. Dr. Peter Mayser
of the Faculty of Medicine of the Justus Liebig University Giessen

First Supervisor: Prof. Dr. Klaus-Dieter Hinsch
Second Supervisor: Prof. Dr. Aria Baniahmad

Committee Members: Prof. Dr. Heinz-Jürgen Thiel (Chairman)
Prof. Dr. Klaus-Dieter Hinsch
Priv.-Doz. Dr. Christine Wrenzycki
Prof. Dr. Andreas Meinhardt

Date of Doctoral Defense: May 11th, 2007

Para

Horacio, Ana, Paula y Gisella

List of abbreviations

List of abbreviations

°C	degree Centigrade
µg	microgram
µl	microliter
µm	micrometer
AEC	3-amino-9-ethyl-carbazol
AS	antiserum
AT	annealing temperature
ATP	adenosine triphosphate
Ca ²⁺	calcium ion
cDNA	complementary DNA
cm	centimeter
CO ₂	carbon dioxide
COC	cumulus-oocytes-complex
CP	crossing point
DNA	desoxyribosenucleic acid
<i>et al.</i>	et alii
FITC	fluorescein-5-isothiocyanat
GAPDH	glyceraldehyde-3-phosphate dehydrogenase
gDNA	genomic DNA
GV	germinal vesicle
H2A	Histone H2A
IVF	<i>In vitro</i> Fertilisation
IVM	<i>In vitro</i> Maturation
KCl	potassium chloride
kDa	kilodalton
M	molar
mg	milligram
MII	metaphase II
min	minute
ml	milliliter
mm	millimeter
mM	millimolar

List of abbreviations

mRNA	messenger RNA
MW	molecular weight
NaCl	sodium chloride
PAGE	polyacrylamide gel electrophoreses
PBS	phosphate Buffered Saline
PCR	polymerase-chain-reaction
pH	pondus hydrogenii
pI	isoelectric point
PI	preimmune serum
PMSF	phenylmethysulfonyl fluoride
RNA	ribonucleic acid
RT-Reaction	reverse transcription reaction
s	second
SD	standard deviation
SDS	sodium dodecyl sulfate
TBS	tris buffer saline
U2snRNA	U2 small nuclear RNA
V	volt
v/v	volume per volume
VDAC	voltage dependent anion channel
w/v	weight per volume

1	Introduction	8
1.1	<i>Voltage Dependent Anion Channel (VDAC).....</i>	8
1.1.1	VDAC structure and expression.....	9
1.1.2	VDAC localization.....	10
1.1.3	Functional relevance of VDAC.....	10
1.1.4	VDAC in mammalian gametes	12
1.2	<i>Fertilization.....</i>	13
1.2.1	Spermatozoon.....	15
1.2.2	Oocyte	16
1.3	<i>Aims.....</i>	19
2	Material & Methods	21
2.1	<i>Expression of VDAC mRNA in porcine and bovine oocytes.....</i>	21
2.1.1	Expression analyses of VDAC mRNA in porcine and bovine oocytes by RT-PCR 21	
2.1.2	Real-time RT-PCR of bovine oocytes.....	24
2.2	<i>Expression of VDAC protein isoforms in porcine gametes</i>	26
2.2.1	Total extraction of porcine spermatozoa proteins	26
2.2.2	Extraction of porcine oocyte protein.....	27
2.2.3	Generation of antibodies against subtype-specific synthetic VDAC peptides.....	28
2.2.4	Protein expression analysis of VDAC in porcine gametes by immunoblotting...	29
2.2.5	Protein identification by MALDI-TOF MS	32
2.2.6	Immunohistochemical detection of VDAC protein in porcine ovaries.....	32
2.2.7	Subcellular localization of VDAC proteins in porcine oocytes by confocal microscopy.....	33
2.3	<i>Functional studies.....</i>	34
2.3.1	Lipid bilayer experiments with purified VDAC protein from porcine spermatozoa 34	
2.3.2	Treatment of mature porcine oocytes with purified VDAC protein from porcine spermatozoa	35
2.3.3	Calcium oscillation measurements after microinjection of purified VDAC protein in mature bovine oocytes.....	37
2.3.4	Influence of anti-VDAC1 antibodies on in vitro maturation of bovine oocytes..	38
3	Results.....	41
3.1	<i>Expression of VDAC mRNA in porcine and bovine oocytes.....</i>	41
3.1.1	Expression analyses of VDAC mRNA in porcine and bovine oocytes by RT-PCR 41	
3.1.2	Real-time RT-PCR of bovine oocytes.....	42
3.2	<i>Expression of VDAC protein isoform in porcine gametes.....</i>	47
3.2.1	Protein expression analyses of VDAC in porcine gametes by immunoblotting..	48
3.2.2	Protein identification by MALDI-TOF MS	54
3.2.3	Immunohistochemical detection of VDAC protein in porcine ovaries.....	57
3.2.4	Subcellular localization of VDAC proteins in porcine oocytes by confocal microscopy.....	60
3.3	<i>Functional studies.....</i>	63

3.3.1	Lipid bilayer experiments with purified VDAC protein from porcine spermatozoa	63
3.3.2	Treatment of mature porcine oocytes with purified VDAC protein from porcine spermatozoa	65
3.3.3	Calcium oscillation measurements after microinjection of purified VDAC protein in mature bovine oocytes	67
3.3.4	Influence of anti-VDAC1 antibodies on in vitro maturation of bovine oocytes..	68
4	Discussion	73
4.1	<i>Expression of VDAC mRNA in porcine and bovine oocytes</i>	73
4.1.1	Real-time RT-PCR of bovine oocytes.....	74
4.2	<i>Expression of VDAC protein isoforms in porcine gametes</i>	76
4.2.1	Immunobiochemical detection and lipid bilayer experiments of VDAC proteins from porcine spermatozoa	77
4.2.2	Immunobiochemical detection of VDAC proteins in porcine oocytes	81
4.2.3	Immunohistochemical detection of VDAC protein in porcine ovaries.....	83
4.2.4	Subcellular distribution of VDAC proteins in porcine oocytes	84
4.3	<i>Functional studies</i>	87
4.3.1	Treatment of matured porcine and bovine oocytes with purified VDAC from spermatozoa	87
4.3.2	Influence of anti-VDAC1 antibodies on in vitro maturation of bovine oocytes..	91
4.4	<i>Perspectives</i>	94
5	Summary	96
6	Zusammenfassung	98
7	Bibliography.....	100
8	Acknowledgements	119
9	Curriculum Vitae.....	120

1 Introduction

1.1 Voltage Dependent Anion Channel (VDAC)

VDAC, also known as mitochondrial porin, is a pore-forming protein (30-35kDa) originally identified in eukaryotic cells in 1976 (Schein *et al.*, 1976) and lately found in bacteria, plants (Heins *et al.*, 1994; Abrecht *et al.*, 2000), yeast (Mihara and Sato, 1985), insects and mammals (Linden *et al.*, 1982b; De Pinto *et al.*, 1989). At least three related but distinct isoforms of VDAC have been reported in vertebrates, VDAC1, VDAC2 and VDAC3 (Blachly-Dyson *et al.*, 1993; Sampson *et al.*, 1997). The channels are integral membrane proteins, mainly found in the outer membrane of mitochondria and despite the numerous studies and reports on VDAC proteins there is no available crystal structure in eukaryotic cells. However, computer modeling of VDAC primary amino acid sequence has led to the development of models showing the possible transmembrane organization, consisting of one polypeptide having stretches of alternating hydrophobic and hydrophilic amino acids that form 13 or 16 transbilayer β -strands composed of a single α -helix at the N-terminus (Figure 1). The β -strands layers are connected by several peptide loops of different sizes on both sides of the membrane that serves as potential protein-interaction sites (Blachly-Dyson and Forte, 2001; Casadio *et al.*, 2002; Colombini, 2004; Shoshan-Barmatz *et al.*, 2006).



Figure 1: VDAC membrane topology model and oligomeric structure (Shoshan-Barmatz *et al.*, 2006)

When reconstituted into planar phospholipid membranes, VDAC exhibits a high conductance anion selective fully open state and multiple, often cation selective, substates adopted upon

application of voltages $>20\text{mV}$ (Benz, 1994; Rostovtseva and Colombini, 1996). The channels formed show current increases with a predominant single channel conductance of about 4nS (in 1M KCl) and a slight preference for anions over cations (2:1). Experimental approaches have been used to show that single VDAC channels are formed by a single protein of 285 amino acids (30kDa). The channel can form a large voltage pore ($\sim 3\text{nm}$ open channel diameter, 1.8nm closed channel diameter, Figure 2) that can exist in multiple conformational states with different selectivity and permeability (Colombini *et al.*, 1987; Blachly-Dyson and Forte, 2001). VDAC is not ion-specific and it also transports adenine nucleotides, Ca^{2+} and other metabolites. The molecular nature of VDAC gating mechanism is still under research.

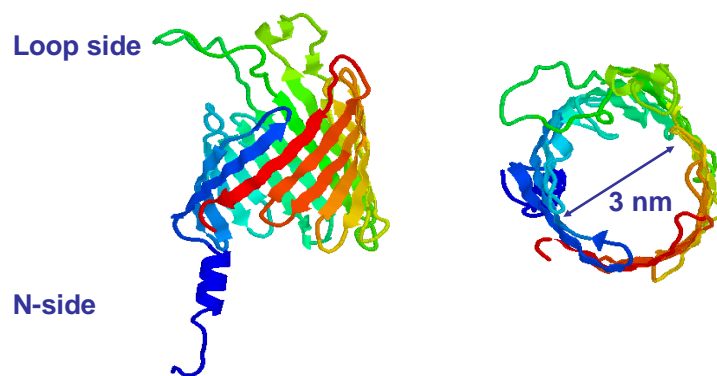


Figure 2: Hypothetical 3-D model of an eukaryotic VDAC1 using *Neurospora crassa* (Casadio *et al.*, 2002)

1.1.1 VDAC structure and expression

Genes encoding VDAC have been sequenced in several eukaryotic organisms. In mammals three VDAC genes have been demonstrated to encode functionally active isoforms (Blachly-Dyson *et al.*, 1993; Sampson *et al.*, 1997; Rahmani *et al.*, 1998). The three genes share a highly similar organization, the exon/intron junctions are conserved and relevant differences are concentrated at the 5' and 3' untranslated regions of mRNA. The promoter region is rich of G+C and it does not contain any classic TATA box element. These two points are characteristic of housekeeping genes which can be associated with the broad expression and distribution of the three mammalian isoforms in a variety of tissues.

In all mammalian species, VDAC1 and VDAC2 isoforms are widespread, although in mice, MVDAC2 is highly expressed in testis, whereas MVDAC1 is not present in this tissue (Sampson *et al.*, 1996). Human VDAC3 is widely distributed with especially high expression in the testis, a similar distribution was observed for the rat isoform (Rahmani *et al.*, 1998).

Although channel gating and selectivity properties are highly conserved, VDAC proteins from different species show little conservation of primary amino acid sequence in opposite to the highly conserved pattern of secondary structure motifs. The reason for this characteristic is still under investigation.

1.1.2 VDAC localization

VDAC is the most abundant protein in the mitochondria outer membrane (OMM) where it was originally described to be exclusively located. In 1989, the presence of VDAC in extramitochondrial localizations was reported by the group of Thinnes and co-workers. VDAC (Porin 31HL) was purified and sequenced from crude B-lymphocyte membranes resulting the first complete primary structure of VDAC in the animal kingdom (Thinnes *et al.*, 1989). After this finding, several studies have revealed that VDAC is also located in other cell compartments like: nuclear envelope (Thinnes, 1992) caveolae and caveolae-like domains (Bathori *et al.*, 1999), sarcoplasmic reticulum (Lewis *et al.*, 1994; Junankar *et al.*, 1995; Jurgens *et al.*, 1995; Shoshan-Barmatz *et al.*, 1996; Shafir *et al.*, 1998), Golgi apparatus and endoplasmic reticulum (Okada *et al.*, 2004), endosomes (Reymann *et al.*, 1998), presynaptic vesicles in cortex from rat brains and in astrocytes (Guibert *et al.*, 1998) and also in the outer dense fibers (ODF) of sperm flagella (Hinsch *et al.*, 2004).

1.1.3 Functional relevance of VDAC

The proposed physiological functions of VDAC are numerous. A growing body of evidence indicates that VDAC is involved in the regulation of metabolite flow in and out of mitochondria resulting in the regulation of mitochondrial functions. The gating of VDAC channels play an important role in controlling the rate of metabolic flux. Mitochondrial VDAC has been found to form complexes with ANT (adenine nucleotide translocase), these junctional complexes bind several cytosolic kinases and other proteins that facilitate the export of mitochondrial high energy phosphate to the cytosol, or that are implicated in apoptosis (Crompton *et al.*, 2002). Within this role in cellular energy metabolism, VDAC interacts with hexo- glycerol- and creatine kinases (Adams *et al.*, 1991; McEnery *et al.*, 1992; Beutner *et al.*, 1998; Crompton *et al.*, 2002). Furthermore, some studies indicate that mitochondrial bound hexokinase selectively uses intramitochondrial ATP, an observation in

concert with the demonstration of direct flow of ATP through isolated VDAC (Rostovtseva and Colombini, 1996). It is also described that VDAC can be integrated with cytoskeleton proteins like MAP2 (microtubule associated protein 2), Dynein-light chain and G-actin (Linden and Karlsson, 1996; Krimmer *et al.*, 2001; Xu *et al.*, 2001; Schwarzer *et al.*, 2002). Using this approach it is possible for VDAC to be involved in mitochondrial movement or implicated in cell motility (Roman *et al.*, 2006). Another attributed function is the regulatory volume decrease (RVD, opening of volume sensitive chloride/anion channels) (Thinnes *et al.*, 2000a; Thinnes *et al.*, 2000b). This postulated function was questioned with gene knockout and inspection of single channel properties. It was concluded that the maxianion channel activity in mouse fibroblasts does not correlate with the presence of any VDAC (Sabirov *et al.*, 2006).

Only speculations can be drawn concerning the possible roles of VDAC in extramitochondrial location. A preliminary assumption is that VDAC forms regulate wide pores which may function in the transport of ions, metabolites and macromolecules.

The existence of three different isoforms and differences in their expression patterns suggests specialized functions for all of them. Until now, it was not possible to purify VDAC2 and VDAC3 isoforms from animal tissue. The existing information derives from mouse recombinant proteins expressed in yeast (Xu *et al.*, 1999). The recombinant proteins were analyzed by reconstitution into liposomes and each isoform induced permeability with a similar molecular weight cut off. In contrast, electrophysiological studies on purified proteins displayed different channel properties between each isoform. VDAC1 and VDAC2 can insert easily and form channels into a phospholipid membrane. VDAC2 may exist as two different populations, one with normal gating activity and one with a lower conductance and selectivity. In contrast VDAC3 can also form channels but does not insert readily into membranes and generally does not gate efficiently even at high membrane potentials (up to 80mV) (Xu *et al.*, 1999). These differences suggest the possibility that VDAC subtypes have distinct physiologic functions.

Other approach to the functional characterization of VDAC was performed by Wu *et al.*, in which it was shown that mouse embryonic stem cells lacking each isoform are viable but exhibit a 30% reduction in oxygen consumption. VDAC1 and VDAC2 deficient cells exhibited reduced cytochrome *c* oxidase activity, where VDAC3 had normal activity, indicating that VDAC subtypes are not essential for cell viability (Wu *et al.*, 1999).

Mice with homozygous deletion of the MVDAC1 gene have been generated and exhibited a strain-specific partial lethality and have respiratory deficiencies (Anflous *et al.*, 2001). Mouse

strains deficient for MVDAC3 and double MVDAC1-MVDAC3 are viable, but growth retarded and occurs less frequently (Weeber *et al.*, 2002). In the case of MVDAC3 deficient strains males are sterile meanwhile females are fertile (Sampson *et al.*, 2001).

VDAC1 is highly involved with the regulation of apoptosis. It is part of the permeability transition pore (PTP) and the triggering from the apoptotic caspase cascade (Bernardi *et al.*, 2001). VDAC2 is proposed to interact and prevent the activity of the pro-apoptotic BAK regulating apoptosis (Cheng *et al.*, 2003).

1.1.4 VDAC in mammalian gametes

Despite the numerous studies of functions of these proteins in somatic cells few reports concerning characterization and roles were available in mammalian gametes until now.

Steinacker *et al.* (2000) described the localization of endogenous VDAC1 in *Xenopus laevis* oocyte plasma membranes. It appears as a disjunctive pattern of spots in confocal laser microscopy images (Steinacker *et al.*, 2000). In the same year a human voltage dependent anion channel was expressed in the plasmalemma of *Xenopus laevis* oocytes to corroborate the data on the extra-mitochondrial expression of eukaryotic VDAC.

Guarino and colleagues specified the expression and localization of VDAC2 in *Drosophila melanogaster*, showing the highest transcription level in testis. Western blot analysis confirmed a high level of expression in spermatozoa and lower in ovaries (Guarino *et al.*, 2006). The same expression pattern of VDAC2 was detected in bovine testis (Hinsch *et al.*, 2001). Further studies in bovine spermatozoa detected VDAC2 and VDAC3 as a soluble protein in extracts of bovine outer dense fibers (ODF). Immunofluorescence studies revealed a clear bound to the sperm flagellum, in particular to the ODF (Hinsch *et al.*, 2004). Studies in mice lacking VDAC3 show healthy infertile males. Although the sperm number was normal, their motility was reduced. Structural defects were detected in the axonemes, like the loss of a single microtubule doublet (Sampson *et al.*, 2001).

Which are the specific roles that the different VDAC isoforms play in the female and male gametes is still unknown.

1.2 Fertilization

The final steps of mammalian oogenesis and spermatogenesis prepare eggs and sperm, respectively, for fertilization. During ovulation fully-grown oocytes from antral follicles undergo meiotic maturation and become unfertilized eggs prepared to interact with sperm.

At insemination several hundred million sperm are released into the female genital tract (Wassarman, 2002). During their transport through the uterus and oviduct the spermatozoa pass through capacitation and subsequently undergo a change in motility called hyperactivation, a prerequisite for the sperm's ability to fertilize the oocyte. Capacitated spermatozoa pass through several layers of cumulus cells to reach the zona pellucida (ZP). After the spermatozoon has become tightly bound to the ZP, it is induced to undergo the acrosome reaction, a secretory event by which hydrolytic enzymes are released from the acrosome of the sperm head (Saling *et al.*, 1979).

This allows the spermatozoa to degrade and penetrate the ZP matrix by a combination of enzymatic digestion of the ZP-glycoproteins and vigorous propulsion by the spermatozoon tail. Eventually a sperm reaches the perivitelline space and fuses with the plasma membrane thereby fertilizing the oocyte, to form a single activated cell, the zygote. When the sperm head binds, the membranes are fused and the sperm nucleus, mitochondria, centriole and flagellum are engulfed by the ooplasm (Yanagimachi, 1994). Upon the first spermatozoon fusion with the oocyte, a series of events referred to as activation are triggered. These events include the exocytosis of cortical granules of the oocyte (cortical reaction) modifying the oocyte membrane and the ZP (plasma membrane-block and/or zona-block to polyspermia) preventing further penetration (Yanagimachi, 1994).

The activation is dependent on an increase in the concentration of free calcium ions within the egg. This reaction of the egg to the sperm can be divided into early and late response (Xu *et al.*, 1994; Ben Yosef and Shalgi, 2001). Early events include a transient rise in intracellular calcium concentration that activates a series of metabolic reactions, like activation of NAD⁺-kinase, cortical granule exocytosis and prevents polyspermy (Ducibella *et al.*, 1990; Raz and Shalgi, 1998). Later events include stimulation of protein synthesis, DNA replication, cytoplasmic movements of morphogenetic material, extrusion of second polar body, decondensation of the sperm head, formation of pronuclei and cleavage (Xu *et al.*, 1994). Recent data suggest that the production of inositol 1,4,5-trisphosphate (IP₃) is the primary mechanism for releasing calcium ions from their intracellular storage and responsible for egg

activation (IP_3 -pathway) are summarized in Figure 3, Kline and Kline, 1992; Xu *et al.*, 1994; Gilbert, 2000; Rice *et al.*, 2000).

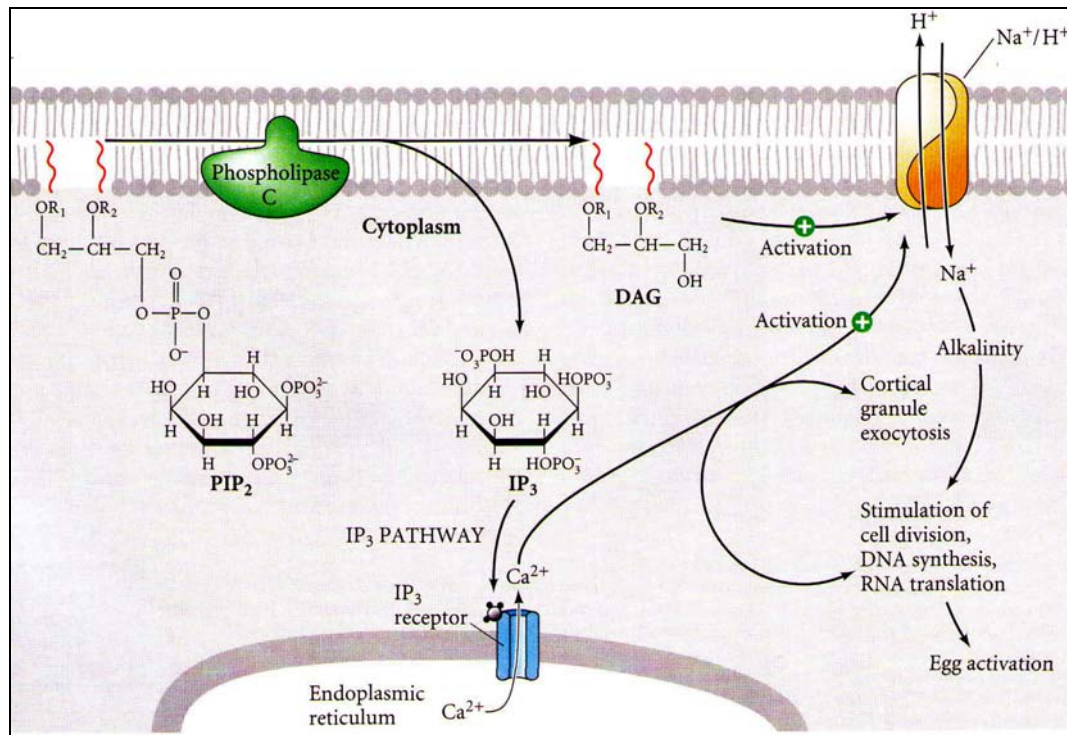


Figure 3: The roles of inositol phosphates in initiating calcium release and the initiation of development (Gilbert, 2000)

In this scenario one important question is which protein initiates the production of IP_3 ? One of the proposed mechanism models suggests that egg activation is initiated after sperm-egg fusion, by introducing a soluble activator from the sperm cytosol, activating the releasing of the sequestered calcium (Yanagimachi, 1994; Wu *et al.*, 1997; Raz and Shalgi, 1998; Swann and Parrington, 1999). This model is supported over the binding receptors and plasma membrane activation models by the clinical procedure intracytoplasmic sperm injection (ICSI) used to treat infertility. Here, a single sperm is injected directly into the ooplasm and is capable of activating the egg, bypassing sperm-egg binding and fusion. Artificial egg activation in mammals can be produced by a wide variety of physical and chemical stimuli as well as by isolated sperm factors. The sperm factor is proteinaceous and does not appear to be species-specific since sperm extracts from vertebrates are effective in a wide variety of species (Wu *et al.*, 1997; Stricker *et al.*, 2000). It is noteworthy that the main candidate to generate IP_3 and calcium increases is the sperm derived PLC (phospholipase C) (Malcuit *et al.*, 2006a)

Observing the previously described events of fertilization, it is clear that a complex dialogue exists between egg and sperm. The egg activates the sperm metabolism that is essential for fertilization and the sperm reciprocates by activating the egg metabolism needed for the onset of development. To understand these aspects of fertilization it is necessary to be acquainted with the structures of the sperm and the egg. The present work will be mainly address to the relevance of VDAC in the oocyte.

1.2.1 *Spermatozoon*

Each sperm (Figure 4) consists of a haploid nucleus, a propulsion system to move the nucleus and a sac of enzymes that enables the nucleus to penetrate the egg. Most of the sperm cytoplasm is eliminated during maturation, leaving certain organelles. The sperm nucleus located in the head is covered by a membrane-bound secretory vesicle, the acrosome, which is derived from the Golgi apparatus, and contains enzymes that are involved in the acrosomal process (Yanagimachi, 1994; Eddy and O'Brien D., 1994). The sperm is propelled by its flagellum. It consists of four distinct segments: the connecting piece (neck), the middle piece, the principal piece and the end piece (Figure 4, A). The major components are the axoneme, the mitochondrial sheath, the outer dense fibers and the fibrous sheath. The axoneme is composed by microtubules emanating from the centriole at the base of the sperm nucleus. The core of the axoneme consists of two central microtubules surrounded by a row of nine doublet microtubules ("9+2" complex, Figure 4, B) (Eddy and O'Brien D., 1994; Inaba, 2003). Although tubulin is the basis for the structure of the flagellum, other proteins are also critical for flagellar function e.g. dynein, a protein attached to the microtubules that hydrolyze molecules of ATP. The ODF are a flexible sperm tail-specific system of accessory cytoskeletal structures surrounded by the mitochondrial helix (Baccetti *et al.*, 1973; Fawcett, 1975; Bradley *et al.*, 1981).

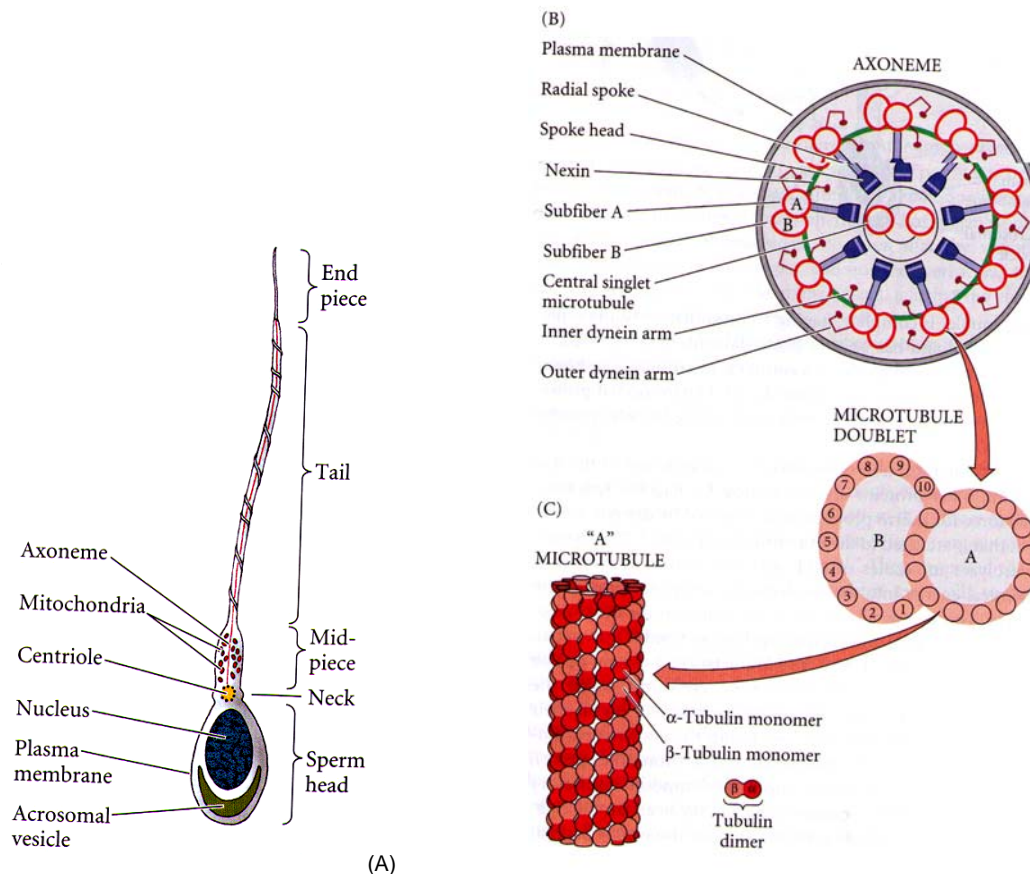


Figure 4: The motile apparatus of the sperm. (A) mature mammalian spermatozoon. (B) interpretative diagram of the axoneme, showing the “9+2” arrangement. A-first portion of the doublet, B-second portion. (C) a three-dimensional model of an “A” microtubule (Gilbert, 2000)

1.2.2 Oocyte

The female germ cell, the oocyte (Figure 5), has haploid nuclear component and a remarkable cytoplasmic store that accumulates proteins, ribosomes, tRNA, mRNA, morphogenetic factors and protective chemicals during its maturation, which are required for fertilization and the initiation of zygotic development. Lying beneath the plasma membrane there is a thin layer of gel-like cytoplasm called the cortex. This region contains high concentrations of globular actin molecules, which form microfilaments necessary for cell division during the fertilization. Also after maturation within the cortex area are the cortical granules, Golgi-derived organelles containing proteolytic enzymes. Outside the plasma membrane is the zona pellucida, which is involved in sperm-egg recognition, surrounded by cumulus cells.

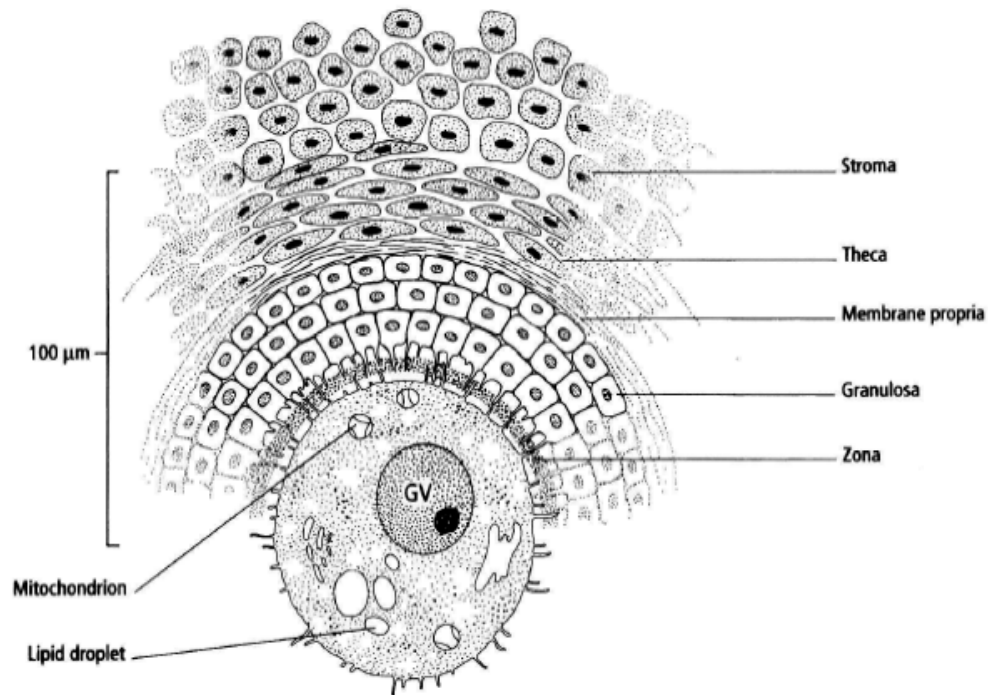


Figure 5: The morphology of a preantral primary follicle (Johnson and Everitt, 1995)

1.2.2.1 General aspects of oogenesis and oocyte maturation

Oocytes meiosis is initiated at early stages of development, often during fetal life. Briefly, oogenesis begins with primordial germ cell formation to oogonias, from oogonias to oocytes where the cessation of meiosis in the dictyate stage is prolonged until oocyte growth and re-initiation of meiosis and the egg ovulation (Gilbert, 2000). Meiosis is arrested in late prophase of the first meiotic phase (germinal vesicle, GV; Figure 6), and the division does not take place until the ovulation, where is finally completed at fertilization (Ben Yosef and Shalgi, 2001; Fan and Sun, 2004). During first meiosis when the oocyte reaches diplonema, it becomes enclosed in a follicle together with the supporting granulosa cells and where it will finish the maturation. The follicular development steps consist of primordial, primary, secondary and tertiary follicles. Primary follicles begin to form in the inner part of the ovarian cortex where they grow concomitantly with the oocyte from a single layer of flattened cells to three layers of cubical granulosa cells. After the oocyte undergoes approximately a 200-fold increase in volume and completes its growth, the follicular cells divide resulting in a graafian follicle which exhibits an incipient antrum (secondary follicle) (Moor *et al.*, 1990). This enlargement indicates a period of intensive metabolic activity. The antrum expands, the oocyte takes up an acentric position surrounded by layers of granulosa cells from which some

will constitute the corona radiata (tertiary follicle) (Dellmann and Eurell, 1998). These cells are connected with the oolema through desmosomes and gap junctions (Sathananthan *et al.*, 2006). Just prior to ovulation the oocytes complete the first meiosis and overcome nuclear progression from dictyate of the first meiotic prophase to metaphase II (meiotic maturation, egg). They remain in this stage of meiosis until stimulated to complete meiosis during fertilization. Only oocytes that have undergone meiotic maturation are capable of being fertilized and developing normally.

The acquisition of meiotic competence apparently occurs in two steps: first the ability to go through nuclear envelope breakdown (GVBD) followed by chromatin condensation and microtubule re-organization with progression to metaphase I, following to metaphase II (MII) (Tosti, 2006). During meiotic maturation significant changes of cortical granules occur, spindle formation and the first polar body emission. Oocytes become arrested at MII until fertilization or parthenogenetic activation. The oocytes released from MII arrest complete the second meiotic division and enter the mitotic cell cycle (Fan and Sun, 2004). Many of the proteins comprising or regulating the maturation process have yet to be identified. Localization and characterization will provide a better insight into the regulation of maturation and fertilization.

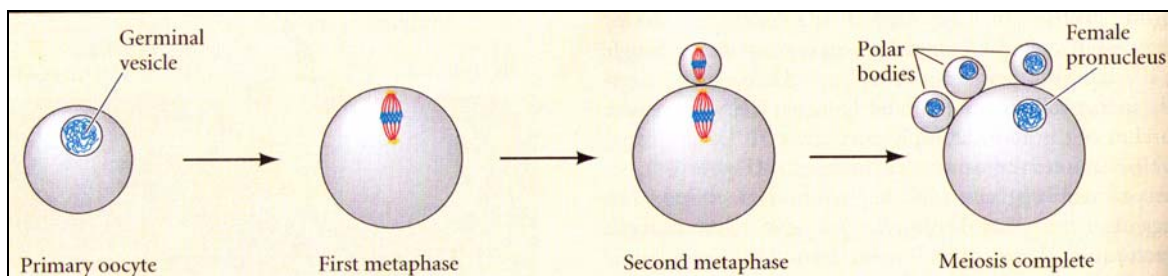


Figure 6: Different nuclear stages present in the oocyte during gametogenesis (Gilbert, 2000)

1.3 Aims

Based on the background information, the aims of the present study were to characterize the different VDAC subtypes present in mammalian gametes. Three main points were studied in order to provide, for the first time, the widest information regarding expression, translation and possible functional role of VDAC in oocytes.

1. Detection of VDAC gene expression in porcine and bovine oocytes

The first aim was to detect the gene expression of VDAC isoforms by RT-PCR in porcine and bovine GV and MII stage oocytes. On the basis of increasing importance to study not only qualitative but also quantitative differences in gene expression levels, relative abundance of the three VDAC isoforms transcripts was intended to be monitored in bovine oocytes originated from three different follicle sizes by real-time RT-PCR.

2. Identification and localization of VDAC protein isoforms in porcine oocytes and follicle cells

In order to further characterize VDAC in mammalian oocytes the second main point was to focus at the protein level.

- a) The first intended aim was to detect VDAC protein expression in porcine ovaries. Immunohistochemical studies were planned using specific anti-VDAC1, 2 and 3 antibodies to evidence eventual changes in terms of the protein expression level and cellular localization of each VDAC protein isoform during folliculogenesis.
- b) Detail distribution was targeted for subcellular localization of VDAC protein subtypes on porcine oocytes in GV and MII stage oocytes by confocal microscopy.
- c) Further immunobiochemical characterization of VDAC protein in porcine oocytes was aimed to be carried out. The purpose was to perform western blot analysis followed by specific VDAC antibodies immunodetection in porcine oocytes regarding their maturation status (GV and MII stage oocytes). The subsequent aim was to isolate and to perform MALDI TOF MS analyses of isolated VDAC protein originated from porcine oocytes.

3. Functional importance of VDAC in mammalian oocytes

The third main point was planned with the aim of studying a possible functional role of VDAC in oocytes. Based on the described events during fertilization, it is clear that a complex dialogue exists between egg and sperm.

a) Thus, VDAC protein from spermatozoa was prompted to be investigated as an accessory mediator which could trigger egg activation. The first intention was to identify VDAC protein subtypes from porcine spermatozoa. For this purpose VDAC spermatozoa proteins were planned to be isolated, purified and subsequently characterized electrophysiologically. Functional VDAC protein was purified from porcine spermatozoa for the purpose of subsequently use it in functional studies related to oocyte activation.

b) The second functional goal was to detect a possible correlation of VDAC1 protein in respect of the regulation of the maturation process. This event is of huge importance since it prepares oocytes for fertilization, hence, localization and characterization of proteins involved in it will provide a better insight on this subject. Therefore, the intended aim was to investigate a potential functional role of VDAC1 during the maturation process of bovine oocytes using specific anti-VDAC1 antibodies which might affect *in vitro* maturation.

2 Material & Methods

2.1 Expression of VDAC mRNA in porcine and bovine oocytes

2.1.1 *Expression analyses of VDAC mRNA in porcine and bovine oocytes by RT-PCR*

2.1.1.1 *Collection of oocytes and cumulus cells*

Porcine and bovine ovaries were obtained from local slaughterhouses (Giessen and Minden/Lübbecke, Germany) and transported to the laboratory in 0.9% NaCl. There was no control over the ovaries collected and no available information regarding breed, age, health or physiological status of the donor.

After being washed, porcine and bovine ovaries were punctured using a scalpel blade. Cumulus oocyte complexes (COCs) were released from antral follicles (3-5mm in diameter) by repeated washing, using a syringe to distribute 0.9% NaCl. Follicular contents were transferred to Petri dishes and observed under a stereomicroscope (Stemi SV11, Zeiss).

2.1.1.2 *RNA-extraction from porcine and bovine oocytes*

Oocytes were denuded by repeated sucking using a mouth-operated glass micropipette with a bore size not greater than the diameter of the oocytes. Denude oocytes were washed 3 times in 0.9% NaCl, collected in RNase free siliconized reaction tubes with 300µl of lysis buffer (Qiagen) and stored at -80°C until RNA-extraction. Ten denuded oocytes were collected per tube.

Isolation of total RNA was performed using the RNeasy mini kit (Qiagen) according to the manufacturer instructions. Briefly, cell lysates were homogenized by directly pipeting onto a QIAshredder spin column (Qiagen) placed in a 2ml collection tube, which was centrifuged for 2min at 13800xg. Afterwards ethanol 70% was added 1:1 to the samples and applied to the RNeasy mini-column. After binding of the RNA to the column the membrane was washed three times, the final RNA was eluted with 30µl RNase-free water and immediately proceeded with the reverse transcription (RT) reaction.

2.1.1.3 Reverse Transcription (RT) procedure

Isolated total RNA was reversely transcribed into complementary DNA (cDNA) using the Omniscript RT-Kit (Qiagen) following manufacturers instructions. In the first tube, first strand cDNA synthesis was performed under optimized conditions; the reaction mixture contained 1X RT buffer, 0.5mM mix of each dNTP (Eppendorf), 10IU RNase inhibitor (Invitrogen), 1 μ M random hexamers (Promega) and 4IU Omniscript reverse transcriptase (Qiagen). The RT-reaction was carried out at 37°C for 60min in a thermal cycler ending with a denaturation step at 95°C for 5min (PTC 200 Pelther thermal cycler. MJ Research). cDNA was pooled, aliquoted and stored at -20°C.

2.1.1.4 Polymerase Chain Reaction (PCR) procedure

The subsequent amplification of the desired genes was performed by PCR, using Taq DNA-polymerase (Eppendorf). PCR-reactions were optimized and the specific annealing temperature was chosen by the best band intensity with only one correct product size observed upon agarose gel analysis.

To reach a final reaction volume of 50 μ l the following components were added: 1X PCR-buffer (NH₄), dNTPs (0.2mM each dNTP, Eppendorf), forward and reverse primers (2pmol each), 2.5IU Taq DNA-polymerase (Eppendorf), DEPC-water (Ambion) and template (cDNA).

All components were gently mixed and added to a thermal cycler (PTC 200 Pelther thermal cycler, MJ Research). The PCR-conditions were 35 cycles of cDNA denaturation at 94°C for 45s, annealing temperature (AT, optimization specified for each primer) for 45s and primer extension at 72°C for 90s with a final step of 72°C for 5min.

To assess the specificity of the obtained products, the following controls were performed:

- PCR was performed using total RNA as template (no RT-step) to detect genomic DNA (gDNA) contamination
 - RT-reaction and PCR were performed omitting templates in order to detect cross contamination
 - PCR was performed using gDNA as a template, to check the ability of utilized primers to span between exons
-

2.1.1.5 Primer design

Using available on-line computer software (http://www-genome.wi.mit.edu/cgi-bin/primer/primer3_www.cgi) and published sequences in Data Bank Pub Med, primers were designed to recognize cDNA of VDAC1, VDAC2, VDAC3 and the housekeeping genes GAPDH, U2snRNA and Histone H2A (Table 1). Primers for each target gene were selected with minimal internal structure (hairpins and primer-dimer formation as determined by the software) and having compatible T_m (melting temperature, each within 1°C of the other). All primers were synthesized by MWG Biotech AG.

Table 1: Primers for PCR

Protein / species	Primer sequence	Amplicon size (bp)	GenBank Accession No.
VDAC1-porcine	F: caaaatctgagaatggactggaa R: ttggtgagaaggatgaatcaaag	219	NM213960
VDAC2-porcine	F: aaatcaaagctgacaaggaa R: gacttttgagaaatggaag	231	NM214369
VDAC3-porcine	F: gaaaggctccaaggatgt R: aggtgcctgatgctttcc	142	NM214364
VDAC1-bovine	F: tgggtctgggttatgaagg R: cgaagcgagtgttgctgtt	234	NM174485
VDAC2-bovine	F: ttcggctgtcttcggttatg R: tcctgatgtccaagcaagg	220	NM174486
VDAC3-bovine	F: gcagtaacaacacccgcttc R: caaatcccagaccgacctt	201	NM174729
Histone H2A-murine ^a	F: gtcgtggcaagcaaggag R: gatctcgccgtaggtactc	182	U62674
U2snRNA-human ^a	F: ctcgcccttttgctaagat R: cggtcctggaggtactgcaa	172	U57614
GAPDH-bovine	F: ccagaagactgtgatggcc R: ctgacgcctgcttcaccacc	248	U85042

Sequences are for forward (F) and reverse (R) primers.

^a Published primers (Robert et al., 2002)

2.1.1.6 Analysis of PCR products

The resulting product from the PCR was run in an agarose gel 1.5% (Invitrogen) in 1X TBE and visualized with ethidium bromide staining (0.5µg/ml, Fluka). Electrophoresis was performed for 90min at 100V. The banding pattern of PCR fragments resolved through the gel was recorded by photography (Canon and Biometra) using a UV transilluminator (wave length 366nm). As molecular standard a 100bp molecular ruler (Bio-Rad) was used.

Gel loading buffer		TBE buffer 5X stock solution/liter	
0.25%	Bromophenol blue	54g	Tris Base
0.25%	Xylenen cyanol FF	27.5g	Boric acid
40% (w/v)	Sucrose in water	20ml	0.5M EDTA (pH 8.0)

2.1.1.7 Sequencing of PCR products

For confirmation of product specificity the fragments with the expected size were sequenced. Therefore PCR products were purified with a QIAquick PCR purification Kit (Qiagen). Amplification products were sequenced by MWG Biotech.

2.1.2 Real-time RT-PCR of bovine oocytes

Antral follicles from 3 different sizes, small (group 1, <3mm) medium (group 2, 4-6mm) and large (group 3, 8-11mm) were isolated from bovine ovaries and dissected under a stereomicroscope (Stemi SV 11, Zeiss) with a surgical blade and fine forceps. Follicles were opened and cumulus oocyte complexes were released, subsequently oocytes were cleaned from cumulus cells. Each single oocyte was collected in lysis buffer (RNeasy mini kit, Qiagen). Total RNA was isolated from each single oocyte using RNeasy mini kit (Qiagen) as previously described. Total RNA was reversely transcribed into cDNA in a total volume of 20µl using a mixture of random hexamers (Promega) and oligo-dT₁₅ primers (Promega) to get the widest array of cDNAs. The reaction mixture consisted of 1X RT buffer, 10IU RNase inhibitor (Invitrogen), dNTPs mix (0.5mM each dNTP), template and sensiscript reverse transcriptase (Qiagen). The RT-reaction was carried out at 37°C for 60min followed by a 5min denaturation step at 95°C.

For real-time RT-PCR reactions, the LightCycler FastStart DNA Master plus SYBR Green 1 (Roche) was used, the reaction mix consisted of DEPC-water (5 μ l, Ambion), PCR primers 10X (0.5 μ l) and PCR master mix 5X (2 μ l). Eight μ l of mastermix were filled into glass capillaries and 2 μ l of cDNA (1:4 dilution) were added as PCR template. Capillaries were closed, centrifuged and placed into the LightCycler rotor (Roche). The following experimental protocol was used: an initial denaturation step (95°C for 10s.), annealing temperature (57°C) was constant for 5s. Elongation was performed at 72°C for 16s. The amplification and quantification program was repeated 45 times (with a single fluorescence measurement) and finally the temperature was raised to 95°C at a heating rate of 0.2°C per second for melting curve analyses. The fluorescence was measured continuously during this step. Cooling program was set down to 40°C.

Fluorescence acquisition was done in every cycle at the end of the second step. To reduce detection of non-specific products with low melting temperature, such as primer-dimers, the acquisition temperature was chosen approximately 3°C below the specific melting temperature of each primer pair.

2.1.2.1 Data analysis

A total of nine CP (crossing point) values of the VDAC samples were acquired apart from the housekeeping genes (U2snRNA and Histone H2A). All investigated genes were amplified in triplicates and were tested in three different experiments at different days, to reduce inter- and intra- assay variation and to confirm reproducibility of real-time RT-PCR results. For further analysis the CP values of every sample were used. The CP is defined as the cycle at which fluorescence rises considerably above background. The CP values were calculated by the LightCycler™ Analysis Software 3.5 (Roche) in the second derivative maximum method. The PCR efficiency was calculated for each sample individually by using LinRegPCR software tool (Ramakers *et al.*, 2003). For every primer pair the mean of evaluated efficiencies respectively was utilized for further analysis. REST-XL was used for evaluation of the expression ratio of the three VDAC mRNA in the three different sizes (Pfaffl *et al.*, 2002; Bustin *et al.*, 2005). REST-XL calculates the expression ratio normalized by the housekeeping gene and corrects for varying PCR efficiencies.

2.2 Expression of VDAC protein isoforms in porcine gametes

2.2.1 *Total extraction of porcine spermatozoa proteins*

Fresh ejaculates from boars (Deutsche Landrasse) were kindly donated by the Clinic for Obstetrics and Andrology of Large and Small Animals, Justus Liebig University, Giessen.

Protein extraction of fresh ejaculates was performed following Hinsch *et al.* protocol (Hinsch *et al.*, 2003). Porcine ejaculates were washed in PBS two times to separate spermatozoa from the seminal plasma for 5min at 700xg. The concentration of spermatozoa was adjusted to 330×10^6 cells/ml and resuspended in 0.6M NaCl PBS to remove loosely attached seminal plasma proteins from the sperm surface. Finally, protease and phosphatase inhibitors were added (EDTA 1mM, benzamidin 10mM, DTT 2mM and PMSF 0.2mM). The suspension was incubated on ice for 1h and afterwards centrifuged at 6000xg for 30min at 4°C. The supernatant was stored at -20°C.

Following the PBS step, two additional extractions with Triton X-100 (TX-100, Serva) were performed. The pellet was resuspended in 0.2% TX-100 and extraction buffer (150mM NaCl, 1mM CaCl₂, 1mM MgCl₂, 1mM KCl, 2mM DTT, 1mM EDTA, 10mM benzamidine, 0.2mM PMSF, 50mM Tris-HCl, pH 7.4) for 1h at 4°C. The spermatozoa were centrifuged at 6000xg for 30min. The supernatant was saved at -20°C and the pellet was resuspended in extraction buffer containing 2% TX-100 and incubated for 1h at 4°C. Finally, the sperm suspension was centrifuged at 6000xg, and the protein supernatant of interest was stored at -80°C until use.

2.2.1.1 *Hydroxyapatite-celite purification of VDAC protein from porcine spermatozoa*

To obtain purified VDAC protein from the TX-100 cell extract, a single step hydroxyapatite-celite chromatography of the TX-100 protein was performed as described by De Pinto *et al.* (De Pinto *et al.*, 1987a). In detail, the spermatozoa protein TX-100 extraction (500µl) was mixed with 2% TX-100 (500µl) and applied to a well packed 600mg hydroxyapatite-celite (ratio 2:1) column (glass 0.5X14cm). Elution was performed with 2% TX-100 buffer at 4°C. One ml was recovered and used for subsequent analyses.

2.2.1.2 Protein precipitation from total extractions and purified samples

Whole cell protein extract and hydroxyapatite-celite purified samples were precipitated using 9ml cold acetone (-20°C) plus 1ml sample at 4000xg for 30min at 4°C. The supernatant was discarded and the pellet air dried. The dry samples were solubilized in laemmli (1X) 5% mercaptoethanol for one dimensional SDS-PAGE or in sample buffer for two dimensional SDS-PAGE.

2.2.1.3 Determination of protein concentration from purified samples

Protein quantification assays were performed using non-interfering Protein Assay kit (Calbiochem). The assays were conducted to settle a comparable amount of VDAC protein purified samples for use in functional experiments. A calibration curve was performed using BSA standard. The quantification kit uses a universal protein substance for removing interfering agents from protein solutions like TX-100. This assay is based on the specific binding of cooper ions to the peptide backbone of the protein. It measures the concentration of unbound cooper, which is inversely related to the amount of protein present in the solution (Biuret-reaction). The detection was performed at 480nm by an ELISA-Reader (Tecan).

2.2.2 Extraction of porcine oocyte protein

Collection of porcine Cumulus-Oocytes-Complex and *in vitro* maturation (IVM)

Oocyte collection and maturation were kindly performed under routine procedures (Rath *et al.*, 1999) in the Dept. of Biotechnology, Institute for Animal Breeding (FAL, Germany). In summary, porcine ovaries were obtained from the local slaughter house (Lübbecke, Germany) and germinal vesicle stages oocytes were isolated from follicles of 2-8mm size with the help of 18-Gauge needle attached to a vacuum pump (VM AR-5100, Cook). The recovered follicular fluid was washed with PBS and 1% new born calf serum (NBCS), allowed to stand for 10min for sedimentation of the COCs and subsequently checked under a stereomicroscope. For collection of germinal vesicle stage oocytes, the oocytes were denuded immediately after selection with the aid of a mouth pipette. For collection of metaphase II

stage oocytes, COCs of good quality (approximately 2-3 cumulus cell layers and homogenous cytoplasm in the oocyte) were selected for maturation.

The medium used for maturation was sterile North Carolina State University (NCSU)-37 media (Petters and Wells, 1993) supplemented with porcine follicular fluid, cysteine, glutamine, mercaptoethanol and Epidermal Growth Factor (EGF). During the first 22h of maturation EGF, cAMP and hCG/eCG were added. COCs were incubated for 22h at 38.5°C, 5% CO₂ and 95% humidity. After 22h new media with only EGF was added and incubated for another 18h, counting up to a final maturation time of 40h. IVM oocytes were denuded with Tyrode's lactate (TL) - Hepes 296- media, calcium and 0.1% hyaluronidase (Sigma) for 5min at 38.5°C. Afterwards cumulus cells were mechanically removed from the oocyte and washed twice in TL- Hepes 296 and calcium.

The cumulus free germinal vesicle (GV) and metaphase II (MII) stage oocytes were washed three times in PBS and frozen immediately in a minimal volume of PBS at -80°C.

Oocytes in PBS utilized for SDS-PAGE and immunoblot experiments were incubated at 70°C for 1h and then dissolved 1:1 (v/v) in oocyte buffer (2X) 5% 2-mercaptoethanol (Bio-Rad) and vortexed for 5 minutes, with a last heat step at 95°C.

2.2.3 *Generation of antibodies against subtype-specific synthetic VDAC peptides*

In previous studies antisera were generated and characterized against synthetic peptides. The sequences of the synthetic peptides used as antigens are shown in Table 2. The sequences were either derived from VDAC2 or VDAC3 amino acid sequences identified in bovine sperm ODF protein proteolytic peptides and/or deduced from cDNA clones coding for bovine VDAC1, 2, and 3 (Hinsch *et al.*, 2004). Accession numbers and amino acid residue numbers were as follows: VDAC1 *Bos taurus* (POR1_BOVIN) P45879: amino acids 271–282; VDAC2 *Bos taurus* Q9MYV7: amino acids 236–247; VDAC3 *Bos taurus* (POR3_BOVIN) Q9MZ13: amino acids 16–25. Antibody binding activity and specificity of the antibody reaction were evaluated (Hinsch *et al.*, 2004).

Table 2: Description of used antibodies

Antibodies	Peptide sequences	Peptide
anti-VDAC1 (AS P6)	GHKLGLGLEFQA	1b
anti-VDAC2 (AS P45)	YQLDPTASISAK	H1
anti-VDAC3 (AS P31)	SVFNKGYGFM	H4
anti-VDAC common (AS P_{common})	GHKVGLGFEL	3-2

2.2.4 Protein expression analysis of VDAC in porcine gametes by immunoblotting

2.2.4.1 SDS- Polyacrylamide Gel (SDS-PAGE) electrophoresis of proteins

SDS-PAGE was performed according to Laemmli (Laemmli, 1970) with some modifications. Solubilized proteins were loaded using a Hamilton syringe (Hamilton Bonaduz AG) onto a Mini Protean IITM Bio-Rad electrophoresis system.

SDS-Polyacrylamide gels (8x9cmx0.75mm thick) were composed of 6% (w/v) acrylamide stacking gel and of 12% running gel. Electrophoresis was performed under reducing conditions at room temperature in electrophoresis buffer (1X) at constant 200V until the bromophenol blue tracking dye had reached the bottom of the running gel.

Determination of molecular masses was based on standard proteins Precision Plus Protein Standard (Bio-Rad).

Oocyte buffer (pH 7-7.4)	
100mM	Tris/HCl
25mM	EDTA
5% w/v	SDS
12%	Glycerol

Electrophoresis buffer (10x) pH 8.3	
192mM	Glycin
25mM	Tris
0.1% w/v	SDS

Running gel (5ml)	
1.25ml	Running gel (0.5M Tris-HCl pH 6.8)
2ml	30% Acrylamide
1.7ml	Dist. water
50µl	10% SDS
2.5µl	Temed
25µl	10% ammonium persulfate

Stacking Gel 6 % (5ml)	
1.25ml	Stacking gel (1.5M Tris-HCl pH 8.8)
1ml	30% Acrylamide
2.7ml	Dist. water
50µl	10% SDS
5µl	Temed
25µl	10% ammonium persulfate

2.2.4.2 Two Dimensional SDS- PAGE electrophoresis of proteins (2D SDS- PAGE)

2D-electrophoresis was used to determine the identity of VDAC1, VDAC2 and VDAC3 proteins in porcine spermatozoa. Protein samples were separated on the basis of their pI in IPG (immobilized pH gradient) strips (pH gradient 3-10, Bio-Rad and pH 6-11, GE Healthcare). Proteins were solubilized using 130µl sample buffer. Probes were subjected to one- and two-dimensional gel electrophoresis. The first dimension was carried out loading samples to the IPG at the time that passive rehydration was conducted over night. Each isoelectric focusing (IEF) was run in a linear ramping mode to a maximum voltage increase of 15000V. After IEF, the IPG gels were removed and, if necessary, stored at -80°C. The IPG gels were prepared for the second dimension by equilibration, first 10min in equilibration buffer containing 2% DTT (room temperature) and then in 2.5% iodoacetamide-equilibration buffer (10min room temperature). IPG gels were placed on a 1.5mm 6% stacking and 12% running SDS-PAGE gel and electrophoresis was carried out as previously described for SDS-PAGE electrophoresis (2.2.4.1).

Sample buffer (pH 3-10)	
8M	Urea
50mM	DTT
4%	CHAPS
0.2%	Carrier ampholytes
0.0002%	Bromophenol Blue
	Water

Sample buffer (pH 6-11)	
8M	Urea
50mM	DTT
2%	CHAPS
0.2%	IPG buffer
0.0002%	Bromophenol Blue
	Water

Equilibration buffer	
6M	Urea
20%	SDS
1.5M	Tris/HCl pH 8.8
0.2%	Carrier ampholytes
50%	Glycerol
	Water

2.2.4.3 Western Blot

Following one- and two-dimensions SDS-PAGE gel electrophoresis, proteins were transferred from polyacrylamide gels to nitrocellulose membranes (Amersham Pharmacia Biotech) by means of a buffer tank electroblotting method. The transfer time was 90min at 70V in western blot buffer.

Then gels were stained for total protein to verify transfer efficiency with Coomassie Blue staining. The polyacrylamide gels were covered with Simply Blue (Invitrogen) overnight in a rocking platform and finally water destained (washing) and dried (50% ethanol and 2% glycerin) to maintain a permanent gel record with cellophane membrane.

To verify electrotransfer efficiency, the nitrocellulose membranes were gently shaken in Ponceau S solution (Sigma) for 5min at room temperature. Then washed with distilled water until banding patterns were visible.

Western blot buffer	
192mM	Glycin
25mM	Tris
20%	Methanol
0.0375%	SDS

2.2.4.4 Immunoblotting

The nitrocellulose membranes were blocked for 1h in 5% (v/v) teleostean gelatin (Sigma) in TTBS to prevent non-specific binding and high background signal. The primary antibody was allowed to bind at appropriate dilution in TTBS supplemented with 3% skimmed milk powder (Euroclon) for 60min. Subsequently, membranes were washed 3 times for 5min in TTBS at room temperature; and the second antibody protein A labeled with horseradish peroxidase (Bio-Rad) was added in a 1:3000 dilution (TTBS 3% skimmed milk powder) for 30min. After several wash steps in TTBS the location of the second antibody was determined by the enhanced chemiluminescence Western blotting detection reagents (ECL, Amersham Pharmacia Biotech). Finally the membranes were exposed to x-ray film (Super RX-Fuji) and developed.

To assess the specificity of the immune reaction, the following controls were used:

- Substitution of the primary or the second antibody with the corresponding buffer

- The control with the corresponding preimmune serum
- Pre-absorption of the antiserum with the peptide employed as immunogen (Table 2). Antisera were pre-incubated at the same working dilution with 15µg of peptide/ml for 1h at room temperature centrifuged for 3min at 13800xg then the supernatant was taken and subsequently assayed in immunoblotting.

TTBS	
10mM	Tris pH 7.5
100mM	NaCl
0.1%	Tween 20

2.2.5 Protein identification by MALDI-TOF MS

After visualization with Coomassie blue or silver staining, spots and bands were subjected to MALDI-TOF MS mass spectrometry for protein identification by the Chromatech Company (Germany). Peptide mass fingerprinting (PMF) database searching was carried out using available online software (<http://www.matrixscience.com/>).

2.2.6 Immunohistochemical detection of VDAC protein in porcine ovaries.

For immunohistochemical studies, porcine ovaries were sliced into small cubes, fixed in Methacarn, and processed as previously described (Bogner *et al.*, 2004). Briefly, the material was cut into sections of 5µm and deposited in glass slides which were beforehand coated with chromalaum. Ovaries sections were deparaffinized with xylene, rehydrated through a graded sequence of ethanols (Fluka), and rinsed with distilled water and PBS. They were treated with hydrogen peroxide 3% (Merck) in PBS for 15min, then washed in PBS and subsequently blocked for 1h in skimmed milk powder 1% PBS. Specimens were treated with anti-VDAC1 (AS P6), anti-VDAC2 (AS P45), anti-VDAC3 (AS P31) and commercially available monoclonal antibody, anti-VDAC1 31HL (P31HL, Calbiochem) for 60min diluted in 1% skimmed milk powder PBS.

Antigen-antibody reaction was visualized with the corresponding second antibodies using streptavidin peroxidase (Labvision) and peroxidase-substratkit AEC as color substrate (Biologo).

Finally, sections were counterstained with hematoxylin (Dakocytomation). As negative control, sections were incubated with preimmune serum following the antibody dilution or with the corresponding IgG in the case of the commercial antibody (mouse IgG_{2a}, Calbiochem).

Chromalaun-gelatin		Methacarn solution	
1g	Gelatine	60% (v/v)	Methanol
0.1g	Chrom (3)-potassium-Dodecahydrot	30% (v/v)	Trichlormethan
260ml	Dist. water	10%	Acetic acid

2.2.7 *Subcellular localization of VDAC proteins in porcine oocytes by confocal microscopy*

Porcine cumulus free GV and MII stage oocytes were obtained as previously described in section 2.2.2. The complete steps were conducted in 100µl drops unless described differently. Oocytes were washed three times in PBS and fixed in 3.7% paraformaldehyde (v/v) PBS for 30min. To permeabilized oocytes, an extra step was carried out, using 1% TX-100 in PBS for 5min, and subsequently washed for 5 times in PBS supplemented with 0.1% skimmed milk powder. Oocytes were blocked in 1% skimmed milk powder diluted in PBS during 60min. The oocytes were incubated with the first antibody diluted in a 30µl drop of 0.1% skimmed milk powder for 60min. Following three washing steps, oocytes were exposed to the FITC-conjugated second antibody, for 30min in 25µl drops. During the last 5min of incubation, 5µl of propidium iodide was added to detect maturation stages. Finally, samples were washed five times and placed in a clean slide with mounting medium (CitiFluor, Agar). The slides were kept in the dark at 4°C until observation. Oocytes were examined and recorded using a laser scanning confocal microscope (LSM 510, Zeiss Axyioplan imaging). The microscope was equipped with an Argon and HNe1 laser.

2.3 Functional studies

2.3.1 *Lipid bilayer experiments with purified VDAC protein from porcine spermatozoa*

For functional characterization the corresponding channel conductance measurements were performed, with purified VDAC protein, extracted from porcine spermatozoa. The purified proteins obtained in section 2.2.1.1 needed to be refolded 1:10 in 1% Genapol X-080 (Fluka) supplemented with 0.5% cholesterol, to get channel-forming activity in lipid bilayer experiments.

The method of reconstitution of purified VDAC protein into artificial lipid bilayer membranes has been carried out following Benz *et al.* (1978). Briefly, membranes were formed from a 1% (w/v) solution of diphytanoyl phosphatidylcholine (DiphPC, Avanti Polar Lipids) in n-decane by painting onto a circular hole (surface area about 0.4mm²) separating the two compartments of a Teflon cell (Figure 7). For standard single channel conductance studies, the Teflon chamber was filled with 1M KCl solution. The voltage across the membrane was applied through silver/silver chloride electrodes inserted into the aqueous compartments on both sides of the membrane. The membrane current was measured with a current amplifier (Keithley 427). The amplified signal was monitored with a storage oscilloscope and recorded on a strip chart recorder. Zero current potential measurements were performed using a high impedance electrometer (Keithley 617).

For voltage dependence studies, the refolded protein was added at a concentration of 500ng/ml to both sides of the membrane. After the reconstitution of VDAC channels into the membrane reached equilibrium, different potentials were applied to both sides starting with ± 10 mV increasing until the membrane was damaged.

The experiments were analyzed using the membrane conductance (G) as a function of voltage. V_m was measured when the opening and closing of channels reached equilibrium, i.e. after the exponential decay of the membrane current following the voltage step V_m . G was divided by the initial value of the conductance (G_0 , which was a linear function of the voltage) obtained immediately after the onset of the voltage.

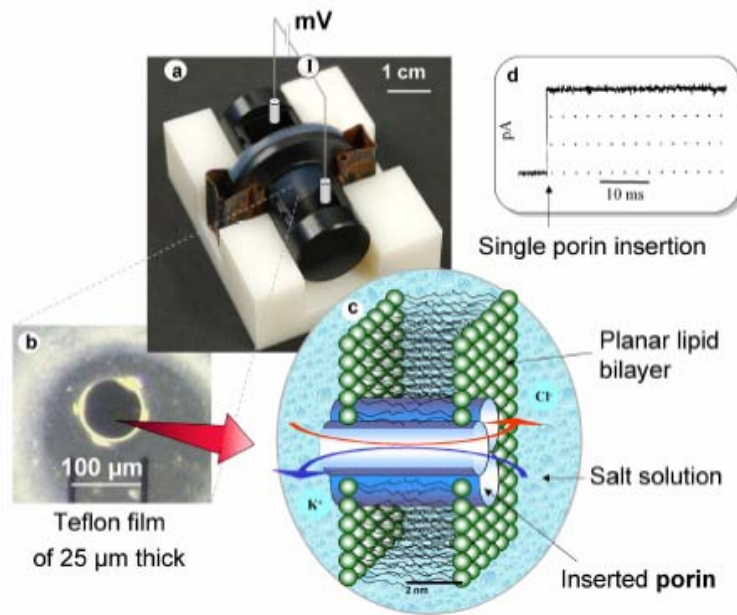


Figure 7: Schematically representation of a planar bilayer set-up for ion current recording. (a) two half cells separated by a Teflon foil with a center hole (b) microscope picture of a Teflon film (c) schema of a lipid bilayer with a reconstitute VDAC pore (d) insertion of a single channel (Berkane *et al.*, 2005)

2.3.2 Treatment of mature porcine oocytes with purified VDAC protein from porcine spermatozoa

2.3.2.1 Pickup procedure and in vitro maturation (IVM) of porcine oocytes

Ovaries were obtained from slaughtered pre-pubertal gilts (Hannover abattoir) transported to the laboratory within 1h in a 0.9% NaCl, 50μg/ml gentamycin solution at 30-35°C, following the procedures described by Meinecke and Meinecke-Tillman (Meinecke and Meinecke-Tillmann, 1979; Meinecke and Meinecke-Tillmann, 1993)

Antral follicles (3-6mm in diameter) were punctured and flushed with an 18 gauge hypodermic needle filled with pre-warmed (39°C) PBS supplemented with 1% (w/v) heat inactivated fetal calf serum (FCS) and 10μg/ml gentamycin. Only oocytes with uniform cytoplasm and surrounded by compact and dense cumulus cell layers were selected. After collection, oocytes were cultured in maturation media for 48h in humidified atmosphere of 5% CO₂ in air at 39°C. The maturation media was modified TC199 (Sigma) supplemented

with 2% FCS, 10µg/ml gentamycin, 1mg insulin, 0.004g L-Glutamin, eCG (10UI/500µl, Intergonan).

At the end of the maturation period, oocytes were denuded with 0.1% hyaluronidase by repeated passage through a glass pipette in PBS supplemented with 10% FCS. The denuded oocytes were kept in culture medium until microinjection without hormone addition and under the same atmospheric conditions used for maturation.

2.3.2.2 Microinjection

Microinjections were performed following previous established procedure (Meinecke and Meinecke-Tillmann, 1993). Therefore, microinjections were conducted at room temperature using standardized glass microinjection needles (Femtotips, Eppendorf) under an inverted microscope using a Leitz mechanical micromanipulator connected to a microinjector system (Transjector 5246, Eppendorf). They were carried out in microdrops of pre-warmed (39°C) PBS supplemented with 10% FCS and 5µg/ml cytochalasin D (Sigma) covered with pre-warmed (39°C) mineral oil. The test solutions were stored at -20°C in 10µl aliquots. Immediately before use samples were centrifuged for 10min at 10000xg at 4°C and loaded by means of a microloader into the glass microcapillaries.

The tip was introduced onto the oolema and in the cytoplasm, during microinjection, the oocyte was held in position with a fire-polished holding pipette. Parameters were adjusted to injection pressure (P_i) 250hPa; a compensation pressure (P_c) of 40hPa and, a fix injection time of 0.5s was maintained throughout the experiments.

After microinjection, oocytes were washed two times in PBS and one time in culture medium. Subsequently oocytes were transferred to culture medium for 24h under *in vitro* maturation atmospheric conditions. Following the 24h culture, assessment of oocyte activation of purified VDAC protein and correspondent control were performed. Results were analyzed by the help of InStat™ from Graph Pad.

2.3.2.3 Assessment of activation

To asses activation oocytes were mounted under posted coverslips and fixed in ethanol/acetic acid (3:1) for 24h. Thereafter, slides were stained for 3-5min with 2% aceto-orcein (Merck) and washed with 25% acetic acid. The stained oocytes were examined under a phase contrast

microscope (Olympus) at 200-400X magnification, activation was considered to have occurred if oocytes had one pronucleus or more.

2.3.2.4 Experimental design

The following experimental protocols were performed in order to elucidate a possible activation effect of purified VDAC protein from spermatozoa in MII stage oocytes:

a) Microinjection of purified VDAC protein

To determine whether purified VDAC protein from sperm can promote the activation of porcine oocytes mature *in vitro*, groups of 10-20 mature oocytes were microinjected with the purified VDAC sample obtain in the section 2.2.1.1. The enriched VDAC protein was acetone-precipitated as previously described and resuspended in PBS at a final concentration of 1g/ml. The experiment was replicated 5 times. To rule out possible effects of the microinjection procedure or buffer systems, oocytes were pierced with an injection capillary (only physical stimulus) or injected with control buffers used for VDAC protein extraction or dilution.

b) Incubation of purified VDAC protein

In order to determine if the incubation of purified VDAC protein from porcine spermatozoa can promote the activation of mature oocytes, groups of 10-20 oocytes were incubated with enriched VDAC protein or with acetone precipitated samples dissolved in dimethyl sulfoxide (DMSO). For treatment of oocytes, the purified VDAC or VDAC/DMSO solution was diluted to experimental concentrations in media and equilibrated at an atmosphere of 5% CO₂. As a control treatment oocytes were incubated in the protein extraction buffer, dissolved like the test sample. Incubations at different times were observed. The experiment was replicated 4 times.

2.3.3 Calcium oscillation measurements after microinjection of purified VDAC protein in mature bovine oocytes

Metaphase II bovine oocytes were kindly provided by the Institute of Animal Breeding Science (University of Bonn). Briefly, follicles of 1-8mm were punctured with an 18G needle and follicular fluid was checked under microscope after sedimentation. Selected oocytes were

set to mature after washing in maturation media. Maturation time was 22h at 5% CO₂ with 95% humidity.

2.3.3.1 *Calcium oscillation patterns in bovine oocytes after VDAC protein microinjection*

Mature bovine oocytes were incubated for 60min at 37.5°C with 100µM of the Ca²⁺ sensitive probe Fura-4 AM (stock in 1mM DMSO, Molecular probes). After 3 times washing with TCM, oocytes were settled for 30min with TCM, until microinjection procedure.

Oocytes were microinjected with different treatments of the enriched VDAC protein from porcine and bovine spermatozoa and their respective buffers as control.

- a) Purified VDAC protein after acetone precipitation resuspended in PBS
- b) Purified VDAC protein without precipitation in elution buffer (2% TX-100)
- c) Purified VDAC protein in elution buffer (2% TX-100) lyophilised diluted in Genapol 1% (1:10)
- d) Purified VDAC protein in elution buffer (2% TX-100) lyophilised diluted in media (1:1)
- e) Purified VDAC protein in elution buffer (2% TX-100) lyophilised, resuspended in PBS and cleaned with Nanosep microconcentrators columns (Pall)

The microinjection procedure was carried out with the help of a micromanipulator (Narishige) and a microinjector (Eppendorf) under the microscope (Leica). Oocytes were held with a self-made pipette and microinjector Femtotip capillaries were used (Eppendorf). A volume of 25.5pl was microinjected into the cytoplasm of each oocyte. For every experiment five oocytes were injected consecutively and calcium oscillations were measured at the same time. The Ca²⁺ was monitored by measuring the fluorescence at 497nm from individual oocytes, loaded into a Petri dish, placed on an inverted microscope. The wavelengths obtained from the oocytes were recorded using a camera and analyzed by the AquaCosmos 1.3 software (Hamamatsu) which digitized in a graphic curve.

2.3.4 *Influence of anti-VDAC1 antibodies on in vitro maturation of bovine oocytes*

Bovine cumulus oocyte complexes used for functional studies were isolated via ovary slicing (Eckert and Niemann, 1996). Briefly, ovaries were cut with razor blades in PBS containing

BSA and heparin. The resulted suspension was passed through a filter to isolate COCs and was allowed to sediment at room temperature for 10min. Oocytes with an evenly cytoplasm surrounded by compact cumulus cells were selected for IVM. The oocytes were collected in TCM199 air medium and then washed three times in 100µl TCM199 maturation media without hormone addition.

Groups of 20 cumulus oocytes complex were placed in 100µl of TCM maturation medium supplemented with suigonan (5IU/ml, Intervet) and the diluted antibody or respective control. Finally, oocytes were overlaid with mineral oil and incubated for 24h at 5% CO₂ in a humid atmosphere at 39°C.

After 24h, oocytes were collected in Hyaluronidase 0.1% for 10min and vortexed for 5min. The denuded oocytes were washed in PBS/BSA, stained with Hoechst (5µl/ml PBS for 10min) and assessed under a fluorescence microscope to be classified according to the meiotic maturation stage.

2.3.4.1 Experimental design

The following blocking treatments were carried out in order to assess a possible role of VDAC1 during oocyte maturation:

a) Treatment of oocytes during maturation with P31HL (anti-VDAC1, Calbiochem)

Effect of P31HL antibody (anti-VDAC1, Calbiochem) during oocyte maturation was examined. Cumulus oocytes complexes (50-70 oocytes each group) were treated during the 24h of maturation, with 8µg of anti-VDAC1 dissolved in 100µl maturation media. For control experiments, oocytes were treated with corresponding amounts of mouse IgG subtype (IgG_{2a}, Calbiochem). A normal maturation rate without exposure to treatment was also examined. P31HL and the correlated control were cleaned of sodium azide using Zeba desalt spin columns (Pierce) and probed their activity by ELISA assay.

b) Treatment of oocytes during maturation with anti-VDAC1 (ASP6)

Complement deactivation of the antibody and preimmune serum was performed by heating for 60min at 56°C. Finally, samples were centrifuged for 3min at 13800xg and the supernatant reaction was controlled and compared to the original batch by ELISA.

In **experiment 1**, anti-VDAC1 (AS P6) antibody or the correlate preimmune serum (PI P6) were incubated during the total maturation process with a final concentration of 2µg in 100µl media

In **experiment 2**, in order to examine whether the intracellular transfer of antibody can affect the maturation process, COCs were treated with an antibody delivery kit (Pulsin, Polyplus transfection) diluted in the maturation media. COCs were treated during the first 4h and the total 24h of incubation. After treatment, COCs incubated for 4h, were washed 3 times in maturation media and incubated in fresh maturation drops for another 18h. COCs treated only with the transfection reagent were used as control. To assess the efficiency of the delivery system, a positive control included in the Pulsin kit was carried out (R-phycoerythrin, red fluorescent marker) was incubated as previously described and observed under a fluorescence microscope.

In **experiment 3**, COCs were cultured for 24h with 6µg of anti-VDAC1 (AS P6) antibody in 100µl media with the addition of 2µl delivery reagent (Pulsin). The procedure was performed as previously described.

2.3.4.2 Statistical analysis

Results were presented as means±SD. Percent data were analyzed after angular transformation by the formula $y = \arcsin[\sqrt{x/100}]$. Statistical analysis was performed by the help of InStat™ from Graph Pad.

3 Results

3.1 Expression of VDAC mRNA in porcine and bovine oocytes

3.1.1 Expression analyses of VDAC mRNA in porcine and bovine oocytes by RT-PCR

RT-PCR of porcine oocytes

RT-PCR revealed that VDAC1, VDAC2 and VDAC3 mRNAs were expressed in porcine oocytes (Figure 8) in GV (lane A, B and C) and MII (lane D, E and F) stage. The predicted fragments for the four genes were generated using cDNA preparations. An amplicon of 219bp was observed with VDAC1 primer (Figure 8; lane A and D), a 231bp fragment with VDAC2 (Figure 8; lane B and E) and a 142bp VDAC3 product was acquired (Figure 8; lane C and F). GAPDH control primer gave a 248bp (Figure 8, lower panel) and no amplification fragments were observed in negative control experiment (data not shown).

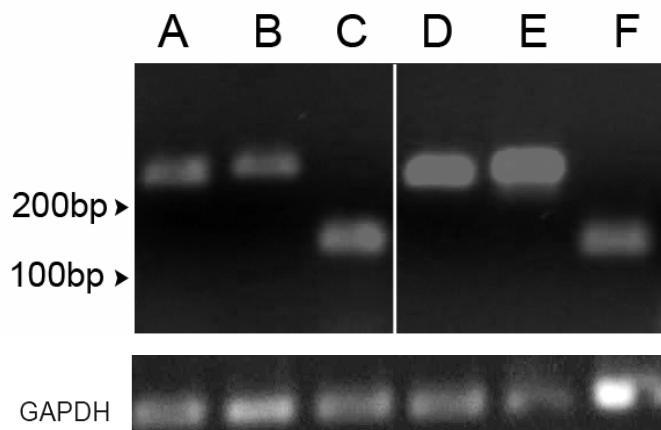


Figure 8: VDAC1, VDAC2 and VDAC3 gene expression in porcine oocytes. GV (lane A, B and C) and MII (lane D, E and F) stage oocytes were assayed with specific primers. VDAC1 (lane A and D; 213bp), VDAC2 (lane B and E; 231bp), VDAC3 (lane C and F; 142bp) and GAPDH (lower panel, 248bp).

All three cDNA amplicons derived from germinal vesicle oocytes were sequenced on both strands. The resulting sequences were compared with published data showing an identity between 98-100% in respect of porcine cDNAs for VDAC1, 2 and 3.

RT-PCR of bovine oocytes

Messenger RNA for VDAC genes was detected in bovine (Figure 9) germinal vesicle (lane A, B and C) and MII (lane D, E and F) stage oocytes. In lanes A and D of Figure 9 an amplicon of 234bp was generated by VDAC1. In lanes B and E the VDAC2 primer amplified a 220bp product and in the lanes C and F the expected fragment of 201bp was observed for VDAC3

(Figure 9). The control housekeeping gene GAPDH gave a 248bp product (Figure 9, lower panel) and no fragment was detected in negative control experiments (data not shown). All three VDAC products, amplified from GV oocytes were sequenced on both strands. The obtained sequences were compared with published data resulting in 98-100% similarity compare to bovine VDAC1, 2 and 3 cDNA.

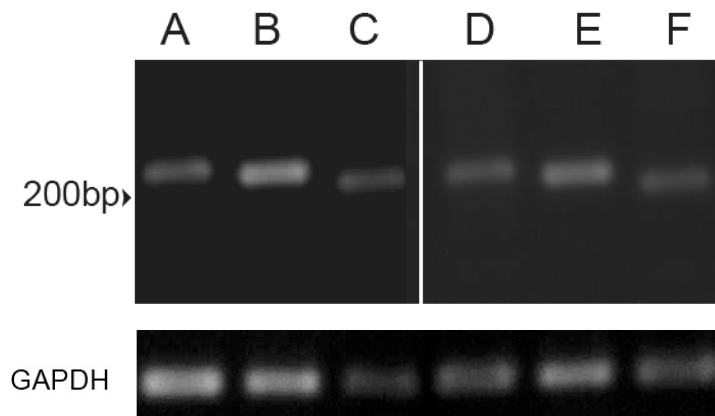


Figure 9: Detection of VDAC gene expression in immature (lane A, B and C) and mature (lane D, E and F) bovine oocytes. Oocytes were assayed with VDAC1 (lane A and C; 234bp), VDAC2 (lane B and E; 220bp), VDAC3 (lane C and F; 201bp) and GAPDH (lower panel, 248bp) primers.

Based on the results of the RT-PCR experiments, the expression of the three VDAC subtypes was detected in bovine and porcine GV and MII stage oocytes. The mRNA pattern seemed to remain stable during meiotic maturation. No quantification analysis could be performed by common RT-PCR protocol; therefore, the expression of VDAC subtypes in bovine oocytes of different follicle sizes was further analyzed by semi-quantitative PCR implementing real-time RT-PCR

3.1.2 *Real-time RT-PCR of bovine oocytes*

Three oocytes populations were recovered separately from small (group 1, <3mm) medium (group 2, 4-6mm) and large (group 3, 8-11mm) follicles and subsequently analyzed by relative quantification studies. The real-time RT-PCR reaction was optimized to run PCR with single oocytes. All primers designed for the block PCR could be utilized with an annealing temperature of 57°C for the Roche LightCycler. Histone H2A and U2snRNA were described to be stable housekeeping genes as discussed in detail below (4.1.1). Products were identified by melting curve profile analyses and confirmed by ethidium bromide stained agarose gel electrophoresis (data not shown). Melting curves were produced after amplification. Thereby,

the fluorescence of the samples was monitored as the temperature was increased. The purpose of melting curve analysis was to determine the characteristic melting temperature of the target gene, supplying information for product identification, primer dimers and possible mutations. No detectable primer dimer formations were generated during the 45 amplification cycles.

Figure 10 displays a representative amplification curve from the fluorescence raw data that was acquired for one of the three runs for VDAC3 during the extension phase of each cycle and the two housekeeping genes (H2A and U2snRNA). Amplification was evident from the three categories of follicles (group 1, group 2 and group 3) and the target genes, with an average threshold PCR cycle of 30. The negative controls, which lacked template (NTC), did not present fluorescence increases, meaning that no product was generated. Replicates obtained were similar and were statistically analysed.

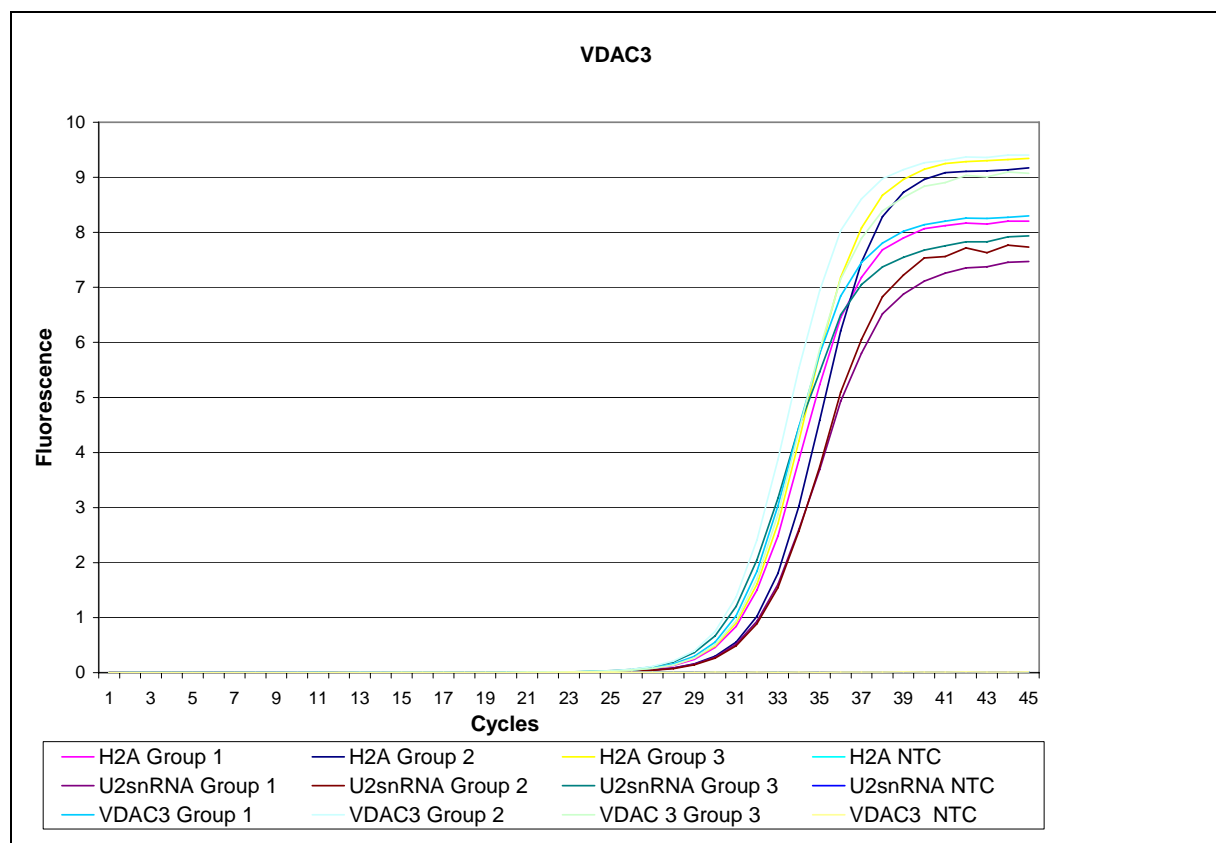


Figure 10: Display of the amplification plot results from real-time RT-PCR of VDAC3. Results illustrate the three follicle categories group 1 (<3mm), group 2 (4-6mm) and group 3 (8-11mm). NTC represents the negative template control. Each sample was run in triplicates but only one single curve is shown for each. The X-axis represents the fluorescence and the y-axis the PCR cycles.

A crossing point (CP) was calculated based on the time (measured in PCR cycle numbers) at which the reporter fluorescent emission increased beyond a threshold level. The CP was correlated to input target mRNA levels, a greater quantity of input mRNA target thereby resulted in a lower CP value, as a result of requiring less PCR cycles for reporter fluorescent emission intensity to reach the threshold (Winer *et al.*, 1999).

Table 3 describes the crossing points and their respective standard deviations for each target gene and the different sample groups. Each gene (VDAC1, VDAC2, VDAC3, H2A and U2snRNA) was plotted in a chart (Figure 11) to compare the groups and their different crossing points.

Table 3: Crossing points analysis for each target gene and sample group

	Group 1	Group 2	Group 3
VDAC1			
Crossing points mean ^a	31.27	32.065	31.822
SD ^b	0.340	0.738	0.497
VDAC2			
Crossing points mean ^a	32.295	33.003	32.767
SD ^b	0.585	0.797	0.312
VDAC3			
Crossing points mean ^a	30.505	30.477	30.626
SD ^b	0.242	0.250	0.182
Histone H2A			
Crossing points mean ^a	30.986	31.922	30.752
SD ^b	0.414	0.308	0.431
U2snRNA			
Crossing points mean ^a	32.137	32.116	30.333
SD ^b	0.792	0.643	0.780

^a Overall mean from all investigated samples from triplicates in three independent experiments

^b Standard deviation of the mean

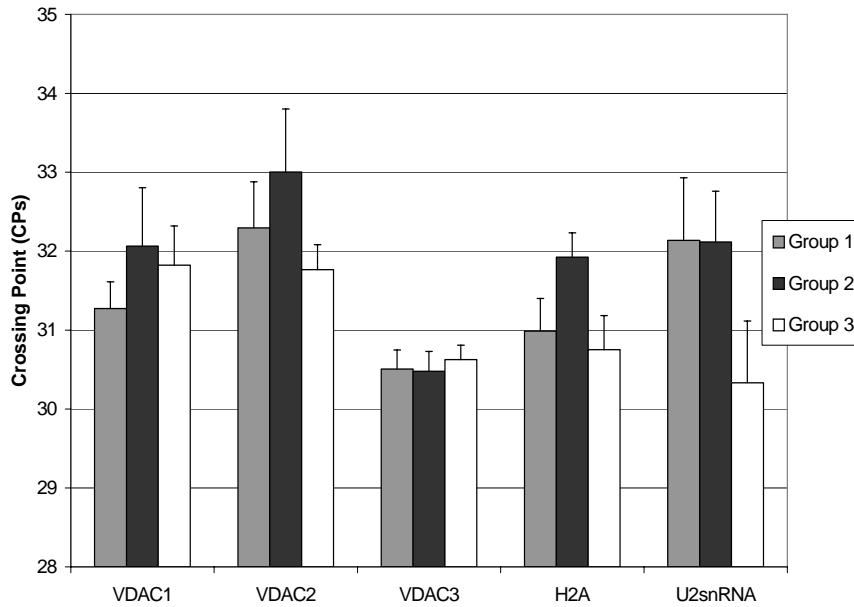


Figure 11: Display of the crossing points for each gene and the housekeeping gene (U2snRNA and H2A) in the three different categories of follicles. The indicated CPs are means obtained from 3 different real-time RT-PCR experiments.

The following equation shows one mathematical model for relative sample comparison, which includes an efficiency correction for real-time RT-PCR efficiency of the individual transcripts.

$$\text{Ratio} = (E_{\text{target}})^{\Delta CP_{\text{target (control-sample)}}} / (E_{\text{ref}})^{\Delta CP_{\text{ref (control-sample)}}}$$

The relative expression ratio of the target gene was computed, based on its real-time RT-PCR efficiencies (E) and the difference (Δ) of the crossing point (CP) of an unknown sample group versus a control group ($\Delta CP_{\text{ref (control-sample)}}$). In mathematical models the target gene was normalized by two non-regulated genes (housekeeping gene). Using REST-XL (Relative Expression Software Tool) the relative calculation procedure was based on the mean CP of the experimental groups, which compares two groups, sample group versus control group, and analyses the group differences for significances with a randomization test.

The relative expression ratio for VDAC1, VDAC2 and VDAC3 mRNA was calculated from oocytes of different follicle categories. Oocytes of group 1 (<3mm) were chosen as control, while group 2 (4-6mm) and group 3 (8-11mm) were compared to the former. All sample and control groups were normalized against the housekeeping genes H2A and U2snRNA.

The expression of the three VDAC subtypes did not show significant differences ($p > 0.05$) between the groups 1 and 2 (Figure 12). In the case of the group 3 compared with group 1,

only VDAC1 shows a tendency of down regulation by an approximated factor of 2.4 ($p=0.011$), where VDAC2 and 3 were not significantly different (Figure 12, $p>0.05$).

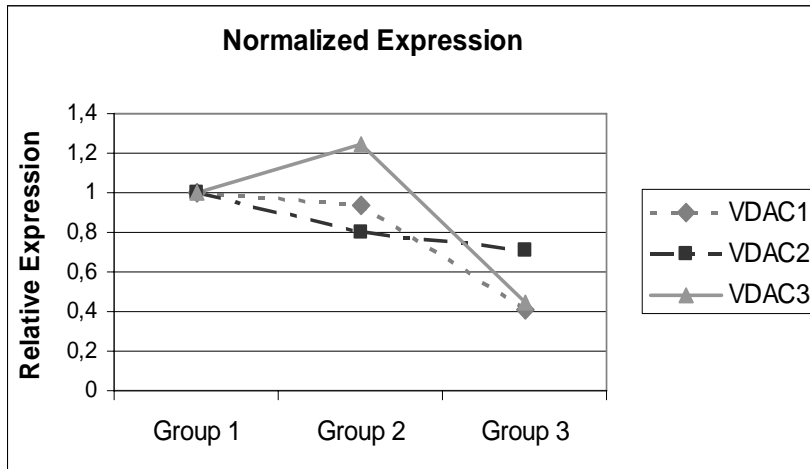


Figure 12: Expression of the three VDAC isoforms. Relative expression calculated with REST-XL for the three categories of follicles. The expression is normalized with the two housekeeping genes (H2A, U2snRNA) and is drawn in relation with the control group 1.

Monitoring the expression of the housekeeping genes (not normalized), shows a higher transcript level in the group 3. Assuming a stable expression of the housekeeping genes during folliculogenesis, this might result from increased total RNA level. Significant changes in total RNA abundance between group 1 and 3 were observed for all examined samples for U2snRNA (Figure 13, VDAC1 $p=0.002$, VDAC2 $p=0.001$ and VDAC3 $p<0.001$) and in one case for H2A (Figure 14, VDAC3 $p=0.001$). The tendency observed for VDAC1 and 2 ($p>0.05$) was not significant.

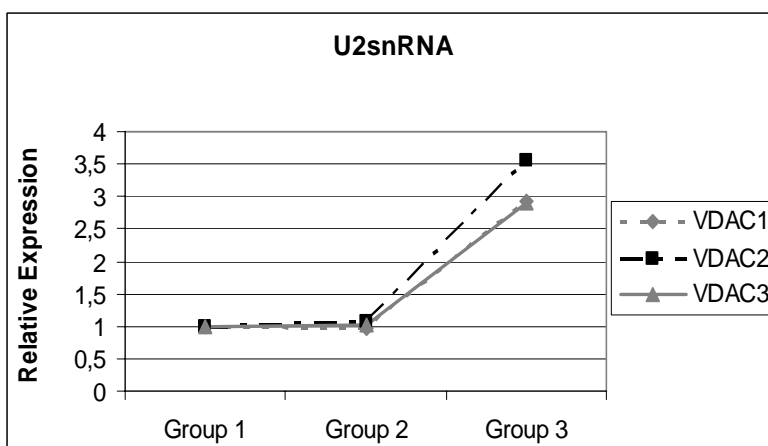


Figure 13: Not normalized expression of U2snRNA obtained during amplification experiments for each VDAC isoform. Relative expression calculated with REST-XL for the three categories of follicles. In the three cases significant differences were observed (VDAC1 $p=0.002$, VDAC2 $p=0.001$ and VDAC3 $p<0.001$).

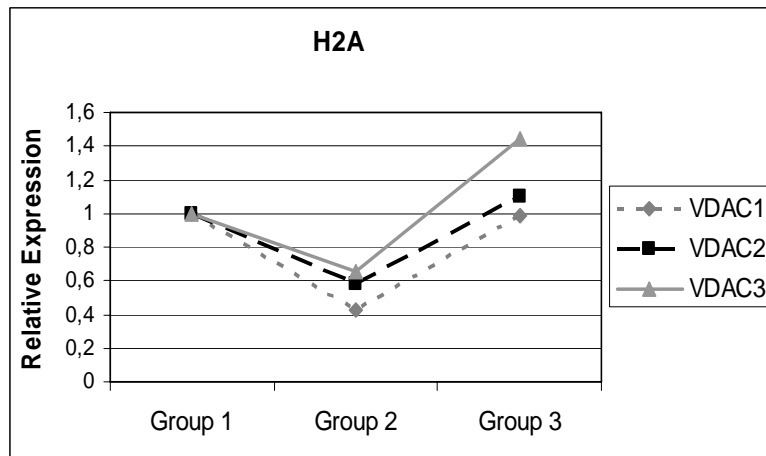


Figure 14: Not normalized expression of H2A obtained during amplification experiments for each VDAC isoform. Relative expression calculated with REST-XL for the three categories of follicles. In the experiment of VDAC3 a significant difference between group 1 and 3 was observed ($p=0.001$).

PCR efficiencies

All amplifications of VDAC isoforms had a typical sigmoid trend and exponential phase. The real-time RT-PCR efficiencies were calculated with LinRegPCR. The program acquires the efficiency for each sample individually by doing linear regression analysis out of the LightCycler raw data.

Table 4: PCR efficiency calculated with LinRegPCR.

	VDAC1	VDAC2	VDAC3	H2A	U2snRNA
Mean^a (n:27)	1.928	1.919	1.918	1.909	1.892
SD^b	0.0681	0.060	0.0559	0.0012	0.0172

^a Overall mean from all investigated samples from triplicates in three independent experiments

^b Standard deviation of the mean

The expression of VDAC mRNA seemed to be stable between three different follicle sizes excepting VDAC1. VDAC1 presented down-regulation behavior between group 1 and 3 of the follicles with a factor of the magnitude of 2.4.

3.2 Expression of VDAC protein isoform in porcine gametes

In order to identify the expression of VDAC proteins, immunobiochemical studies were performed. The expression was detected with the help of antibodies against different epitopes for VDAC1, VDAC2 and VDAC3 proteins. The characterization was carried out by:

(1) Western blot analysis and subsequent immunodetection in porcine oocytes and spermatozoa; (2) immunohistochemistry was conducted to compare VDAC protein expression during porcine folliculogenesis and (3) the subcellular distribution of VDAC protein was detected in porcine oocytes by confocal microscopy.

3.2.1 Protein expression analyses of VDAC in porcine gametes by immunoblotting

Solubilized proteins were subjected to one- and two dimensional electrophoresis. Detection was achieved by immunoblotting using anti-VDAC1, 2, 3 and a common antibody that recognizes the 3 isoforms of VDAC (Table 5). In previous studies, the specificity of the four different anti-VDAC antibodies were verified using immunoblots and recombinant VDAC proteins from the three different subtypes (Hinsch *et al.*, 2004).

Table 5: Used antibodies for immunodetection of VDAC proteins

Antibodies	Negative control	Dilution (in 3% skimmed milk powder/TTBS)
anti-VDAC1 (AS P6)	Preimmune serum (PI P6)	1:100
anti-VDAC2 (AS P45)	Preimmune serum (PI P45)	1:100
anti-VDAC3 (AS P31)	Preimmune serum (PI P31)	1:100
anti-VDAC _{common} (AS P _{common})	Preimmune serum (PI P _{common})	1:200
anti-VDAC1 (P31HL, Calbiochem)	IgG _{2a}	1:100
Second antibody protein A-HRP (Bio-Rad)		1:3000

3.2.1.1 Immunoblot detection of VDAC proteins from porcine spermatozoa

The study of VDAC proteins from porcine spermatozoa after 2% TX-100 extraction was effective as well as the protein purification through a hydroxyapatite-celite chromatography. Immunocharacterization of total protein extraction (2% TX-100), was performed by solubilization and loaded protein from approximately 25×10^6 spermatozoa/per lane. In the case of purified hydroxyapatite-celite product circa 165×10^6 spermatozoa/per lane were charged (Figure 15).

Characterization studies were performed to analyze each VDAC isoforms protein expression in porcine spermatozoa. As seen in Figure 15, total TX-100 protein extraction (I) and enriched

VDAC obtained through hydroxyapatite-celite chromatography (II) were compared. Total protein extractions showed a higher quantity of faint bands (I) than the purified samples (II). Anti-VDAC1 (AS P6) antibody clearly detected, for total extraction, two strong bands in the area above 50kDa (Figure 15, AS, panel A, lane I) and several slight immunoreactive bands at different molecular weights. In the case of the purified material an extremely weak immunoreactive band was observed at 30kDa (Figure 15, AS, panel A, lane II). Using anti-VDAC2 (AS P45) two strong bands were detected in both samples around 30-35kDa (Figure 15, AS, panel B, lane I and II) and extra bands were detected for the TX-100 total extraction. One strong immunoreactive band was detected at 50kDa range. In the case of anti-VDAC3 (AS P31) only in the TX-100 total sperm extraction were bands observed with 3 different molecular masses, approximately 15kDa, 30kDa and above 50kDa (Figure 15, AS, panel C, lane I).

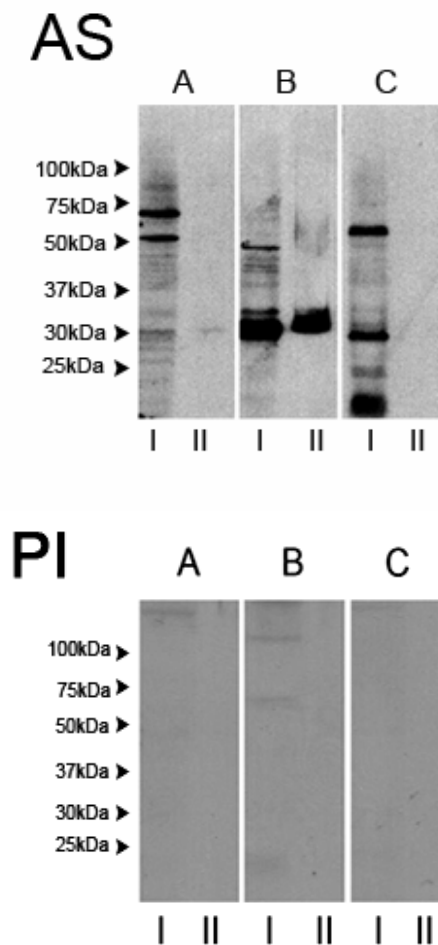


Figure 15: Immunoblotting of porcine spermatozoa protein and hydroxypapatite-celite purified fraction. Triton X-100 protein extract of porcine spermatozoa (25×10^6 spermatozoa/per lane, **I**) and hydroxypapatite-celite purification (165×10^6 spermatozoa/per lane, **II**). Proteins were separated by SDS-PAGE and transferred to nitrocellulose membranes. (**AS**) The blot **A** was incubated with antiserum AS P6 (panel A, 1:100), **B** was exposed to AS P45 (panel B, 1:100) and **C** to AS P31 (panel C, 1:100). (**PI**) The blot **A** was incubated with preimmune serum PI P6 (panel A, 1:100), **B** was exposed to preimmune serum PI P45 (panel B, 1:100) and **C** to PI P31 (panel C, 1:100). The bound antibody was detected with protein A-HRP (1:3000).

To avoid false positives which could result from unspecific binding of secondary antibodies to the target protein, negative controls were included. The second antibody did not exhibit positive reaction. The specificity of the reactions was also probed by using the correspondent preimmune serum (preimmune serum PI P6, PI P45 and PI P31) featuring negative response (Figure 15, PI). Successful antibody blocking was obtained with their respective synthetic peptides (15µg/ml, data not shown).

In summary immunoblotting indicates the presence of VDAC1, 2 and 3 proteins in porcine spermatozoa after 2% TX-100 extraction. In purified hydroxyapatite-celite samples VDAC1 and VDAC2 isoforms were revealed and no specific immunodetection was observed for VDAC3.

Porcine spermatozoa protein (total TX-100) was further studied by the help of 2D electrophoresis. Probes from approximately 87.5×10^6 spermatozoa per strip were subjected to 2D-electrophoresis. The first dimension was carried out using immobilized pH gradient (IPG, pH range 3-10, Bio-Rad). Proteins were then separated by SDS-PAGE on 12% acrylamide gels. In Figure 16 demonstrates the spot pattern of VDAC protein detected with anti-VDAC_{common} antibody (AS P_{common}).

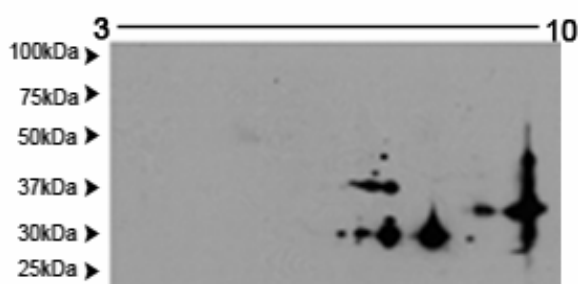


Figure 16: Characterization of porcine VDAC protein from spermatozoa by 2D-electrophoresis. Sperm homogenates (87.5×10^6 spermatozoa/per strip, 2% TX-100) were loaded in IPG strips pH range 3-10. Run in a 12% SDS-PAGE gel and transferred to nitrocellulose membranes. The immunoreactive spots were detected by anti-VDAC_{common} antibody (1:200) and protein A-HRP antibody (1:3000).

To further elucidate the distribution of VDAC protein isoforms and to avoid difficulties during MALDI-TOF MS due to the great quantity of spots, 2D gels were further studied with chromatography purified spermatozoa proteins were used.

One ml sample (ca. 165×10^6 spermatozoa), after chromatographic purification, was acetone precipitated and resuspended in 125µl rehydration 2D buffer. Two different pH intervals of

IPG strips were tested to find a suitable pH range that could improve the isoelectric focusing of all proteins of interest. The results observed for the hydroxyapatite-celite acquired material using pH strips with a 3-10 interval (Figure 17, blot A), showed a clear presence of 8 spots for AS P_{common}. They were distributed between pH 6-9. Five spots were gathered in a group with an approximately molecular mass of 30-35kDa. The immunoreactive spots were divided in two lines; the upper line indicated 2 spots with different intensity. The lower line presented 3 spots with increasing intensity from lower to higher pH. Extra spots were distributed through the membrane; two present in the same pH interval but with higher MW (>50kDa) and a third one was detected on the area of pH 8-9 and 30kDa. To improve the identity of the spot observed at the basic pH range of the 3-10 pH strips, immobilized strips gels with a pH 6-11 were tested (Figure 17 blot B incubated with AS P_{common}). The results displayed the two lines of spots previously observed and the case of the single spot observed in the 3-10 pH range (blot A), appeared as a row of 3 not well focused spots with an equal intensity and similar molecular weight (Figure 17, blot B).

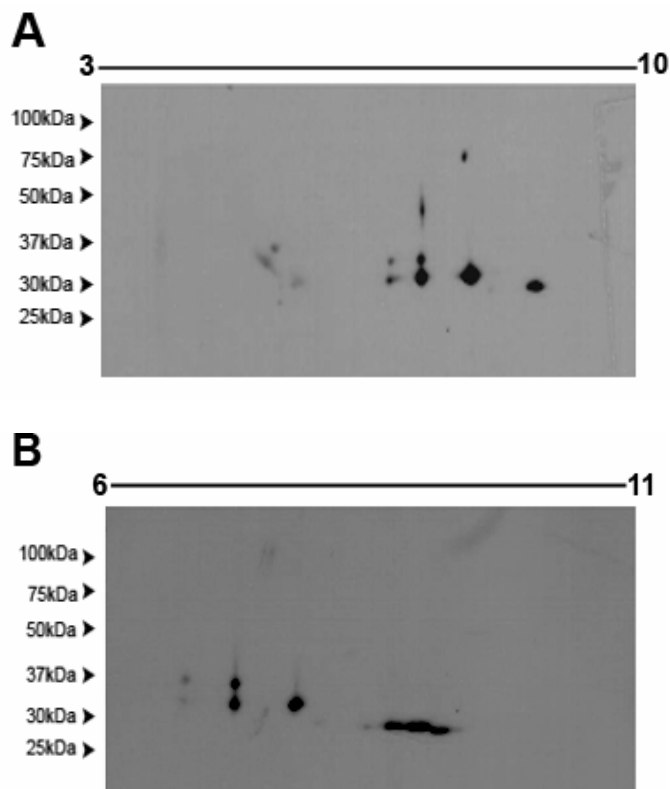


Figure 17: Electrophoretic and immunoblot analysis of porcine spermatozoa protein samples after hydroxyapatite-celite chromatography (165×10^6 spermatozoa/per strip). Enriched VDAC material was loaded in IPG strips pH 3-10 (blot A) and pH 6-11 (blot B) run in a 12% SDS-PAGE gel and transferred to nitrocellulose membranes. Blot A and B were tested with anti-VDAC_{common} antibody (AS P_{common}, 1:200) and detected by protein A-HRP antibody (1:3000).

The observed spots were further analyzed by immunoblotting experiments with the specific isoform antibodies. The results observed in Figure 18 (blot A) corresponded to the anti-

VDAC1 antibody (AS P6). A single spot was detected in 30-32kDa range with the polyclonal (AS P6) and monoclonal (P31HL, Calbiochem) antibodies.

In the case of anti-VDAC2 antibody (AS P45), 5 immunoreactive spots were observed in two different MW ranges, following the previously observed pattern of anti-VDAC AS P_{common} antibody observed in the Figure 17. Due to the great intensity and protein quantity the spots seemed not to be well focused causing extra artifacts (Figure 18, blot B). The results of the third isoform antibody (AS P31) presented a faint line in the 30kDa area (Figure 18, blot C arrow) similar to the anti-VDAC_{common} antibody (Figure 17, blot B).

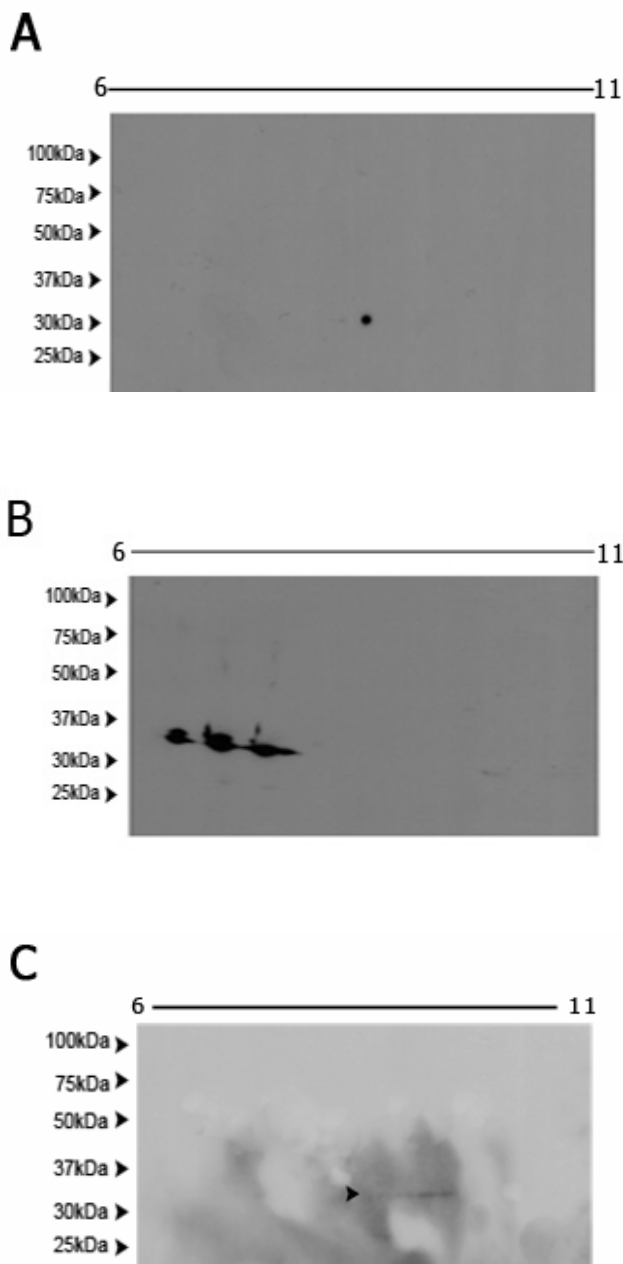


Figure 18: Electrophoretic and immunoblot analysis of porcine spermatozoa protein samples after hydroxyapatite-celite chromatography (165×10^6 spermatozoa/per strip). Enriched VDAC material was loaded in IPG strips pH 6-11. Second dimension was run in 12% SDS-PAGE gel and transferred to nitrocellulose membranes. Blot **A** was tested with anti-VDAC1 antibody (AS P6, 1:100). Blot **B** was incubated with anti-VDAC2 antibody (AS P45, 1:100) and blot **C** with anti-VDAC3 antibody (AS P31, 1:100). The specific binding was detected by protein A-HRP antibody (1:3000).

In summary, with the help of 2D-electrophoresis and specific antibodies, VDAC1, 2 and 3 could be detected in proteins extracted from porcine spermatozoa and purified by hydroxyapatite-celite chromatography. In the three cases the negative controls (preimmune serum PI P6, PI P45 and PI P31) displayed no specific immunoreaction (data not shown).

3.2.1.2 Immunoblot detection of VDAC proteins from porcine oocytes

Solubilized proteins from 300 porcine oocytes (per lane) were separated in 12% SDS-PAGE gels under reducing conditions. The separated oocyte proteins from GV and MII stage oocytes were transferred to nitrocellulose membranes and immunoanalysed with anti-VDAC antibodies (Table 5, Figure 19).

GV stage oocytes (Figure 19, panel A) with anti-VDAC1 (AS P6; panel A, lane I) detected an approximately 32kDa protein. Meanwhile, anti-VDAC2 immunodetection (AS P45; panel A, lane II) presented a reactive band of 30kDa and a slightly positive one in the 50kDa area. In contrast anti-VDAC3 did not show specific reactivity (AS P31; panel A, lane III).

II stage oocytes blots (Figure 19, panel B) displayed specific binding at approximately 32kDa for anti-VDAC1 (AS P6, panel B, lane I) similar to GV stage oocytes (panel A, lane I). In the case of anti-VDAC2 (AS P45) a strong immunoreaction was detected at the molecular mass range of 50-55kDa (panel B, lane II). The blot with anti-VDAC3 (AS P31) showed no immunoreacted band (panel B, lane III).

Negative controls were included in GV and MII stage oocytes blots to avoid false positives. The specificity of the reactions was probed by the appropriate preimmune serum, in the three cases the negative controls (preimmune serum PI P6, PI P45 and PI P31) displayed no specific immunoreaction (Figure 19, panel C, sample for MII stage oocytes) and also by blocking the antibodies with their respective synthetic peptides (15µg/ml; data not shown).

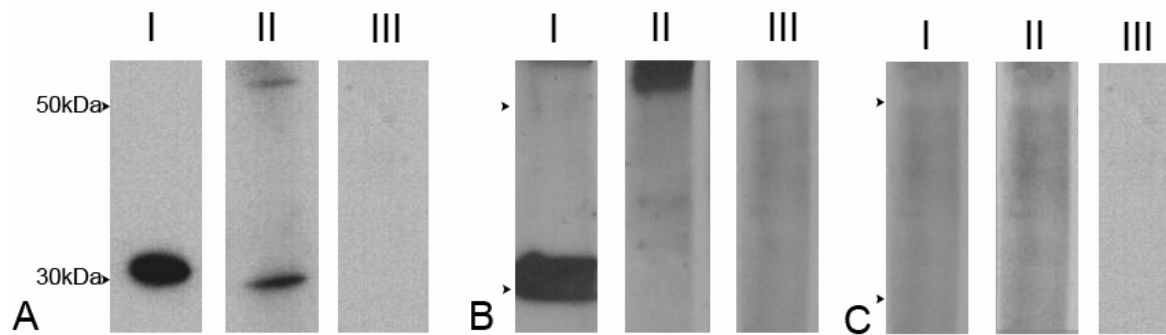


Figure 19: Detection of VDAC isoforms in porcine GV (panel **A**) and MII (panel **B**) stage oocytes. Proteins of 300 oocytes per lane were analyzed by 12% SDS-PAGE and transferred to nitrocellulose membrane. The membrane in lane **I** was incubated with anti-VDAC1 (AS P6, 1:100). Lane **II** was immunoprobed with anti-VDAC2 (AS P45, 1:100) and lane **III** with anti-VDAC3 (AS P31, 1:100). Negative control, sample for MII stage oocytes (Panel **C**), lane **I** preimmune serum for VDAC1, PI P6 (1:100); lane **II** for VDAC2, PI P45 (1:100) and lane **III** for VDAC3, PI P31 (1:100). Bound antibody was detected with protein A-HRP followed by detection with an ECL system.

Briefly, based on the results of the experiments, VDAC1 and VDAC2 protein expression could be confirmed by immunoblot with protein extracts derived from GV and MII stage oocytes. The blots suggested the presence of VDAC1 with a steady immunoreaction at 32kDa for oocytes of both maturation stages. In contrast, between GV and MII stage oocytes, a shift on the MW was observed in the reactivity of AS P45 (anti-VDAC2). The anti-VDAC3 (AS P31) antisera showed no positive reaction in both samples (GV/MII).

3.2.2 Protein identification by MALDI-TOF MS

A second step was conducted to confirm the results after immunoblotting of porcine material. Following the results obtained from the immunoblotting experiments with the specific anti-VDAC antibodies immunoreactive spots and band pattern were excised. Preparative gels stained with simply blue (Coomassie staining, Invitrogen) or silver stained (SilverQuest, Invitrogen) were used to detect the material of interest and sent for protein sequence (ChromaTec). The peptide fragments were analyzed by MALDI-TOF MS followed by database searching (Mascot). The Mascot database normally used a MOWSE score, which represents the quality of the obtained peptide mass fingerprint (PMF) and the peptide

sequence described in the databank. For each search a significant limit in form of MOWSE score is given for successful protein identification.

In Figure 20 a one-dimensional 12% polyacrylamide gel with spermatozoa protein extracts (165×10^6 spermatozoa/per lane) from porcine after chromatography procedure is observed. The purified proteins gave two bands with Coomassie staining (Figure 20). After Mascot search the band labeled as I (Figure 20), was detected as VDAC2 (*Sus scrofa*) with a MOWSE score of 132 and 32kDa of mass (significant $p < 0.05$). The second band tagged as II (Figure 20) was characterized as VDAC3 (*Sus scrofa*) with a MOWSE score of 165 and a mass of 30kDa (significant $p < 0.05$).

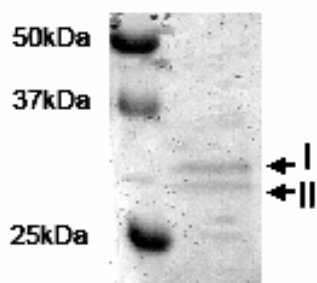


Figure 20: SDS-PAGE of hydroxyapatite-celite purified porcine spermatozoa proteins. Chromatographically purified proteins from 165×10^6 spermatozoa/per lane were visualized by Coomassie Blue staining after SDS-PAGE separation on a 12% polyacrylamide gel. The two indicated bands (arrows) were excised for MALDI-TOF MS analyses. After peptide mass fingerprinting **I** represents VDAC2 (*Sus scrofa*) and **II** VDAC3 (*Sus scrofa*).

Chromatography-purified samples (ca. 495×10^6 spermatozoa/per strip) were run in 2D-SDS PAGE in IPG strips (pH 6-11) silver stained and analyzed by MALDI-TOF MS (Figure 21). The obtained results were summarized in Table 6. In the case of spots 6 and 7 no clear results were obtained.

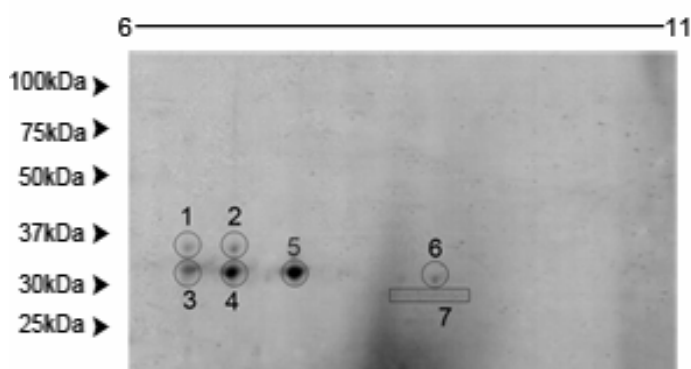


Figure 21: Electrophoretic analysis of porcine spermatozoa protein samples after hydroxyapatite-celite chromatography (495×10^6 spermatozoa/ per strip). Enriched VDAC material was loaded in IPG strips (pH 6-11). Silver staining was performed after SDS-PAGE separation on a 12% polyacrylamide gel. The indicated spots (numbers) were excised for MALDI-TOF MS analyses. Results from peptide mass fingerprinting were summarized in Table 6.

Table 6: Results from the MALDI-TOF MS and Mascot search analysis of hydroxyapatite-celite purified proteins from porcine spermatozoa.

Spot	Protein	Coverage (%)	Mass (Da)	pI	Acc.n° (SWISS-PROT)	Ms ^a	Peptides matched
1	VDAC2_PIG	42	31573	7.49	Q9MZ15	103	11
2	VDAC2_PIG	44	31573	7.49	Q9MZ15	103	11
3	VDAC2_PIG	42	31573	7.49	Q9MZ15	103	11
4	VDAC2_PIG	53	31573	7.49	Q9MZ15	164	15
5	VDAC2_PIG	44	31573	7.49	Q9MZ15	89	14
6	VDAC1_PIG	4	30596	8.6	Q9MZ16	N/S	1
7	VDAC3_PIG	7	30578	8.9	Q9Y277	N/S	2

^a MOWSE scores were determined using the search engine Mascot. This program uses a probability-based

MOWSE scoring program to determine significant peptide matches. Scores are reported as $-10 \cdot \log(P)$, where P is the probability that the observed match is a random event. Protein scores greater than 59 are considered significant ($p < 0.05$).

N/S Protein scores lower than 59 consider not significant

In the case of oocytes the solubilization and purification procedure was adapted from the classic isolation method developed for mammalian VDAC protein (De Pinto *et al.*, 1987a). 3300 porcine GV stage oocytes were resuspended in 1ml 2% Triton X-100 extraction buffer (150mM NaCl; 50mM Tris-HCl, pH 7.4; 2mM DTT; 1mM EDTA; 10mM benzamidine; 0.2mM PMSF). The suspension was incubated for 90min at 4°C and finally centrifuged at 13800xg for 15min. The supernatant (sample A) was stored at -20°C until use. A second extraction (sample B) was performed from the pellet first obtained and following the previous steps including disruption of the cells with a micropestle (Eppendorf). The one ml suspension was incubated for 90min at 4°C and centrifuged at 13800xg for 45min; finally the supernatant was stored at -20°C. The two obtained 2% Triton X-100 supernatants extracts (sample A and B) from 3300 oocytes were separately applied to two dry hydroxyapatite-celite (2:1) columns (De Pinto *et al.*, 1987a) and eluted with 2% Triton X-100 extraction buffer. Two elution fractions of 1ml were collected for each sample (elution I and II). Thereafter, 900μl plus 100μl water from each fraction was precipitated with 9ml of cold acetone. The acetone-

sample mixture was left to settle for 30min at -20°C to improve precipitation and then was centrifuged at 6000xg at 4°C for 30min.

The protein enriched pellets were resuspended in 20µl laemmli buffer. SDS-PAGE was performed as previously described and gels were stained with SilverQuest Staining Kit (Invitrogen). In the first extraction procedure (sample A) no protein was observed, neither in the first fraction (elution I) nor the second elution (elution II) after purification (Figure 22, lane A/II). The second extraction (sample B) step gave satisfactory results showing in the first elution a faint band (data not shown) meanwhile a higher amount of protein was observed in the second fraction of elution (Figure 22, lane B/II). The labeled band displayed the known pattern for VDAC and MALDI-TOF MS followed by PMF analyses classified the band as VDAC2 (*Sus scrofa*) Mass 31573Da; $p < 0.05$, this indicated identity or extensive homology.

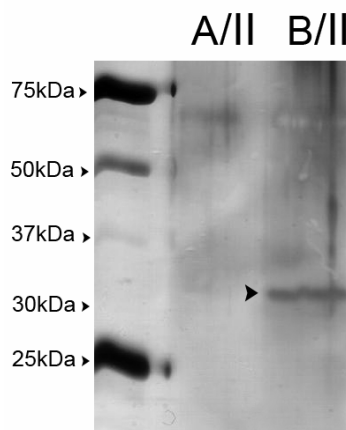


Figure 22: Protein extraction and hydroxyapatite-celite purification of 3300 GV stage porcine oocytes. Proteins were isolated in two steps (A and B) and purified with two elutions. Proteins from second elution (II) from sample A and B were separated in 12% SDS-PAGE and silver stained. First sample, second elution (lane A/II) did not present stained bands. The second elution obtained from the second sample (lane B/II), presented a single stained band (arrow). Mascot MS/MS ion search identified the tagged band (arrow, B/II) as VDAC2 (*Sus scrofa*).

MALDI-TOF MS and peptide fingerprinting analyses confirmed the presence of VDAC2 and VDAC3 protein in one-dimension electrophoresis of purified porcine spermatozoa protein. Meanwhile investigation of 2D-gels proved the protein expression of only VDAC2 protein, and only indications of VDAC1 and 3 were observed. MALDI-TOF MS analyses of porcine GV stage oocytes consolidated the expression of VDAC2 protein.

3.2.3 Immunohistochemical detection of VDAC protein in porcine ovaries

During porcine ovarian follicle maturation, the localization of VDAC subtypes was examined using specific subtype antibodies. Tissue sections of Methacarn fix ovaries, embedded in

paraffin were incubated with the primary antibodies (Table 7) and the detection of the specifically bound antibody was performed by a biotin labeled second antibody followed by AEC system. All experiments were carried out in serial cuts and repeated three times for confirmation.

Table 7: Working dilutions of the antibodies used for immunohistochemistry

Antibodies	Negative control	Dilution (in 1% skimmed milk powder/PBS)
anti-VDAC1 (AS P6)	Preimmune serum (PI P6)	1:30
anti-VDAC2 (AS P45)	Preimmune serum (PI P45)	1:30
anti-VDAC3 (AS P31)	Preimmune serum (PI P31)	1:30
anti-VDAC1 (P31HL, Calbiochem)	IgG _{2a}	1:50
Second antibody anti-rabbit (Sigma)		1:500
Second antibody anti-mouse (Sigma)		1:200

VDAC1 (AS P6 and P31HL) protein localization in porcine follicles did not vary according to the stage of folliculogenesis as observed in Figure 23 (A-A2). Primordial (PF, A1) and primary follicles (not observed on the selected slide) displayed immunoreactivity in the ooplasm as well as in the surrounding follicle cell layers. The ooplasm of primary and primordial oocytes was clearly above the background, with a large counterstained blue nucleus. The surrounded squamous and cuboidal follicular cells from the primordial and primary follicles, respectively, were positive labeled despite the scarce cytoplasmic area (Figure 23; Fc, A1). For later preantral developmental stages a positive reaction remained to be detected in all the regions. In secondary follicles (Figure 23; SF, A1) VDAC1 labeled the oocyte ooplasm and the granulosa and theca cells. Additionally, in tertiary follicles (Figure 23; TF, A2), color development was detected within the surrounding granulosa and theca cells and in the ooplasm of the growing oocyte. In the surrounding tissue, no specific detection was observed.

Without exception, VDAC2 protein (AS P45; Figure 23, B-B2) was found in ooplasm and follicle cells (granulosa and theca cells) independent of the developmental stage. A faint but definitive staining was observed in primary (not observed on the selected slide) and primordial follicles (Figure 23, B1). The staining was also visualized as a distinct light color in secondary (Figure 23, B1) and tertiary follicles (Figure 23, B2).

Sections treated with the preimmune serum (PI P6 and PI P45) and IgG_{2a} did not display any specific color development (sample for PI P6, C-C2).

No specific results were achieved for the localization of VDAC3 protein (AS P31) in ovary tissue (data not shown). Two different antibodies originated from diverse peptides were tested as well as protein A purified anti-VDAC3 antibody. Color deposition was observed within the ooplasm and in scattered follicle cells incubating with the antibody or the respective negative controls (preimmune serum and peptide blocking of the antibody).

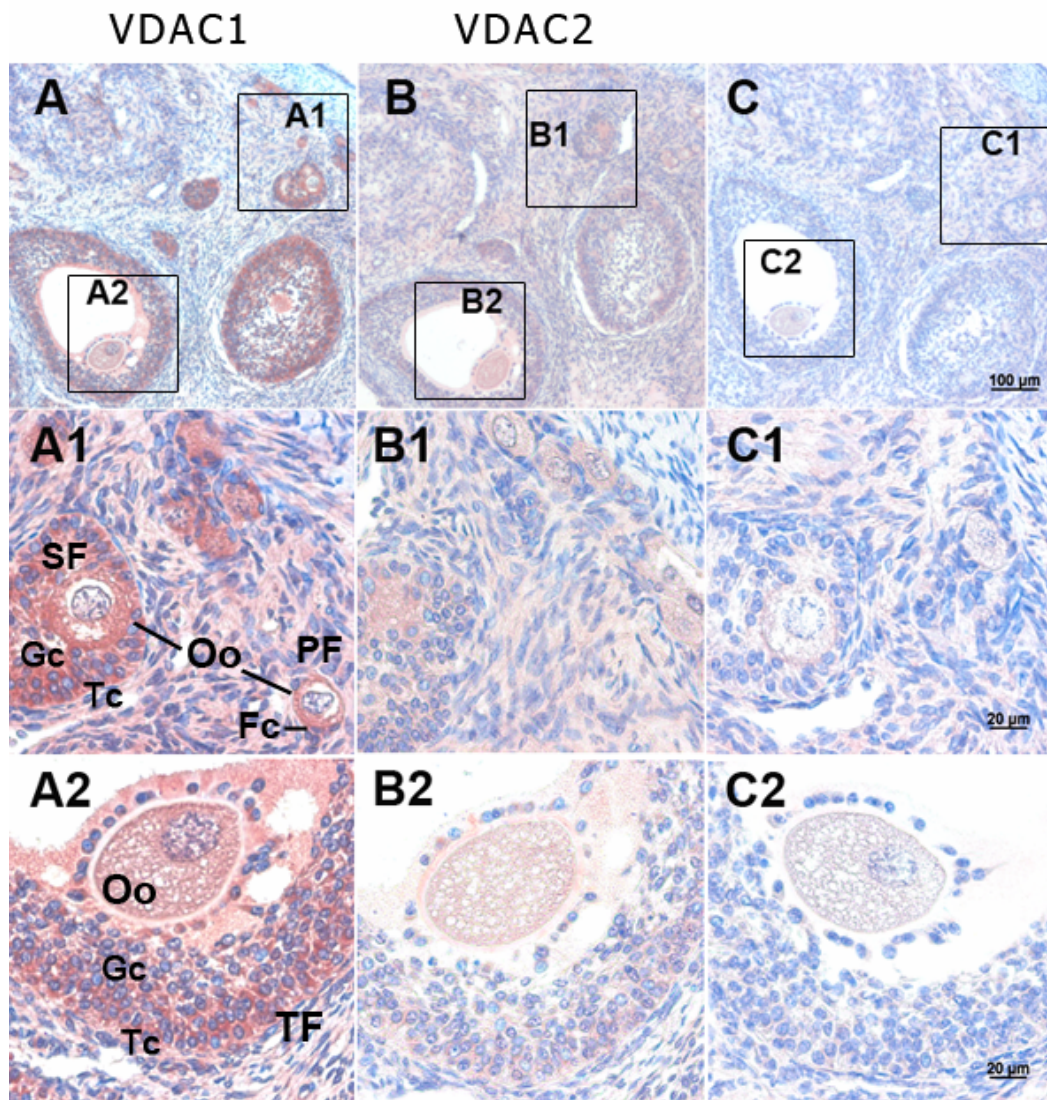


Figure 23: Immunohistochemical localization of VDAC1 and VDAC2 proteins in the porcine ovaries. Methacarn-fixed and paraffin embedded sections were incubated with antisera AS P6 (A, A1-A2; 1:30 dilution) and AS P45 (B, B1-B2; 1:30 dilution). Control sections were treated with preimmune serum, sample for PI P6 (C, C1-C3; 1:30 dilution). Binding of antibodies was visualized using streptavidin-peroxidase AEC method. PF= primordial follicle SF= secondary follicle; TF= tertiary follicle; Oo= oocytes; Fc= follicle cells; Tc=theca cells; Gc=granulosa cells. Bar: A-C 100μm; A1-C2 20μm

The results of the antibodies AS P6, P31HL and AS P45 in porcine ovary tissue indicated the presence of VDAC1 and VDAC2 protein in the ooplasm of oocytes and in surrounding cells of porcine follicles with no explicit variation according to the stage of folliculogenesis.

3.2.4 *Subcellular localization of VDAC proteins in porcine oocytes by confocal microscopy*

Subcellular localization of VDAC protein subtypes was researched in porcine oocytes using anti-VDAC specific antibodies (Table 8). The samples were examined using a laser scanning confocal microscope.

Table 8: Working dilutions of the experimental antibodies used for confocal microscopy

Antibodies	Negative control	Dilution (in 1% skimmed milk powder/PBS)
anti-VDAC1 (AS P6)	Preimmune serum (PI P6)	1:80
anti-VDAC2 (AS P45)	Preimmune serum (PI P45)	1:40
anti-VDAC3 (AS P31)	Preimmune serum (PI P31)	1:40
anti-VDAC1 (P31HL, Calbiochem)	IgG _{2a}	1:30
anti-VDAC2 (Santa Cruz)	goat IgG	1:5/1:10
Second antibody anti-rabbit IgG:FITC (Sigma)		1:60
Second antibody anti-mouse IgG: FITC (Sigma)		1:100
Second antibody anti-goat IgG: FITC (Santa Cruz)		1:25

As initial attempt, porcine oocytes were manipulated as shown in earlier published data obtained by Steinacker *et al.* in *Xenopus laevis* oocytes (Steinacker *et al.*, 2000). In Figure 24 GV stage oocytes were prepared omitting the permeabilization step, in order to observe a possible binding of VDAC1 antibodies in the plasma membrane. Anti-VDAC1 (AS P6, 1:20) and monoclonal anti-human type 1 VDAC antibodies (P31HL, Calbiochem, 1:4) were incubated followed by FITC conjugated second antibodies (anti-rabbit 1:20, and anti-mouse 1:8 respectively). Both antibodies showed a dense dot-wise arrangement of fluorescent labeling over the whole oocyte surface (Figure 24, A and B). In the case of the polyclonal antibody (AS P6) unspecific binding was observed around the zona pellucida (Figure 24 A, arrow indicates zona pellucida), but it did not present a barrier to the antibody, showing the

same results as P31HL (Figure 24, B). No distinct labeling was observed in control oocytes, which were treated only with the second antibody and with the respective preimmune serum or IgG (Figure 24, C; sample for IgG_{2a}).

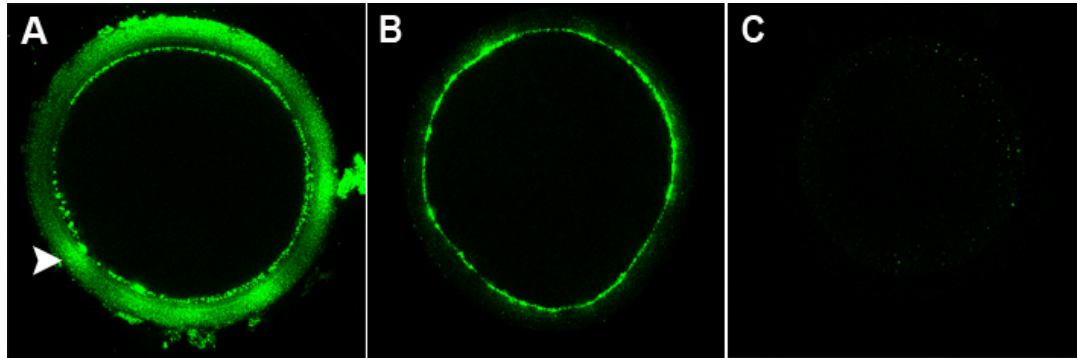


Figure 24: Confocal laser microscopy images of immature porcine oocytes in the equatorial plane without permeabilization step. Oocytes were incubated with anti-VDAC1 antibodies. **A:** AS P6 (1:20) and **B:** P31HL (1:4) and revealed by FITC-labeled second antibody. Zona pellucida non-specifically stained (A, arrow). **C:** sample for negative control, oocyte exposed to IgG_{2a}. Original magnification X600.

Subcellular localization of VDAC protein isoforms was detected in permeabilized, ZP- intact porcine oocytes. Paraformaldehyde fixed oocytes (GV and MII stage) were handled with anti-VDAC antibodies (Table 8). Oocytes were completely scanned and photographed in three planes; however, only the equatorial plane data was included since it gave the most descriptive information. As seen for GV stage oocytes in Figure 25, AS P6 (A) and AS P31 (E) present a dense specific reaction around the cortical area. In contrast AS P45 showed no specific reaction giving a high unspecific background in the negative controls (data not shown). To overcome the unspecific reaction of anti-VDAC2 antibody different approaches were carried out, including protein-A purification, peptide blocking and several blocking solutions. However, no validated results were obtained. In this case a commercially available VDAC2 polyclonal antibody was tested (Santa Cruz), revealing specific immunoreaction (Figure 25, C). The staining was not consistent between oocytes and in contrast to VDAC1 and VDAC3 the localization was observed as variable spherical clusters, not evenly distributed through the cortical area (details observed in Figure 26).

Oocytes stained using control preimmune serum and no immune IgG exhibited no staining (Figure 25; B, D and F).

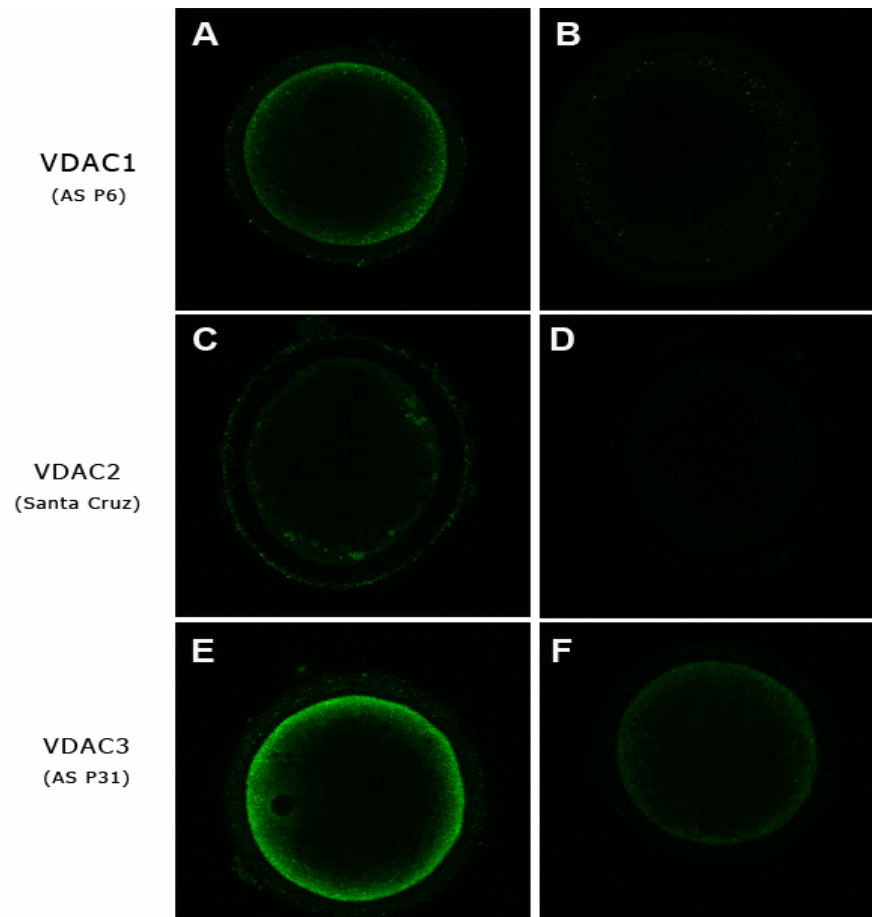


Figure 25: Subcellular immunolocalization of VDAC protein isoforms in porcine GV stage oocytes. Indirect immunofluorescence and confocal microscopy of paraformaldehyde fixed oocytes was performed. Cells were treated with **A:** AS P6 (1:80), **C:** anti-VDAC2 (Santa Cruz; 1:5) and **E:** AS P31 (1:40). Control experiments were performed with **B:** PI P6 (1:80), **D:** goat IgG (Santa Cruz; 1:10) and **F:** PI P31 (1:40). Bound antibodies were detected with FITC labeled second antibodies. Original magnification X600.

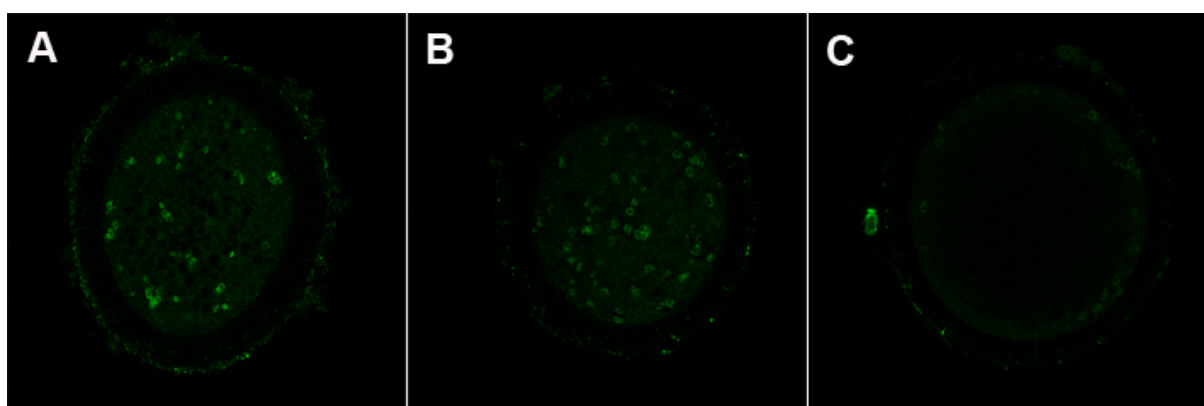


Figure 26: Exemplary detail immunofluorescence pattern of bound anti-VDAC2 antibody to porcine GV stage oocyte. Indirect immunofluorescence and confocal microscopy was performed. The oocyte was treated with anti-VDAC2 antibody (Santa Cruz, 1:5). Bound antibody was detected with second antibody anti-goat IgG: FITC (Santa Cruz, 1:25). (**A/B**) two different plains from a cortical image of the same oocyte (**C**) equatorial image. Original magnification X600.

Similar results were achieved with *in vitro* mature oocytes. Metaphase II oocytes incubated with anti-VDAC1 (AS P6) and anti-VDAC3 (AS P31) antibodies revealed the presence of a punctual pattern in the cortical area as previously observed (data not shown). In the case of anti-VDAC2 antibody (Santa Cruz) no positive immunoreaction was observed (data not shown).

Consequently, based on the results, VDAC1 and VDAC3 isoforms were constantly detected in GV and MII stage porcine oocytes. In the case of VDAC2, a specific spherical distribution was observed in a fraction of GV stage oocytes which lately disappeared in mature oocytes.

3.3 Functional studies

3.3.1 *Lipid bilayer experiments with purified VDAC protein from porcine spermatozoa*

The functional characterization of the samples obtained from porcine spermatozoa after hydroxyapatite-celite chromatography (referred as purified or enriched VDAC) was assayed by incorporation into planar bilayer. The electrophysiological properties of the enriched VDAC isoforms (consisting of VDAC1, 2 and 3 by immunoblot and MALDI-TOF MS results) were studied into artificial membranes made from diphytanoyl-phosphatidylcholine and compared with previously known data.

VDAC like channel activity was observed by adding purified protein from porcine spermatozoa into the artificial membranes. Results were specific for the addition of the purified VDAC; there were no channel formations upon the sole addition of the buffer. Single channel experiments performed with purified VDAC protein in 1M KCl showed current increases in discrete steps with a predominant single channel conductance of 1.6nS (Figure 27).

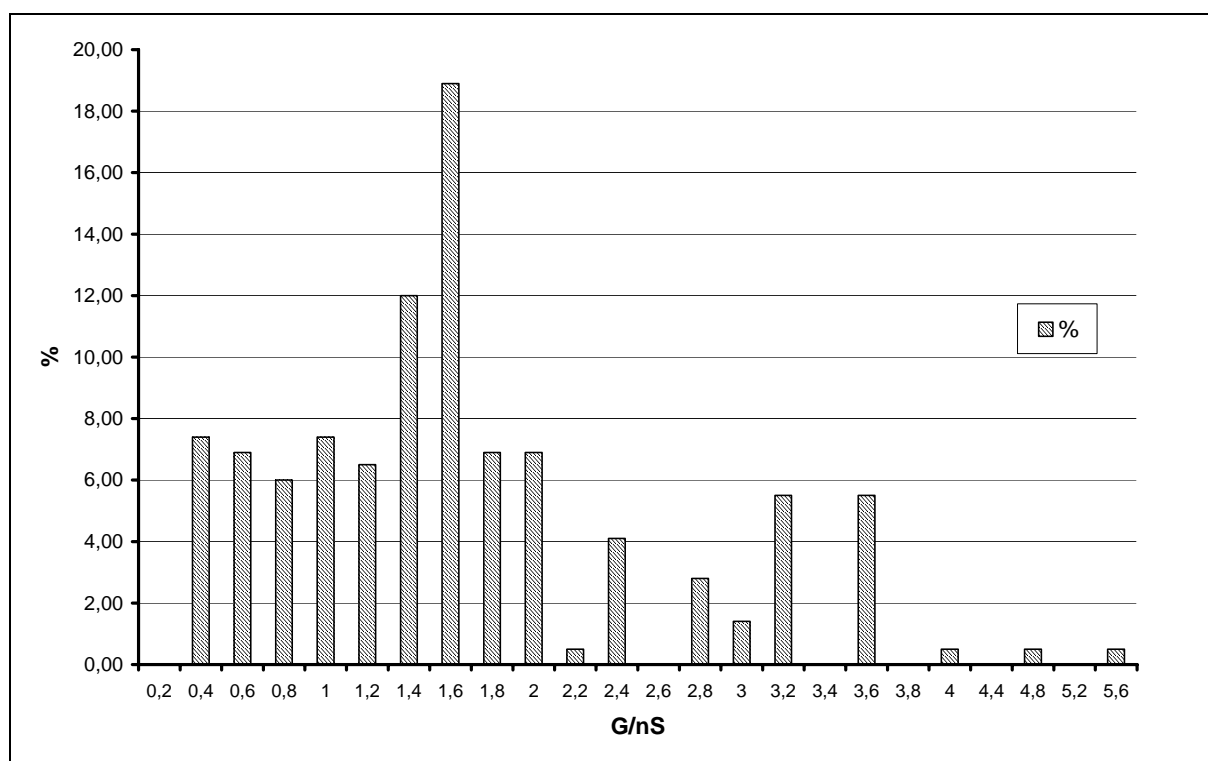


Figure 27: Histogram of the probability for the occurrence of a given conductivity unit observed with membranes formed of diphytanoylphosphatidylcholine/n-decane in the presence of purified porcine VDAC protein. In the y axis is the percentage (%) of transition events with a given conductance increment observed in the single channel experiments, the x axis is G/nS. The calculus was made by dividing the number of transitions with a given conductance increment by the total number of conductance transitions. The aqueous phase contained 1M KCl and the applied voltage was 10mV at 20°C.

In the next step the voltage dependence of the purified VDAC was analyzed. Voltage dependence is a typical feature of VDAC channels (Benz, 1994). The experiments were performed setting different potentials ranging from 10 to 100mV, while membrane currents were monitored. Immediately after application of the voltage, the current was a linear function of the applied membrane potential. Starting with 30mV, the membrane current decreased in an exponential way for both positive and negative potentials. The observed results were summarized in the Figure 28. The figure displays the relative conductance G/G_o as a function of the applied voltage (V_m). The plot demonstrates a symmetrical response of the purified VDAC to the applied voltages.

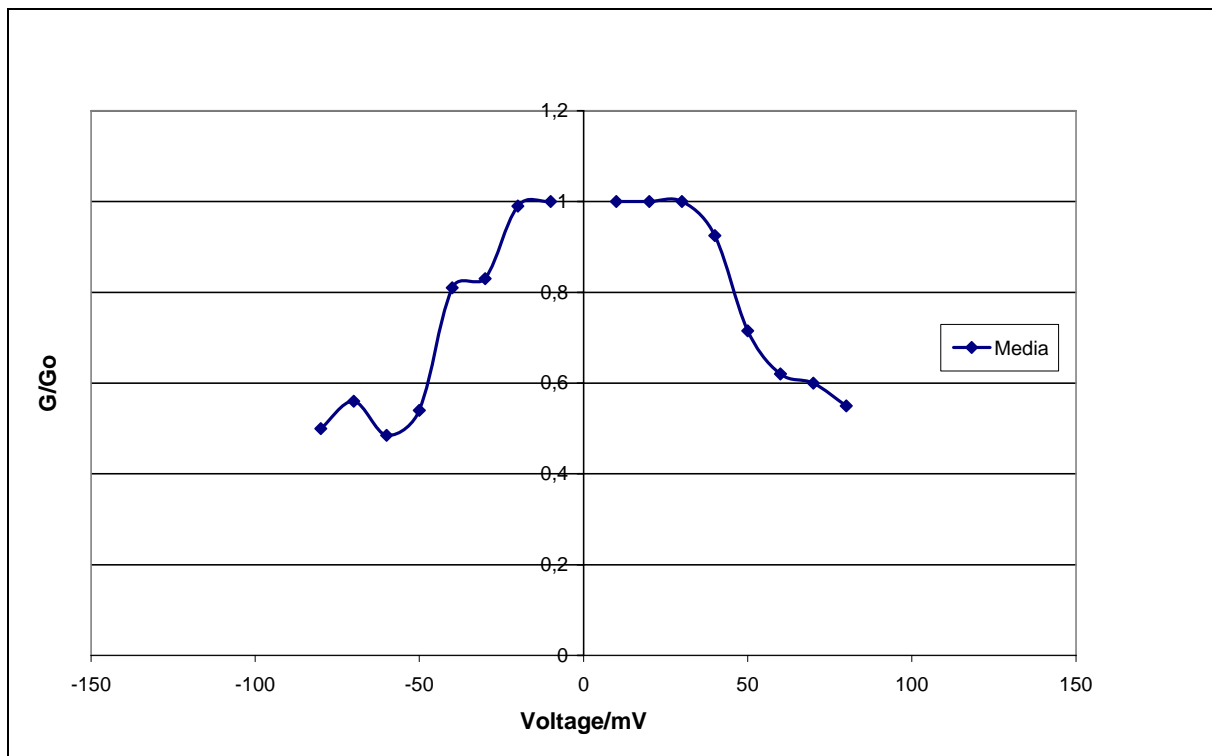


Figure 28: Bell-shaped curve for voltage dependence G/G_0 of purified VDAC. Voltage dependence G/G_0 was a function of the applied voltage (V_m).

Briefly, functional experiments indicate that purified VDAC from porcine spermatozoa was successfully renatured showing voltage dependence activities and single conductance channel of 1.6nS.

3.3.2 *Treatment of mature porcine oocytes with purified VDAC protein from porcine spermatozoa*

To investigate a possible role of spermatozoa VDAC protein on oocyte activation, MII stage oocytes were microinjected or incubated with enriched VDAC protein obtained from porcine spermatozoa after hydroxyapatite-celite chromatography. Evaluation of activation was performed after 24h post-manipulation by aceto-orcein staining and checked for the presence of one or more pronuclei. Oocytes with pronuclei were considered activated.

a) Microinjection of purified VDAC protein

The functionality of spermatozoa VDAC in oocyte activation was assayed by microinjection of purified VDAC protein. Samples were prepared by protein extraction from porcine

spermatozoa and a hydroxyapatite-celite chromatographic purification. The purified sample was acetone precipitated and resuspended in PBS (1mg/ml). Ten μ l aliquots were stored at -20°C until microinjection procedure. Oocytes were matured *in vitro* for 48h, microinjected and assessed for activation after an additional 24h of incubation. In experiments designed to monitor the activation mediated by the microinjection procedure itself, oocytes were either injected with buffers used to elute and extract the spermatozoa protein or pierced with an injection capillary.

Microinjection of VDAC purified samples resulted in activation rates of 12.25%, without a significant difference when compared to controls 1.54-5.4% (Table 9). Randomly, treated and controlled oocytes exhibited a pronucleus-like structure (data not shown). However, the variation among the results was not significantly greater than expected by chance ($p=0.26$). The rate of maturation was between 80-90%.

Table 9: Porcine MII stage oocytes injected with hydroxyapatite-celite purified spermatozoa protein lyophilized and resuspended in PBS. Oocytes were incubated for 24h and then activation was assessed.

Treatment	n ^a	% of oocytes activated *
VDAC purified sample in PBS	48	12.25±14 ^b
Buffer in PBS (control)	35	5.4±8 ^b
Mechanical manipulation (control)	34	1.54±3.4 ^b

Values are expressed as percentage (mean±SD) of 5 independent experiments.

^a Number of oocytes

^{b-c} Values with different superscripts within the column are significantly different ($P<0.05$)

*% of activated oocytes= No. of oocytes activated/ No. of oocytes examined.

b) Incubation of purified VDAC protein

To evaluate if the lack of activation observed after VDAC microinjection was due to the selected procedure, mature oocytes were incubated with purified VDAC protein resuspended in DMSO and diluted in medium. Purified VDAC was dissolved 0.0025 μ g/500 μ l and 0.025 μ g/500 μ l in medium and equilibrated for at least 2h in a humidified atmosphere. Groups of oocytes were exposed in both concentrations for 15-30-60-120-180 and 360min, then rinsed in medium and further incubated for 24h until activation assessment. Oocytes of both tested concentrations, after 30min of incubation, presented lysed or deformed morphology. According to the observed results, incubation time was decreased to 3-6 and 9min (0.0025 μ g/500 μ l). Following incubation, oocytes were washed and cultured for 24h, finally

activation was assessed. The effects of VDAC/DMSO and the control buffer/DMSO diluted in medium were identical. Activation of oocytes was not observed in buffer/DMSO treated oocytes or VDAC/DMSO treated oocytes. Between 80-90% of oocytes had reached metaphase MII stage and none showed pronucleus structures.

To assess a possible block of the functionality of VDAC samples during the acetone precipitation, oocytes were exposed to purified VDAC samples diluted directly in medium. Three different dilutions were examined (1:10, 1:100 and 1:1000) and processed as previously described for VDAC/DMSO experiments. Oocytes were exposed for 5min, washed and incubated for 24h. Manipulated oocytes were evaluated within 30min post-incubation, and observed for deformed or lysed oocytes. The results observed during these treatments were comparable to the long exposure treatment of VDAC/DMSO. Oocytes showed characteristics of degeneration such as ooplasm shrinking, membrane disruption or great presence of granules. Control and VDAC treated oocytes displayed similar effects as previously described. In conclusion, it was not possible to assay maturation or activation status of oocytes treated with purified VDAC protein from porcine spermatozoa.

3.3.3 *Calcium oscillation measurements after microinjection of purified VDAC protein in mature bovine oocytes*

One of the early cellular events observed in all mammalian eggs is an increase in free intracellular Ca^{2+} followed by Ca^{2+} oscillations after the sperm-egg interaction occurs (Malcuit *et al.*, 2006a). Numerous studies support the role of Ca^{2+} transient in egg activation mediating resumption of meiosis. Recent studies attributed VDAC a role in Ca^{2+} trafficking in the cell, which may lead to an important role in the physiological control of Ca^{2+} signaling (see discussion, 4.3.1). The aim of this functional test was to investigate whether VDAC is able to trigger calcium oscillations in bovine oocytes. *In vitro* matured oocytes were microinjected with VDAC protein extracted from porcine and bovine spermatozoa. In experiments designed to control the microinjection procedure itself, MII stage bovine oocytes, were treated with buffers used to isolate and purify the samples. Ca^{2+} oscillations were monitored during 1 to 3h after the injection of purified VDAC protein.

The results observed after microinjection of VDAC purified extract, showed no difference between the treatments and the control group. No specific increases in Ca^{2+} were observed during the monitored time (data not shown).

3.3.4 *Influence of anti-VDAC1 antibodies on in vitro maturation of bovine oocytes*

The present study was designed to investigate a possible role of VDAC1 in bovine oocytes during meiotic maturation. Prophase arrested oocytes were treated with anti-VDAC1 antibodies during the normal *in vitro* maturation protocol. After 24h oocytes were fixed, stained and examined by fluorescence microscope. Progression of normal maturation was based on nuclear status considering metaphase II: extrusion of first polar body and spindle formation.

a) Treatment of bovine oocytes during maturation with P31HL (anti-VDAC1, Calbiochem)

Treatment with P31HL antibody (monoclonal Ab-1, Calbiochem) was performed by diluting the antibody (8µg/100µl) in maturation media and incubating with freshly obtained COCs for 24h (50-70 oocytes each group). In this case, due to the presence of sodium azide (<0.1%) in the antibody and IgG_{2a} control, an extra cleaning step was performed.

After exposure to the respective treatments diluted in the maturation media for 24h, oocytes were assessed. Control group displayed a maximum of 7% of oocytes in MII stage with the correspondent IgG_{2a} (8µg/100µl, Calbiochem). The anti-VDAC1 antibody did not display mature oocytes (P31HL, 0%). Results were not considered to be significant ($p < 0.01$) assuming an identical effect between both treatments. The data obtained with the routine maturation protocol, reached an expected 90% of oocytes in MII stage ($p < 0.0001$) considered extremely significant (Figure 29) compared to the former treatments.

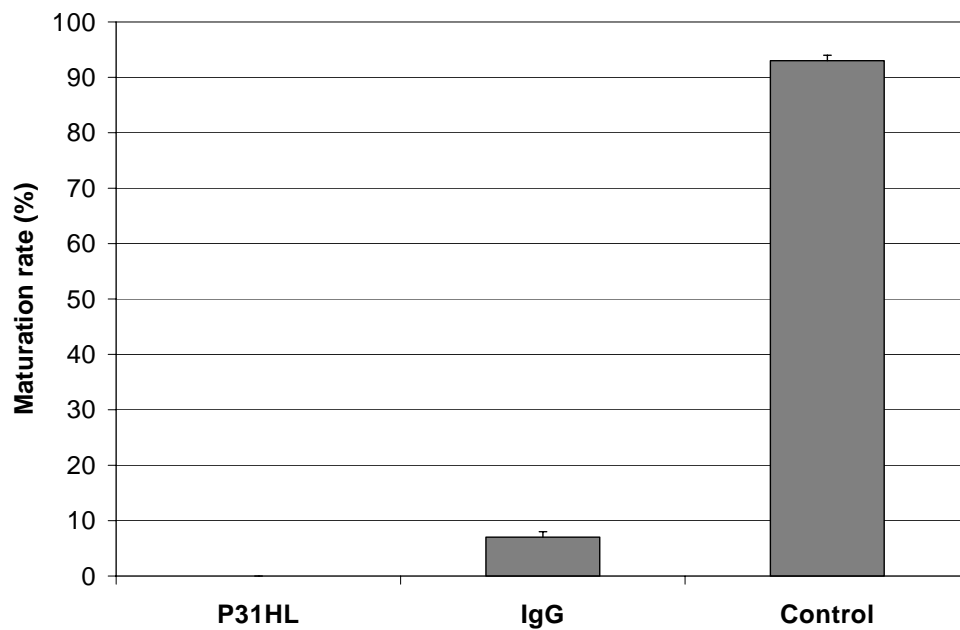


Figure 29: Effect of P31HL on *in vitro* maturation of bovine oocytes. Bovine oocytes were incubated in *in vitro* maturation medium containing P31HL (anti-VDAC1; 8 μ g/100 μ l, Calbiochem) for 24h. IgG_{2a} was incubated in maturation media and used as control (IgG_{2a}; 8 μ g/100 μ l, Calbiochem). The solid bar termed control consisted of the normal maturation media. The values are percentage of the maturation rate observed in each treatment group (mean \pm SD). No significant differences were observed between the P31HL and the IgG_{2a}. The result obtained with the control group was considered significant in respect with P31HL and the IgG_{2a} ($p < 0.0001$).

b) Treatment of bovine oocytes during maturation with anti-VDAC1 (AS P6)

The obtained results could be evidence of toxic activity from the preserving substance found in the monoclonal antibody and IgG_{2a} control. To avoid further failures, the experiments were subsequently performed using the polyclonal anti-VDAC1 antibody (AS P6). The antibody and correspondent preimmune serum control were complement deactivated by heat.

Experiment 1: Incubation with AS P6 (2 μ g/100 μ l) was performed during 24h and a group of control oocytes was exposed to the correspondent preimmune serum and the routine maturation protocol (Figure 30). Neither the antibody (AS P6) nor the preimmune serum stopped the normal meiotic maturation activity. The maturation values were 78 \pm 2% for the anti-VDAC1 antibody treated group, for the preimmune serum 82.5 \pm 11% and for the routine

maturation protocol $81 \pm 9\%$. The results were considered to be not significant ($p=0.890$), the variation among columns means was not significantly greater than expected by chance.

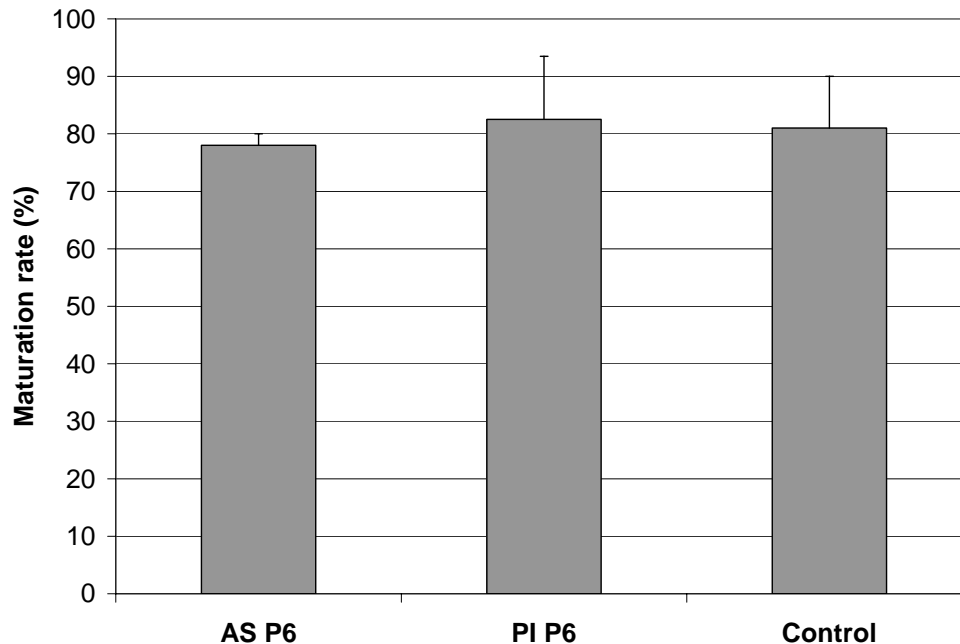


Figure 30: Effect of anti-VDAC1 antibody incubation on the *in vitro* maturation rate of bovine oocytes. Bovine oocytes were incubated with AS P6 ($2\mu\text{g}/100\mu\text{l}$) diluted in *in vitro* maturation media for 24h. PI P6 ($2\mu\text{g}/100\mu\text{l}$) in maturation media was performed as control. The solid bar termed control consisted of the normal maturation media. The values are percentage of the maturation rate observed in each treatment group (mean \pm SD). No significant differences were observed between the three treatment groups ($p=0.890$).

Experiment 2: Due to the lack of response of oocytes to the antibody, an alternative approach was taken. Oocytes were exposed to a delivery reagent (Pulsin), which facilitates antibody delivery into cells. To test the efficiency of the reaction a fluorescent protein was used as positive control. Groups of oocytes were incubated with the fluorescent protein control and the normal maturation protocol. In the two cases the delivery reagent ($2\mu\text{l}/100\mu\text{l}$, Pulsin) was added. Oocytes were exposed for 4 or 24h with each treatment. Oocytes exposed only for 4h were subsequently washed 3 times and the normal maturation protocol was resumed.

The auto-fluorescent protein was mainly observed under the microscope in COCs incubated for 24h. It showed a positive even staining through the whole cumulus cells and some fluorescence scattered spots were observed in the oocytes after hyaluronidase treatment. In the case of four hours incubation only the outside cumulus cells exhibited fluorescence. No fluorescence was detected in the ooplasm (Data not shown)

Experiment 3: Based on the results of experiment 2, oocytes were incubated for 24h with AS P6 (6µg/100µl) and 2µl delivery reagent (Pulsin). Treatment with the AS P6 displayed a significant decrease of the normal maturation rate after 24h of exposure compared with the control groups. The control groups consists of preimmune serum treated oocytes (PI P6, 6µg/100µl) and the normal maturation protocol with addition of the delivery reagent (2µl, Pulsin). The maturation rate observed in both control groups was within the expected values (~80%). In the case of the anti-VDAC1 (AS P6) treated oocytes only 52% reached the MII stage, displaying a significant difference between the two controls groups (Table 10, Figure 31).

Table 10: Effect of AS P6 (6µg/100µl) and delivery reagent (2µl, Pulsin) on the *in vitro* maturation of bovine oocytes after 24h incubation.

Treatment (+delivery reagent)	No. of oocytes examined	% of oocytes in metaphase II
anti-VDAC1 (AS P6)	91	52.8±4.12 ^a
preimmune serum (PI P6)	83	80.4±4.6 ^b
normal maturation protocol	67	77±6.6 ^b

Values are percentage (mean±SD) of 5 independent experiments.

^{a-b} Values with different superscripts within the column are significantly different ($P < 0.05$)

The two-tailed value obtained with antibody and preimmune serum was ($p=0.0010$) considered very significant. In contrast, the data between the preimmune serum and the maturation media including the delivery reagent was considered not significant ($p=0.68$).

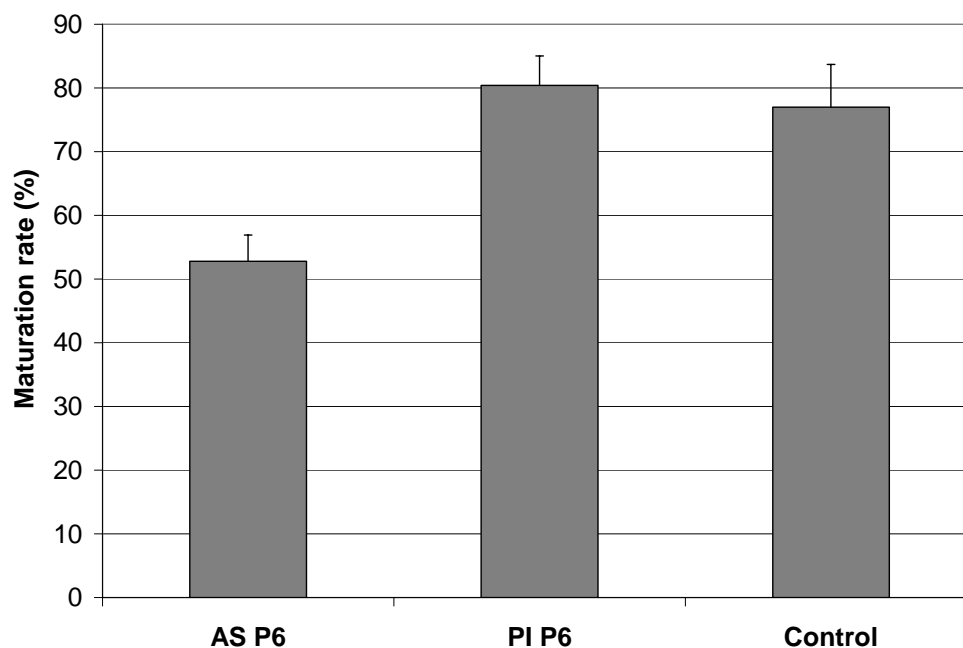


Figure 31: Effect of anti-VDAC1 antibody incubation on the *in vitro* maturation rate of bovine oocytes. Bovine oocytes were incubated with *in vitro* maturation media containing AS P6 (6 μ g/100 μ l) and delivery reagent (2 μ l, Pulsin) for 24h. PI P6 (6 μ g/100 μ l) in maturation media and delivery reagent (2 μ l, Pulsin) was performed as control. The solid bar termed control consisted of the normal maturation media and 2 μ l of the delivery reagent. The values are percentage of the maturation rate observed in each treatment group (mean \pm SD). No significant differences were observed between the preimmune serum PI P6 and the control group ($p=0.68$). A significant difference was observed with the AS P6 antibody treated oocytes ($p=0.0010$).

The preliminary results showed an interruption during the meiotic maturation process; only 50% of the oocytes after treatment with anti-VDAC1 antibody reached MII stage compared to the expected maturation rate of 80-90%.

4 Discussion

This study entails the investigation of the three VDAC isoforms (VDAC1, VDAC2 and VDAC3) in mammalian oocytes. Experiments were carried out to clarify gene and protein expression. Furthermore, preliminary functional studies were conducted to characterize possible roles of VDAC during maturation and oocyte activation. Experiments involving purified VDAC protein from spermatozoa were performed to find a potential relation between high amounts of VDAC protein in spermatozoa and oocyte activation. The second approach concerned oocyte maturation and the participation of VDAC protein in this process through the help of anti-VDAC antibodies. These experiments should constitute the first data obtained from VDAC in mammal oocytes.

4.1 Expression of VDAC mRNA in porcine and bovine oocytes

In order to pursue a detailed analysis of VDAC gene expression, highly sensitive methodologies are required. Different methods are of common use: northern blotting, *in situ* hybridization and RT-PCR. The limitation of the first two methods is their comparatively low sensitivity (Bustin, 2000) while the RT-PCR is the most sensitive method compared with the described techniques, which require large amounts of total RNA (Liu and Saint, 2002). This limitation can play an important role in cases where the research material is difficult to obtain in high quantities.

The expression analyses of VDAC1, 2 and 3 mRNA were possible with RT-PCR. Transcripts of VDAC1, 2 and 3 were detected in oocytes both before and after *in vitro* maturation. This revealed that synthesis of VDAC isoforms occurs in porcine and bovine oocytes. Although several previous reports have confirmed the presence of mRNAs for these isoforms in different tissues (De Pinto *et al.*, 1987b; Blachly-Dyson *et al.*, 1993), these are the first results obtained in female gametes from mammals. Steinacker and colleagues demonstrated in 2000 that the plasma membrane of *Xenopus laevis* oocytes contains VDAC; however it was only described on the protein level (Steinacker *et al.*, 2000). Guarino *et al.* reported the transcription of VDAC isoforms from germinal tissue of *Drosophila melanogaster*. The experiments were performed with homogenized ovaries and showed amplification of VDAC1 and 2 (Guarino *et al.*, 2006). In the present work sequencing of obtained amplicons from porcine and bovine oocytes confirmed that they represent VDAC1, VDAC2 and VDAC3

RNA. Contamination from genomic DNA could be excluded by the use of primers sets that span between introns. No qualitative differences were observed between GV and MII stage oocytes from both species. RT-PCR enabled the analysis of VDAC isoforms but, in terms of quantitation, one cannot rely on the direct measuring of the band intensity stained with ethidium bromide on agarose gel. Therefore, a semi-quantitative PCR method was performed.

4.1.1 *Real-time RT-PCR of bovine oocytes*

Reverse transcription of mRNA followed by polymerase chain reaction is a reliable method of detecting gene expression, but it is of increasing importance to detect not only qualitative but also quantitative differences in gene expression levels. Real-time RT-PCR allows quantification of low amounts of mRNA transcripts; therefore, it offers important physiological insights in mRNA expression levels. The aim was to compare the relative abundance of the three VDAC isoforms transcripts in bovine oocytes. Many reviews provide a careful analysis of a wide spectrum of data concerning gene expression level in bovine oocytes and embryos (Knijn *et al.*, 2002; Mourot *et al.*, 2006). Moreover, semi-quantitative RT-PCR is the most frequent method used in this case (Lechniak, 2002). Therefore, bovine material has been selected for analyzing the relative transcript abundance of VDAC in oocytes.

Oocytes were chosen from three different follicle size categories to observe a possible regulation of VDAC during the last stages of folliculogenesis. The developmental competence of oocytes is acquired gradually and increases with follicular development. It is known that the follicle size influences the efficiency of embryo production *in vitro* (Machatkova *et al.*, 2004). However, little is learned about oocytes genes being able to confer this competence during folliculogenesis. A better understanding of the mRNA profiles of VDAC isoforms in oocytes of different follicle categories could provide further information on gene regulation and on the general characterization regarding VDAC expression in female gametes.

Briefly, SYBR green I fluorescence dye was used for detection of newly synthesized PCR products and the quantification method chosen was the relative expression of a target gene versus two internal reference genes. Relative quantification requires a housekeeping gene for normalization that displayed a minor variation throughout the biological samples examined in the assay. The reference gene corrects for differences in initial sample amount. It also corrects for possible RNA degradation in nucleic acid recovery, lowering the mistakes in sample

and/or nucleic acid quality as well as cDNA synthesis efficiency. The abundance of mRNA in preimplantation stages is variable for most genes, including housekeeping genes, due to gene expression dynamics in early development (Bilodeau-Goeseels and Schultz, 1997). Thus, the election of a suitable housekeeping gene was a problem to overcome; it is common to standardize the measured mRNA levels to β -actin, GAPDH or S18 rRNA. However, the expression profiles of these genes during the preimplantation are not always stable. The following housekeeping genes were deployed in the real-time RT-PCR experiments: U2snRNA and H2A. Histone H2A is a gene involved in chromatin support and often used as control (Mourot *et al.*, 2006). The mRNA of H2A was verified to be constant in oocytes from 2 follicle categories and preimplantation stages by McGraw and colleagues (McGraw *et al.*, 2003). Other studies proposed H2A to be the most reliable candidate because the transcript levels were similar throughout this time in bovine and murine oocytes (Robert *et al.*, 2002; Jeong *et al.*, 2005). U2snRNA (U2 small nuclear RNA) was mostly constant until the eight cell stage and both housekeeping genes showed no differences between two diverse follicle size groups, indicating that the RNA levels are not influenced by follicle size (Watson *et al.*, 1992; De Sousa *et al.*, 1998; Robert *et al.*, 2002). The analyses of the expression was performed in three oocytes populations recovered separately from small (group 1, <3mm), medium (group 2, 4-6mm) and large follicles (group 3, 8-11mm). The data was normalized with the two housekeeping genes as recommended (Bustin and Nolan, 2004) for the utilized analysis software REST-XL (2005). The relative quantification was performed by using group 1 as control with which group 2 and 3 were compared. Successful quantification of transcripts in individual oocytes by real-time RT-PCR was monitored. The three isoforms did not demonstrate significant differences between group 1 (<3mm) and 2 (4-6mm), with the mRNA expression remaining constant. Although VDAC isoforms proteins are of great importance in several metabolic pathways, they do not appear to be mediators of developmental potential. The data could also be related with previous results in which different genes were tested in four different follicle sizes and oocyte obtained from <2 to 6mm follicle size presented the minor differential expression (Mourot *et al.*, 2006). On the other hand, levels of VDAC1 in the group 3 (8-11mm) were approximately 2.4-fold lower than those of group 1 (<3mm). The meaning of this down-regulation is unclear. An assumption would be that if VDAC1 is a channel for cytochrome *c*, a decrease in VDAC1 levels may be associated with lower vulnerability of oocytes to apoptosis. It has been proposed that mitochondrial apoptogenic factors are released through VDAC of the PTP (Shimizu *et al.*, 2001). This model assumes that the functional interaction of proapoptotic members such as Bak and BAX with VDAC or

another PTP component opens the VDAC channel allowing cytochrome *c* release. Previous quantitative studies remarked that the differences in the expression amounts of VDAC mRNAs could be closely related to the regulation of cellular metabolism (Shinohara *et al.*, 2000). It should be noted that the 2.4 fold down-regulation magnitude is not a major value which might not have physiological relevance.

Monitoring the expression of the housekeeping genes (not normalized), they displayed a higher transcript level in the group 3. Assuming this expression to be constant, it might result from increased total RNA levels in oocytes of this group. Nevertheless, data from Mourot *et al.* (2006) detected a gradual increase of H2A RNA from the 5mm follicle size and a substantial increase for the >8mm follicle size (Mourot *et al.*, 2006). The discrepancy observed between Mourot and this work, in reference to the results from Robert *et al.* (2002), could be explained by the fact that only follicles of 3-5mm were studied by Robert and colleagues (Robert *et al.*, 2002). Furthermore, in this work U2snRNA also presented an increase in the amounts of RNA in the larger follicle sizes.

To sum up, the real-time method for the quantification of VDAC isoforms in single oocytes from different sizes of bovine follicles could be established. The results from group 1 (<3mm) and 2 (4-6mm) displayed a constant expression for the three isoforms, while the levels of VDAC1 in the group 3 (8-11mm) were down-regulated compared to those of group 1.

4.2 Expression of VDAC protein isoforms in porcine gametes

Detection of mRNA levels does not determine whether the mRNA is translated into protein or not. Thus, to further identify the expression of VDAC isoforms in gametes and to correlate the data obtained in the RNA level, different approaches had to be performed with the help of anti-VDAC antibodies.

Antisera were previously generated and characterized for their isoform-specificity. The specificity of the antibodies had been tested in immunoblots and proved to be capable of discriminating between isoforms. Using recombinant proteins the antibodies AS P6 recognized VDAC1, AS P45-VDAC2 and AS P31-VDAC3, while anti-VDAC AS P_{common} antibody was able to recognize all three subtypes. These represent the first true monospecific antibodies for all three VDAC isoforms (Hinsch *et al.*, 2004). Monoclonal and polyclonal anti-VDAC antibodies were previously reported (Babel *et al.*, 1991); however, their specificity has been not fully established.

Detection of VDAC1 protein was additionally analyzed with the monoclonal antibody P31HL (Calbiochem). The monoclonal antibody was raised against the N-terminal of porin 31HL (purified from a crude membrane preparation from human lymphocytes). Originally, this antibody was produced against highly enriched human type 1 VDAC protein (Babel *et al.*, 1991) and featured to differentiate between type 1 and 2 VDAC in human (Winkelbach *et al.*, 1994). A disadvantage, is that most of the biochemical results obtained in many laboratories come from this antibody (P31HL), which was reported in frog, shark and turkey to have cross-reactivity with no possible distinction between type 1 and 2 VDAC (Reymann *et al.*, 1999; Steinacker *et al.*, 2000).

The subcellular localization of VDAC2 protein was also analyzed by confocal microscopy experiments with anti-VDAC2 antibody (C-17, Santa Cruz). Anti-VDAC2 is an affinity purified goat polyclonal antibody raised against the peptide mapping near the C-terminus of VDAC2 protein of human origin.

4.2.1 Immununobiochemical detection and lipid bilayer experiments of VDAC proteins from porcine spermatozoa

The aim of identifying and purifying VDAC protein from spermatozoa was to subsequently proceed to functional studies. The approach followed was to isolate, purify and electrophysiologically characterize the porcine spermatozoa VDAC protein. The starting material consisted of fresh ejaculates, following successive solubilization steps with TX-100. Immunobiochemical studies evidenced the presence of the three VDAC isoforms in a 2% Triton X-100 porcine sperm extract with the help of AS P6, AS P45, AS P31 antibodies and the monoclonal anti-VDAC1 P31HL antibody (Calbiochem). The observed results agree with previous reports from VDAC isoforms in TX-100 extracts of bovine spermatozoa (Hinsch *et al.*, 2001; Aires *et al.*, 2003; Hinsch *et al.*, 2004). The MW interval between 30-35kDa was compared to previous described output for different tissues (Benz, 1990). Protein bands with higher molecular masses than the expected for VDAC protein were observed and according to a recent publication this could be explained by the existence of VDAC like protein dimers, trimers or tetramers (Zalk *et al.*, 2005). VDAC protein was also described to exist in mitochondria not only as a monomeric 32kDa protein but as part of a much larger complex (Krimmer *et al.*, 2001). Distler (2006) described the presence of VDAC1 and 2 proteins in the 86 to 90kDa range and explained it as a possible homodimerization/oligomerization of these

integral membrane proteins. In addition it was also identified in the 76 to 80kDa range VDAC1 (Distler *et al.*, 2006).

Following the solubilization steps, and using the protein material recovered from the final treatment with 2% TX-100, samples were chromatographically purified in hydroxyapatite-celite columns (2:1). Solubilization and purification procedures were based on the classic isolation method (De Pinto *et al.*, 1987a). The procedure resulted in two protein bands on SDS-PAGE (Coomassie staining and immunoblotting), which were related with VDAC protein isoforms on the basis of MW, reactivity with polyclonal antibodies, MALDI-TOF MS and characteristically activity displayed in planar bilayer after reconstitution. Results from other tissues after chromatographic purification like liver, heart, brain (De Pinto *et al.*, 1987a), skeletal muscle (Shoshan-Barmatz *et al.*, 1996) or retina (Gincel *et al.*, 2002) mainly showed one single band of approximately 35kDa. A characterization of this 35kDa band by immunobiological studies was generally performed by the commercial available antibody VDAC1 (P31HL, Calbiochem) and no further distinctions were made. The difference between the published data where only one band is observed as VDAC protein and the results obtained in this work, where 2 bands were observed in the hydroxyapatite-celite material could be due to the extraction and elution procedures and/or protein quantity as well as material origin. Interestingly, the bands observed in this work from purified protein which was originated from spermatozoa material were characterized as VDAC1 and VDAC2 protein with the antibodies (AS P6 and AS P45) and the result of the MALDI-TOF MS followed by peptide mass fingerprinting as VDAC2 and VDAC3 porcine protein. However, the data obtained with MALDI-TOF MS revealed identical subtypes previously suggested in bovine spermatozoa (Aires *et al.*, 2003). The specificity of the reaction obtained with the antiserum (AS P6 and AS 45) was demonstrated by successful pre-absorption of the antibodies with the respective peptides and with preimmune serum experiments. This discrepancy between the antibodies results and MALDI- TOF MS could not be entirely resolved; a limitation of the technique compared with 2D gels is that every 1D band analyzed could consist of mixtures of at least two proteins.

In addition to one dimensional SDS analyses, the presence of VDAC proteins was investigated with two dimensional polyacrylamide gel electrophoresis (PAGE), normally used to study complex protein mixtures from biological systems in conjunction with mass spectrometric analysis (Rabilloud, 2002; Barnouin, 2004). The characterization of VDAC isoforms by 2D was mainly performed with hydroxyapatite-celite chromatographically

purified spermatozoa proteins. In this way detection difficulties due to the great quantity of spots were avoided during MALDI-TOF MS analysis.

Surprisingly, clear immune responses were demonstrated for the three VDAC subtypes. Six different electrophoretic spots and a line proved to be immunoreactive with anti-VDAC AS P_{common} antibody in the experimental window (pH 6-11, mass 10-200kDa), showing approximately the same MW but different pI values. VDAC1 protein was observed as a single spot after immunodetection using anti-VDAC1 polyclonal (AS P6) and monoclonal commercial antibody (P31HL, Calbiochem). The presence of VDAC2 protein (anti-VDAC2, AS P45) was observed as 5 spots distributed in different MW and pI areas. This difference could be explained by post-translational modifications (like phosphorylation) or splice variants which are known for human VDAC2 (Ha *et al.*, 1993; Blachly-Dyson *et al.*, 1993; Liberatori *et al.*, 2004). Studies carried out at the mRNA level showed that the VDAC2 gene may generate at least four different isoforms through alternative splicing (Ha *et al.*, 1993). It is also known that phosphorylation adds negative charges on the molecule producing a pI shift. The width of this shift is dependent on the number of added phosphates per molecule. Phosphorylation patterns were described for two out of three VDAC2 spots and one VDAC1 spot in guinea pig brain synaptosomes in normoxic versus hypoxic samples (Liberatori *et al.*, 2004). Nevertheless, to solve this question it seems necessary to sequence the whole protein and the corresponding cDNAs or to analyze phosphorylation profiles of the VDAC protein with anti-phosphorylation (anti-PY) antibodies.

Anti-VDAC3 antibody (AS P31) displayed an unfocussed band. This could result from incomplete solubilization of the sample prior to application; as well as possible interfering substances or an incorrect focusing time during the electrofocusing protocol.

The spots observed by silver staining and related with the immunoblot results were submitted to MALDI-TOF MS. Analysis of peptide mass values gave clear results for VDAC2 for the 5 spots detected by the AS P45 antibody with significant scores; only preliminary clues were observed for the spots detected with VDAC1 and VDAC3. These not significant results could be explained by the difficulty to obtain a clear focus spot for VDAC3 (observed as a band) and higher quantities of protein for VDAC1. In addition, higher amounts of protein were tested; nevertheless, the procedure has a limit of resolution and protein intake. The low sequence coverage of the sequenced data could be explained by partial cleavage of protein that occurs in gel digestion of proteins with many membrane spanning regions (Hellman *et al.*, 1995; Buhler *et al.*, 1998). To keep membrane proteins in solution, detergents are required

and the presence often interferes with enzymatic digestion as well as with the analysis of the proteins and their digestion products by mass spectrometric methods.

The electrophysiological properties of purified VDAC protein inserted into planar bilayers are well established (Gincel *et al.*, 2000; Shoshan-Barmatz and Gincel, 2003). To characterize the channel forming properties of VDAC protein from porcine spermatozoa, proteins were chromatographically purified, added to planar phospholipid membranes and studied by electrophysiological methods. Some typical VDAC activity was found in reconstituted bilayers experiments with material obtained after hydroxyapatite-celite purification of porcine spermatozoa protein extractions. The reconstituted VDAC displayed bell-shaped symmetrical voltage dependence curve when either positive or negative potentials were applied, while exceeding 30mV; VDAC underwent transition to a non-conducting closed state. The increase occurred regardless of whether the protein was added to only one side or both sides of the membrane.

However, some other properties did not match the classic VDAC behavior. The channels normally have a single channel conductance of 4nS in 1M KCl (Shoshan-Barmatz and Gincel, 2003). In the spermatozoa enriched VDAC protein material the most frequently observed single channel conductance in 1M KCl was close to 2nS. This result is in agreement with earlier observation for bovine spermatozoa (Menzel *et al.*, in preparation). It has been previously suggested that the smaller single channel conductance corresponds to a substate of the pore which eventually may revert to the open state. It has to be noted, however, that in preparations of VDAC protein from other species only smaller channel sizes have been observed. To arouse interest a closer similarity of channel conductance values was obtained with those reported by Benz (1979) for *Escherichia coli*. The single channel conductance was described with an electrical conductance of 1-2nS (Benz *et al.*, 1979). This feature was also observed for the isolated Porin31HL, where apart from the 3.5-4.5nS pores, smaller channels around 2nS were found (Thinnes *et al.*, 1989). Smaller conductance have also been observed for yeast (Ludwig *et al.*, 1988), neurospora (Freitag *et al.*, 1982), corn (Aljamal *et al.*, 1993) and reconstitution experiments with eukaryotic VDAC (Benz, 1985; De Pinto *et al.*, 1987b).

An important remark is that it was not possible in this work to obtain pure VDAC after the hydroxyapatite-celite chromatography procedure. After silver staining, VDAC protein was observed as the major protein component of the eluted sample but other minor protein contaminants were present. As reported by De Pinto (De Pinto *et al.*, 1987a), only minor contaminants were seen when no salt was present but increasing presence of other proteins

were found with higher concentrations. However, the extra bands observed with the spermatozoa protein material were not detected by any of the specific subtype antibodies.

The functional results previously discussed should be analyzed like a general characteristic that corresponds to the three isoforms together. Early attempts to isolate each isoform and to analyze them individually gave unsatisfactory results. Constant contamination between isoforms was present when the bands were separated in polyacrylamide gels; intensive optimization work is yet to be done.

To sum up, it was possible to isolate and to obtain enriched VDAC protein material from porcine spermatozoa. Western blot and MALDI-TOF MS demonstrated the presence of VDAC1, VDAC2 and VDAC3 protein after isolation with a nonionic detergent (Triton X-100) and chromatographic purification. Electrophysiological experiments demonstrated a functional active VDAC protein originated from porcine spermatozoa, providing material for functional studies related to oocyte activation.

4.2.2 Immunobiochemical detection of VDAC proteins in porcine oocytes

The aim of the immunobiochemical studies was to identify VDAC proteins in porcine oocytes using different anti-VDAC antibodies. Examination by one dimensional SDS-PAGE and immunoblot revealed the presence of VDAC1 and VDAC2 protein in immature and mature oocytes.

Strong reactions were observed for anti-VDAC1 antibody (AS P6) in both GV and MII stage oocytes, with an apparent molecular 30kDa mass correlating with previous reported data (Benz, 1990). Meanwhile, VDAC2 (AS P45) presented a shift in protein level and MW between GV and MII stage oocytes. These results cannot be quantitatively interpreted due to uncertainty about the relative reactivity of these antibodies with their respective isoforms, or with isoforms of different species, but a tendency is suggested. In GV stage oocytes a high intensity band was observed with anti-VDAC2 antibody (AS P45) in the expected MW range (~30kDa) which was almost not detectable in MII stage oocytes. The same pattern was inversely observed for a band at the 50-55kDa range. In GV oocytes this band presented a low intensity but it strongly increased after the *in vitro* maturation procedure. The presence of the 50-55kDa band agrees with the reported expression of Porin2 (VDAC2) in ovaries homogenates of *Drosophila melanogaster* (Guarino *et al.*, 2006). This band could be

explained by the same previously discussed points for porcine VDAC protein originated from spermatozoa (4.2.1)

It is worth noting that VDAC3 is expressed in a wide variety of tissues (Rahmani *et al.*, 1998; Sampson *et al.*, 2001; Hinsch *et al.*, 2004), but it was neither detected in immature nor mature oocytes. The data presents a discrepancy towards the RT-PCR results presented in this work. That could mean that in oocytes either VDAC3 is expressed at very low level, not translated or it could be lost by the applied protein isolation method. It could also be caused by a steric conformation of the protein in the gel which could produce antibody-antigen recognition failure. The presence of VDAC3 protein could not be answered by this method.

A second step was conducted to confirm the observed immunoblot patterns. The solubilization and purification procedure was adapted from the classic isolation method developed for mammalian VDAC protein isoforms (De Pinto *et al.*, 1987a). The VDAC fraction of 3300 oocytes was obtained by two sequential solubilization of TX-100 and two hydroxyapatite-celite chromatography elutions. First and second eluates from each solubilization step were analyzed. The procedure resulted in one protein band on SDS-PAGE from the second solubilization step after silver staining, which was identified by MW as VDAC isoforms. MALDI-TOF MS and peptide mass fingerprinting was performed from the band corresponding to the second eluate which yielded a higher amount of protein and it was confirmed as porcine VDAC2 protein with a significant score. The observed result agrees with the partial sequencing of the VDAC protein results from *Xenopus laevis* oocytes (Steinacker *et al.*, 2000). The reported band from *Xenopus laevis* oocytes was previously indicated as frog type 1 VDAC protein by the P31HL antibody (Calbiochem), but later explained as a possible cross-reaction of the antibody, and confirmed as frog type 2 VDAC protein by partial sequencing (Steinacker *et al.*, 2000). Schwarzer (2000) also analyzed the expression of VDAC from the supernatant of solubilized *Xenopus laevis* oocytes in relation to recombinant constructs. Following anti-hVDAC1 incubation endogenous VDAC protein from *Xenopus laevis* oocytes was detected in the 30kDa level (Schwarzer *et al.*, 2000). The result is also consistent with earlier MALDI-TOF MS analysis in this work of porcine spermatozoa, where the matchable band was classified as VDAC2 protein, as well.

A substantial improvement should be made to obtain higher VDAC protein yields after protein isolation and purification from oocyte. This will allow further analysis of VDAC1 and 3 as well as the possibility to study their functional properties by incorporation into planar bilayers. A major difficulty is the availability of the studied material, although oocytes are large cells and possess high quantities of mRNA and protein; studies are hampered by the

limited numbers of cells available and time consuming procedure to gather single cell preparations including the manual removal of cumulus cells.

Immunobiochemical results were supported by the RT-PCR in this same study, demonstrating that VDAC1 and VDAC2 proteins are expressed in porcine oocytes. In the case of VDAC3 protein no clear results could be obtained with immunoblotting. Meanwhile by RT-PCR, gene expression could be successfully demonstrated. VDAC2 protein was successfully purified from oocytes and a partial sequence was obtained by MALDI-TOF MS analysis.

4.2.3 *Immunohistochemical detection of VDAC protein in porcine ovaries*

Immunohistochemistry (IHC) is a qualitative method well established for the localization of tissue proteins. In the present study IHC was utilized to detect cellular localization of the three VDAC subtypes during folliculogenesis in porcine ovaries.

Anti-VDAC1 antibodies, AS P6 (Hinsch *et al.*, 2004) and monoclonal P31HL antibody (Calbiochem) detected positive cytoplasmatic staining from oocytes and follicle cells in the three studied follicle stages. This agrees with presented RT-PCR results and western blot data indicating that both transcription and translation occur in the same cell, it also indicates the specificity of the applied IHC method. Concerning VDAC2, there was a weaker reactivity, however, it could be demonstrated in both, protein and mRNA level. Further, specificity of IHC for VDAC1 and VDAC2 was confirmed by lack of non-specific signals in the negative controls.

With respect to VDAC3 no consistent results were obtained as unspecific signals were found in positive and negative samples. RT-PCR revealed transcription but translation could not be detected successfully by immunoblot and immunohistochemistry procedures. These observations can be related to tissue conservation procedures which might mask the targeted antigen-domains (Lehmann *et al.*, 1995) or low protein yield, showing IHC not to be sensitive enough for the detection of VDAC3 protein.

The presence of VDAC1 and 2 proteins in the cumulus cells agrees with preliminary data obtained in western blot analysis with anti-VDAC_{common} antibody (AS P_{common}) and confocal microscopy (AS P6, Anti-VDAC2 and AS P31 antibodies). For the work purposes the localisation of VDAC in cumulus cells was not in focus, the main goal was to concentrate on

the oocyte level. However, the data of the IHC could be corroborated by these tentative results.

4.2.4 Subcellular distribution of VDAC proteins in porcine oocytes

To further study VDAC isoforms in porcine oocytes at the protein level, subcellular distribution was observed using antibodies and confocal microscopy. Experiments were divided in not-permeabilized oocytes, to investigate VDAC1 protein localization as described in a previous study (Steinacker *et al.*, 2000) and permeabilized GV and MII stage oocytes for a precise subcellular localization of VDAC protein isoforms.

The images of not-permeabilized oocytes after anti-VDAC1 antibody incubation displayed a punctuate distribution pattern on the oocyte surface, the observation indicates a possible plasma membrane labeling. This result is in agreement with earlier data obtained in *Xenopus laevis* oocytes (Steinacker *et al.*, 2000), where the regular expression of endogenous VDAC protein was detected in plasma membranes by anti-human type 1 monoclonal antibody (P31HL, Calbiochem). The staining in porcine oocytes was consistent between the two anti-VDAC1 antibodies, AS P6 and P31HL (Calbiochem) antibodies. In both cases, focusing through the oocyte, the staining appears exclusively in the cell surface but not inside the oocyte, which could be explained by the lack of the permeabilization step during the protocol scheme. In 1989, the first data on the extra-mitochondrial expression of VDAC protein in the plasma membrane of human B lymphocytes was published (Thinnes *et al.*, 1989). There were reports on its integration in the plasma membrane of different vertebrate tissues and on intracellular membranes of other organelles (Dermietzel *et al.*, 1994; Reymann *et al.*, 1995; Junankar *et al.*, 1995; De Pinto *et al.*, 2003). The extra mitochondrial localization of VDAC protein was questioned by Yu and co-workers, who investigated the subcellular distribution of epitope-tagged VDAC (Yu *et al.*, 1995). Antibodies against the tagged proteins showed that the three isoforms were exclusively located in fractions or subcellular regions that contained mitochondrial markers. The authors conclude that data supporting extra mitochondrial localization of VDAC protein were probably artifacts or unspecific immunoreactions. On the other side, experiments with NH-SS-biotin and 2D SDS-PAGE strongly suggest that, at least, a fraction of VDAC is localized in the plasma membrane due to NH-SS-biotin specific labeling (Bathori *et al.*, 1999). In this work the observed immunoreaction in the oocyte surface may also appear as artifact from the antibodies. However, the probability is low, since

negative controls were performed. No immunolabeling was observed by incubation with the second antibody or by the presence of the respective negative control like IgG specific subtypes or preimmune serum. By the presented result localization VDAC1 in the plasma membrane seems to be likely, the exact role or function is unknown.

To support previous results in the protein level and to further characterize subcellular localization of VDAC protein isoforms in oocytes, confocal microscopy examination was performed. The subcellular determination scheme includes a TX-100 permeabilization step. Oocytes immunostained with anti-VDAC1 (AS P6) and anti-VDAC3 (AS P31) antibodies revealed intense spots of dense staining distributed in the cortical area of both GV and MII stage oocytes and some lower reaction scattered, throughout the ooplasm. Antiserum AS 45 presented unspecific staining. Color reaction was observed in both positive and negative control samples. Thus, additionally a commercial anti-VDAC2 antibody (Santa Cruz) was tested. In comparison with AS P6 and AS P31 antibodies, anti-VDAC2 antibody presented a remarkable characteristic pattern (like grape clusters or ring forms) in GV oocytes. The immunoreaction was not visible in all the GV stage oocytes samples studied and it was totally absent in MII stage oocytes. This variation substantiates the results of the immunoblot experiments, where differences with anti-VDAC2 antibody (AS P45) band patterns were observed between mature and immature oocytes.

Control preimmune serum and IgG were applied and no labeling was present, demonstrating the specificity of the immunoreaction in the confocal microscopy experiments.

Until now, it was not possible to define the cellular compartments containing the VDAC proteins observed by confocal microscopy. Some candidates, which are not mutually exclusive, come into question. The distribution of VDAC1 and 3 proteins seemed to be stable through out the meiotic maturation. Taking this into account, organelles which remain unchanged during the maturation event and are known to possess VDAC protein were taken in consideration. In the germinal vesicle stage of mammalian oocytes actin filaments are distributed as a relative thick uniform area around the cell cortex and are also found near the GV. After germinal vesicle breakdown (GVBD), microfilaments are predominantly found at the cortex of the cell and around the female chromatin (Wang *et al.*, 2000). A functional interaction between actin and VDAC was reported. VDAC is known to interact *in vivo* with a wide repertoire of cytoskeletal elements (Roman *et al.*, 2006).

The localization of VDAC protein on the outer membrane of mitochondria from eukaryotic cells is well established (Benz, 1990). Thus, the observed pattern by confocal microscopy

experiments could be considered as a possible mitochondrial co-localization staining. During porcine oocyte maturation, the mitochondrial distribution was reported, in the perinuclear area from the GV and large mitochondrial foci form and relocated to the inner cytoplasm in mature oocytes (Sun *et al.*, 2001). Previous observation also revealed that translocation of mitochondria is coordinated with changes in the location of microtubule-organizing centers and that the microtubule-mediated accumulation of mitochondria may be required for nuclear maturation of mouse oocytes. Mitochondria are clustered at the periphery of the large nucleus and the cortical area, but they disperse through the cytoplasm during maturation. This pattern of distribution may be related to the high energy requirement in the cortex, as the oocyte requires the support of cumulus cells at this stage (Sun *et al.*, 2001).

In the case of VDAC2 the pattern of the protein localization apparently depends on the stage of development. The possibility that the reaction could not be detected in MII stage oocytes with confocal microscopy images due to changes in the protein conformation cannot be discarded. Nevertheless, it is known that some of the oocyte organelles such as cytoskeletal elements, cortical granules and endoplasmic reticulum exhibit dramatic changes during meiotic progression. Biochemical evidence supports the presence of VDAC protein in caveolae (Lisanti *et al.*, 1994) of somatic cells. Caveolae are domains of the plasma membrane where specific lipids and proteins are sub-compartmentalized. A family of proteins termed caveolins organizes these membranous domains bearing specific functions in the trafficking between the plasma membrane and the rest of the cell (Razani *et al.*, 2002). Caveolae are enriched with glycosphingolipids and cholesterol and are thought to play a role in cell-signaling, cholesterol homeostasis, clathrin-independent endocytosis, transcytosis and potocytosis. As the oocyte forms, significant fractions of caveolae in the cell begin to appear in large ring-like membrane compartments in the cytoplasm. Just after ovulation and fertilization, the large ring-like organelles apparently fuse with the plasma membrane. The fusion is strongly linked to progression of meiosis. The described location and process corresponds to data obtained from *Caenorhabditis elegans* (Sato *et al.*, 2006). The similarities between the caveolae results from *Caenorhabditis elegans* and the results obtained in this work with anti-VDAC2 antibody are important, nevertheless scarce research is done in mammalian oocytes so as to further relate them.

Apart from the similarities of ring-like forms observed with anti-VDAC2 antibody in this work to cortical granules, the possibility that VDAC protein is part of them is minimal. The cortical granules, membrane-bound organelles, are synthesized during the maturation period and migrate to the periphery of the matured oocytes at the time of completion of GVBD and

formation of the first metaphase (Cran, 1985). During oocyte maturation cortical granules move to the periphery in nearly all examined species. This is linked to the exocytosis function upon fertilization. The pattern of distribution is not related to the described result of VDAC2 protein subcellular localization presented in this work.

It is important to remark that the signal observed by anti-VDAC2 antibody in this work in the GV stage oocytes was not present in all the studied samples. It could be of interest to detect if the difference observed in the labeling is related to individual characteristics like oocyte quality. *In vitro* production (IVP) of pig embryos has been interfered by a high incidence of polyspermy failed or delayed paternal pronucleus formation and decreased development upon culture. There is still an obstacle in most IVP systems (Long *et al.*, 1999) and the finding of quality markers in oocytes would be of great help.

All in all, the presented immunocytochemical studies confirm the presence of VDAC1 and VDAC3 protein mainly in the cortical area of GV and MII stage oocytes. Furthermore, it offers additional clues for a difference of VDAC2 protein expression between GV and MII stage oocytes.

4.3 Functional studies

This work explored the potential relationship of VDAC to oocyte activation or maturation events. However, no supporting references or experimental data were previously cited to support these statements and no published results provides a basis for asserting that VDAC isoforms can be involved in the course of this investigation. In a first series of studies, the relationship of spermatozoa VDAC protein towards oocyte activation was investigated. A second approach was to address the role of VDAC1 during oocyte *in vitro* maturation; anti-VDAC1 antibodies being used to block VDAC1 protein whereas the classic IVM procedure.

4.3.1 *Treatment of matured porcine and bovine oocytes with purified VDAC from spermatozoa*

In all mammalian eggs studied so far, one of the early events after sperm-egg interaction is increase in calcium succeeded by oscillations. The initial calcium transient is followed by a series of subsequent oscillations that can continue for several hours after fertilization. The

single calcium rise is sufficient to induce both early and late events of activation such as second polar body extrusion, cortical reaction, pronuclear formation and DNA synthesis. Parthenogenetic activation of mammalian eggs can be achieved by increasing cytosolic calcium concentrations. The mechanism by which spermatozoa generate calcium transient and oscillation is suggested by the role of a sperm factor that is released into the egg. It has been well documented that a soluble factor extracted from the sperm of swine can elicit fertilization by calcium transients after being injected into unfertilized oocytes obtained from several species (Swann, 1994; Wu *et al.*, 1997; Stricker *et al.*, 2000). Cross-reactivity of sperm factors were well documented; several interspecific crossings have been obtained within the class mammalian and interphyletic (Stricker *et al.*, 2000). The sperm factor appears to be the PLC ζ (sperm-specific) and responds through the second messenger IP $_3$ (Saunders *et al.*, 2002; Cox *et al.*, 2002). Microinjection of porcine PLC ζ RNA revealed the ability to trigger repetitive calcium transients in oocytes and activation, initiating embryonic development up to the blastocyst stage (Yoneda *et al.*, 2006). However, according to Heyers calcium releasing activity and pronucleus formation in murine oocytes seemed to depend on more than one sperm factor (Heyers *et al.*, 2000).

ICSI (intra-cytoplasmatic sperm injection) has been used widely for the production of offspring in species ranging from the mouse (Kimura and Yanagimachi, 1995) to the human (Devroey and Van Steirteghem, 2004). Nevertheless, success in large domestic livestock species is limited, mainly in bovine, porcine and equine species (Bedford *et al.*, 2003; Choi *et al.*, 2004). With exception of the birth of several calves (Galli *et al.*, 2003), conventional ICSI failed to produce high rates of embryonic and fetal development in the absence of exogenous activation stimulus in species of economical relevance. Therefore, it is of importance from an applied stand-point, as well as for a basic understanding any concern regarding the mechanisms of oocyte activation and the identity of sperm factors that are involved in species such as cattle or swine. In cattle it was reported that one of the problems from ICSI could be the inability to initiate calcium oscillations and induction of oocyte activation (Malcuit *et al.*, 2006b).

Recent studies attributed to VDAC roles in Ca $^{2+}$ trafficking in the cell. The report of a tight regulation of Ca $^{2+}$ flow through VDAC (Gincel *et al.*, 2001) and the evidence that over-expression of VDAC facilitates Ca $^{2+}$ signal propagation to mitochondria (Rapizzi *et al.*, 2002) indicate that the OMM (outer mitochondrial membrane), and thus VDAC, may have an important role in the physiological control of Ca $^{2+}$ signaling (Hajnoczky *et al.*, 2002).

Thus, the objective of this study was to investigate the possibility of VDAC purified from spermatozoa as an accessory mediator that could initiate egg activation. The objectives were based in previous reports in cattle, where VDAC2 and VDAC3 were found as an important solubilize protein in spermatozoa extracts (Hinsch *et al.*, 2004) as well as publications of procedure improvements in ICSI. The practices of breaking off the sperm tail or the aggressive sperm immobilization (between the middle piece and the tail) were reported to enhance the rate of egg activation (Dozortsev *et al.*, 1995; Palermo *et al.*, 1996; Yanagida *et al.*, 2001). This was explained by the facilitated release of sperm cytosolic contents including the sperm factor.

The results of this work after microinjection or incubation with porcine enriched VDAC protein from spermatozoa after hydroxyapatite-celite chromatography did not display any activation in mature porcine oocytes. Presence of pronuclei was random and no significant differences were observed between the treated groups (1.5-12%). Inconstant results led to especially high deviation (SD). The obtained percents of activation by chance were in agreement with previous data. Reports from Petr and colleagues demonstrated that piercing with an injection capillary (mechanical control) or injection with water or buffers induced activation between 4-10% of porcine oocytes while treatment with specific activation substances were between 50-64% (Petr *et al.*, 2000).

The lack of activation in this work by the enriched VDAC protein might be due to a reduced potency and/or inadequate concentration of the investigated material. As all the isolation procedures of VDAC protein involve solubilization by Triton, applied in a concentration of 2%, trace amounts of this detergent could be present in all the functional tests carried out with purified VDAC preparations. The properties of VDAC protein may well be modified by isolation/reconstitution, in particular, by the use of detergents. A previous study has demonstrated, by means of a hexokinase assay on intact mitochondria, that traces of Triton may diminish the sensitivity of VDAC to Konigs polyanion (Bathori *et al.*, 1995). Furthermore, the precipitation step with acetone could modify the normal refolding activity of the purified VDAC protein (personal communication with Prof. Dr. Benz). Triton treatment during incubation procedures may have also stressed the oocytes leading to necrotic and apoptotic cell death. The attempts to obtain a functional VDAC protein with no TX-100 traces failed. The demonstrated inability to initiate activation upon injection into porcine oocytes could also be attributed to the fact that certain physiological events important for fertilization were bypassed. It could be imagined that some of the molecular events during capacitation or acrosome reaction could regulate the function of VDAC. It is described for example that

phosphorylation is an important regulator of VDAC function (Lemasters and Holmuhamedov, 2006).

An incorrect penetration of the microinjection needle with VDAC into the ooplasm could not be discarded. Thus, an incubation approach with the aid of DMSO was tested. DMSO is a well-known solvent and delivery reagent for different drugs. It can penetrate membranes without damaging them and can carry other compounds deep into biological systems. The results of VDAC/DMSO incubation were nevertheless comparable to the microinjection procedure.

The possibility that the activity of VDAC itself could be insufficient for second polar body extrusion or pronuclear formation in porcine oocytes can not be excluded. Similar results were obtained by treatments with ionophore where a clear calcium elevation was observed in porcine and bovine oocytes but the drug alone could not effectively produce parthenogenetic activation (Liu *et al.*, 1998; Wang *et al.*, 1998). Combined treatment of calcium ionophore and 6-DMAP (6-dimethylaminopurine) led to effective pronuclear formation but could not provoke second polar body extrusion (Liu and Yang, 1999). Heyers also described one fraction of the sperm factor that contained calcium releasing activity, but did not support pronuclear formation (Heyers *et al.*, 2000).

Although, that enriched VDAC protein originated from spermatozoa injected into mature oocytes did not trigger activation, the possibility that this treatment triggers a more subtle process that pronucleus formation should be considered as well. Thus, based in the previous discussed points, a more sensitive approach was investigated. The purpose was to research the possibility of spermatozoa VDAC protein as an accessory mediator which elicits and maintains calcium oscillations as seen during fertilization. To this end, the enriched VDAC protein sperm extract preparation was injected into bovine oocytes and the calcium responses were monitored. Bovine oocytes were selected for this experiment according to well established calcium oscillations measurements in this specie. Previous reports demonstrated that fertilized bovine eggs exhibited calcium oscillations with intervals of 20-30min after sperm factor microinjection (Fissore *et al.*, 1992; Sun *et al.*, 1994). Moreover, previous reports confirmed the lack of species specificity of sperm extracts to trigger activity (Kimura *et al.*, 1998). Furthermore, artificial activation of porcine oocytes has been attempted using various methods but the ability to promote oocytes to the blastocyst stage is greatly inferior to that in other mammals, such as mice or cattle (Amano *et al.*, 2004).

The examined sperm extracts (enriched VDAC protein) after hydroxyapatite-celite purification neither from porcine nor from bovine had the ability to elicit calcium oscillations.

The experiments suggested that the purified VDAC material had no calcium oscillation activity. However, the previously discussed points should be accounted.

Briefly, in this work both studied systems did not suggest the capability of VDAC protein from spermatozoa to be involved in the egg activation event. These findings encourage amplifying the chosen approaches and material. The results as well do not exclude the possibility that endogenous oocyte VDAC may contribute to the generation of calcium oscillations during mammalian fertilization.

4.3.2 Influence of anti-VDAC1 antibodies on *in vitro* maturation of bovine oocytes

Fully grown oocytes can undergo meiotic maturation during culture *in vitro*, thus providing an advantageous experimental system for biochemical studies. Meiotic maturation is characterized by dissolution of the nuclear membrane of the oocyte germinal vesicle, a process known as germinal vesicle breakdown, condensation of chromatin into bivalents, chromosome alignment in the metaphase I spindle, and separation of homologous chromosomes. These events are followed by emission of the first polar body and arrest of meiosis with the chromosomes aligned at the metaphase II spindle.

In this study the possible correlation between VDAC1 protein and the maturation process was evaluated. Oocytes with the surrounding cumulus cells were incubated with the anti-VDAC1 antibodies (P31HL and AS P6). It is worth mentioning that when studying the immature oocyte under physiological conditions, the oocyte is influenced by the surrounding cumulus cells which are connected to the oocyte via gap junctions. VDAC1 protein was blocked during maturation procedure by anti-VDAC1 antibody. The first approach included the commercial anti-VDAC1 antibody (P31HL, Calbiochem). The low maturation rate obtained for the antibody treatment and IgG control, strongly suggests a possible toxic effect of the sodium azide, a conservation reagent found in both treatments. The antibody (P31HL, Calbiochem) and IgG control (IgG_{2a} Calbiochem) were cleaned up from the conservation agent by special columns. However, the observation points towards the common toxic agent (sodium azide).

To further investigate the possible role of VDAC1 protein on maturation, the AS P6 antibody (anti-VDAC1) was incubated with the COCs during the normal *in vitro* maturation protocol. After 24h of incubation no differences were observed between the studied groups. In this case the maturation rate was approximately 90% for the AS P6 antibody, the PI P6 (control) and the normal *in vitro* maturation protocol. This result did not exclude the possibility that

VDAC1 protein could be involved within the maturation process. Previous, subcellular localization data displayed for VDAC1 protein (AS P6) without a permeabilization step a clear superficial staining, presumably the plasma membrane. However, no specific intracellular reactivity was observed. Most likely, the antibody could not pass through the plasma membrane. Thus, to clarify the results, an antibody delivery reagent was included with the AS P6 antibody incubation during the maturation protocol. In this last approach, meiotic maturation was not observed in 48% of the oocytes after 24h of incubation with anti-VDAC1 (AS P6) antibody and the delivery reagent (2 μ l, PULSIN). In the case of the positive (normal maturation protocol plus delivery reagent) and preimmune serum (PI P6 plus delivery reagent) controls the maturation rate was between the expected 80-90%. These preliminary results outline a possible role of VDAC1 protein during maturation, although further studies are necessary to elucidate its detailed function and pathways.

Currently, dose-response curves are planned to determine if diverse antibody concentrations might lead to a difference in the activity. As well, time-response analysis will be directed to observe if VDAC1 protein plays a role during the complete maturation process or if it is triggered at a specific point before or after the germinal vesicle breakdown occurs. GVBD occurs within 9h of release of the oocyte from the follicle in cow (Homa, 1988). A further point would be to clear out the reversibility of the process and to examine if the lack of maturation was not a sign of cell death caused by the blocking treatment. Studies to determine apoptosis should also be performed since it is known that VDAC plays a role during cell death. VDAC can control coupled regulation and cell survival (Gincel *et al.*, 2001). It is involved in apoptotic cell death; the release of cytochrome *c* through VDAC1 is modulated by pro- and anti-apoptotic members of the Bcl2 family.

This work showed that VDAC1 was expressed in the oocytes from the GV to MII stage, and inhibition of VDAC1 activity blocked maturation. The mechanism in which VDAC1 protein participates during the meiotic maturation event is not clear and in order to find a relation within a pathway only speculations are possible at this time. One well established role of VDAC is its function as an ATP diffusion pathway or hexokinase binding protein, so that it seems logical to propose this as one of its tasks. Hexokinases have been found to associate with VDAC, first evidence showed that VDAC could bind the hexokinase receptor on the mitochondria surface (Fiek *et al.*, 1982; Linden *et al.*, 1982a). Also other kinases such as glucokinase, glycerol kinase, mitochondrial creatine kinase and c-Raf kinase are able to bind (Adams *et al.*, 1991; Le, V *et al.*, 2002). The association of cytosolic kinases with VDAC is thought to give a preferential access to the phosphorylated substrates produced in the

mitochondria. In this respect VDAC might be involved in the coupling of the glucose metabolism with oxidative phosphorylation.

It has been well established that eukaryotic cells require filamentous actin to maintain their shape and for migration, growth, polarization, organelle movement, endocytosis/exocytosis, replication and gene regulation. Meiotic maturation in mammalian oocytes is a complex process that involves extensive rearrangement of microtubules and actin filaments as well as other cytoskeleton-associated proteins providing the framework for various dynamic processes. GVBD and meiotic spindle formation are not regulated by microfilaments, but polarized movement of the chromosomes depends on a microfilament mediated process in maturing oocytes (Kim *et al.*, 2000). Actin cytoskeleton is critical to the migration of cytoplasmic organelles, the nucleus during oocyte maturation and fertilization and to cell cleavage during mitosis. In this system VDAC1 appears to interact with cytoskeletal proteins. By affinity chromatography MAP2 (Microtubule associate protein 2) was shown to bind a porin dimer (Linden and Karlsson, 1996). Human recombinant gelsolin, a Ca^{2+} dependent protein that modulates actin assembly and disassembly, was demonstrated to bind directly to VDAC reconstituted in liposomes and to block its activity (Kusano *et al.*, 2000). VDAC1 might act as a mediator of the interactions between mitochondria and cytoskeletal structures. It also might have a role as a docking structure to support the motion and the distribution of mitochondria to high-energy consuming districts in specialized cells (Leterrier *et al.*, 1994). Little is known about the molecules interacting with actin-filaments in the mammalian egg cortex or proteins that connect to the plasma membrane. Cytoskeletal inhibitors showed that microfilaments are crucial for cortical meiotic spindle positioning and maintenance, formation of the first and second polar bodies, incorporation cone formation, pronuclear apposition and cytokinesis (Simerly *et al.*, 1998). Correct positioning and active movement of organelles are essential for oocyte growth, maturation and fertilization. Previous observations also revealed that translocation of mitochondria are co-coordinated with changes in the location of microtubule-organizing centers and that the microtubule-mediated accumulation of mitochondria may be required for nuclear maturation of mouse oocytes (Van Blerkom, 1991). Thus, analysis of microfilament regulation, oocytes chromosome alignment and spindle status of the oocytes should be performed after inhibition of VDAC1 protein during IVM.

As previously discussed, VDAC is involved in calcium regulation; meanwhile, calcium ions are common messengers in intracellular signaling and play a significant role in the regulation of meiosis, resumption and progression of the meiosis to the stage of metaphase II in mammalian oocytes (Homa *et al.*, 1993). Oscillations of intracellular calcium released from

intracellular stores are typical of the resumption of meiosis in mouse oocytes *in vitro* (Carroll, 2001). The importance of calcium ions for meiosis resumption was further underlined by chelating or blocking of intracellular calcium which resulted in inhibition of resumption of meiosis in porcine (Kaufman and Homa, 1993) and bovine oocytes (Homa, 1988; Homa *et al.*, 1993). The inhibition of calcium channels blocked *in vitro* maturation of swine oocytes at the stage of metaphase I (Kaufman and Homa, 1993). During maturation, mitochondria are found in clusters in close proximity to endoplasmic reticulum (ER) membranes. Mitochondria are a source of ATP and the endoplasmic reticulum is the major site of intracellular calcium release. This juxtaposition may allow an efficient transmission of cytosolic calcium signal into the mitochondria and an efficient supply of ATP (Dumollard *et al.*, 2006). VDAC is a key determinant of calcium permeability at ER-mitochondria contacts and thus is responsible for exposing the uptake systems of the inner mitochondrial membrane to the large calcium gradients needed for rapidly accumulating calcium in the organelle upon stimulation (Rapizzi *et al.*, 2002; Shoshan-Barmatz and Israelson, 2005). VDAC plays a global control over mitochondrial metabolism. Mitochondrial dysfunction with resulting compromising of cellular ATP supply is often an essential event leading to necrotic cell death (Lemasters and Holmuhamedov, 2006). VDAC closes early in the evolution of apoptosis with the consequence that mitochondria cannot release ATP or take up ADP and respiratory substrates from the cytosol. VDAC act as a brake on mitochondrial metabolism (Lemasters and Holmuhamedov, 2006) which could arrest the normal meiotic maturation.

Many pathways are involved concerning maturation and the interaction of VDAC1 protein in one of them could be feasible. The results of this work present the first preliminary data of a possible interaction of VDAC1 protein during maturation, adding a further step in the characterization of VDAC. Blocking VDAC1 by anti-VDAC1 antibody reduced significantly the normal maturation rate of bovine oocytes after normal *in vitro* maturation protocols.

4.4 Perspectives

The present study is, in fact, the only one in which VDAC was extensively examined in mammalian gametes, especially in oocytes. Several points need further investigations but this work provides important basic instruments for future research of VDAC in the reproduction area.

The preliminary data obtained in the present study are the basis for further detailed analyzes of the role of VDAC in germ cells. One important point would be to identify VDAC gene

expression levels for the porcine system in order to study possible species-specific differences. As well the gene expression level in single bovine oocytes with respect to the maturation stage should be studied in a quantitative fashion. Such approach may become particularly valuable when connected with a potential relevance of VDAC during maturation. On the protein level one aim of future studies will be to identify subcellular co-localization of polypeptides with possible relevance to better define pathways or functions of VDAC proteins. The assignment of each isoform to organelles would give great progress in the field. The purification of VDAC protein subtypes obtained from spermatozoa would be of further interest, during an attempt to functionally characterize each isoform. This would be of great importance knowing that VDAC2 and VDAC3 isoforms have never been purified from animal tissues and information about VDAC subtype function has only been obtained from recombinant proteins (Xu *et al.*, 1999). It must also be considered that only the basic and preliminaries electrophysiological studies were performed. Wider characterization related to inhibitory and regulatory effects of VDAC subtypes are suggested to be performed. It is planned to carry out further detailed studies on the role of VDAC during *in vitro* maturation in oocytes at the protein and molecular level. Elucidation of mechanism involved during *in vitro* maturation not only promises to increase the efficiency of this technique, but may also help in understanding the signaling mechanism that underlies mammalian meiotic maturation. Possible disturbances in maturation pattern and regulation may have great clinical relevance. The maturation of GV stage oocytes *in vitro* is an emerging technology that in the future may transform the practice of assisted reproduction. Whereas the frameworks are in place for the clinical exploitation of IVM, considerable effort is still required to develop IVM to its full potential. Extensive research is still needed to fully understand and optimize the chain of events which comprise oocyte maturation.

5 Summary

This thesis comprises the study of the expression of VDAC subtypes in porcine and bovine oocytes in GV and MII stage oocytes by means of RT-PCR. The results demonstrate that VDAC1, 2 and 3 subtypes are expressed within oocytes of both species. Subsequently, quantitative expression of VDAC1, 2 and 3 mRNA transcripts in bovine oocytes from follicles with three different diameters was determined (group 1 <3mm; group 2, 4-6mm and group 3, 8-11mm) by real-time RT-PCR. A distinct difference in the relative expression was observed only for VDAC1 which presented down-regulation of expression with a magnitude factor of 2.4 in group 3 compared to group 1.

Immunoblot studies using subtype specific anti-VDAC antibodies and porcine spermatozoa indicated the presence of VDAC1, 2 and 3 in male germ cells. Further characterization of VDAC polypeptides by MALDI-TOF MS and PMF analyses of 2D-gels from hydroxyapatite-celite purified VDAC from porcine spermatozoa protein confirmed the detection of VDAC2. Functional experiments in artificial membranes showed that biochemically isolated VDAC was successfully renatured by demonstrating voltage dependent electrophysiological channel properties and a single conductance of 1.6nS.

In porcine oocytes VDAC1 and VDAC2 protein expression could be demonstrated by immunoblot experiments assaying VDAC proteins that derived from GV and MII stage oocytes. A shift of intensity of protein stain as well as differences in apparent molecular masses were observed with anti-VDAC2 antibody between GV and MII stage oocytes. MALDI-TOF MS and PMF analyses confirmed the presence of VDAC2 protein in GV stage oocytes.

Using specific antisera against synthetic peptide sequences from VDAC subtypes immunohistochemical data suggest the presence of VDAC 1 and 2 in ooplasm of porcine oocytes as well as in the follicle cells with no clear change of localization during folliculogenesis. Subcellular localization of VDAC1 by confocal laser microscopy exhibited a dense arrangement of particular dotted fluorescent labeling over the entire oocyte surface suggesting the presence of VDAC1 in the porcine oocyte plasma membrane. Data obtained from permeabilized oocytes assayed with anti-VDAC1 and anti-VDAC3 antibodies show a clear pattern of spotlike immunofluorescent labeling localized particularly around the cortical area in GV and MII stage oocytes. Anti-VDAC2 immunostaining yielded ring-like clusters structures distributed on the cortical area in some but not in all GV stage oocytes.

Microinjection of matured porcine and bovine oocytes with VDAC protein purified from porcine spermatozoa was performed in order to detect possible oocyte activation and/or calcium oscillation activity. The results showed no clear change of oocyte activity or calcium oscillation after intraooplasmic injection of purified sperm VDAC protein.

Finally, blocking VDAC1 activity in *in vitro* maturing bovine oocytes using anti-VDAC1 antibodies resulted in a significant interruption of physiological maturation events.

These results obtained in this study are the first that show particular biochemical characteristics, distributions and possible functions of VDAC subtypes during maturation and fertilization of porcine and bovine oocytes.

6 Zusammenfassung

Ziel dieser Arbeit war es, das Vorhandensein, die Lokalisation und die mögliche funktionelle Relevanz der VDAC Isoformen VDAC 1, VDAC2 und VDAC3 in porcinen und bovinen Gameten zu untersuchen. Mit Hilfe der RT-PCR wurde die Synthese der VDAC Subtypen in porcinen und bovinen Oozyten unterschiedlicher Entwicklungsstadien (GV- und MII-Stadium) nachgewiesen. In den Oozyten beider Spezies konnte die Expression aller drei Subtypen (VDAC1, 2 und 3) detektiert werden. Zusätzlich zum qualitativen Nachweis erfolgte die quantitative Bestimmung von VDAC1, 2 und 3 mRNA-Transkripten in bovinen Oozyten mittels real-time RT-PCR. Untersucht wurden Oozyten verschiedener Follikelgrößen (Gruppe 1 <3mm; Gruppe 2, 4-6mm und Gruppe 3 8-11mm). Nur für VDAC1 wurde ein relevanter Unterschied in der relativen Expression in Form einer Herunterregulierung der Transkriptmenge in der Größenordnung eines Faktors von 2,4 in der Gruppe 3 verglichen mit der Gruppe 1 beobachtet.

Unter Verwendung subtypen-spezifischer anti-VDAC Antikörper gelang es mit immunbiochemischen Untersuchungsmethoden VDAC1, 2 und 3 Protein in porcinen Spermatozoenproteinextrakten nachzuweisen. Nach der Reinigung der Spermatozoenextrakte über einen Hydroxyapatite-Celite Säule und anschließender Auftrennung in einer 2D-SDS PAGE erfolgte eine weitere Charakterisierung der gewonnenen VDAC Polypeptide mittels MALDI-TOF Massenspektrometrie und PMF-Analyse. Diese Untersuchungen bestätigten eindeutig das Vorhandensein von VDAC2 in Proteinextrakten aus porcinen Spermatozoen. Abschließende Ergebnisse zum Nachweis von VDAC1 und VDAC3 liegen zurzeit noch nicht vor.

Funktionelle Experimente in künstlichen Membranen (Lipid bilayer membrane) zeigten, dass aus porcinen Spermatozoen biochemisch isolierte VDAC Proteine erfolgreich renaturiert werden konnten, was sich in spannungsabhängigen elektrophysiologischen Kanaleigenschaften und einer Einzeleitfähigkeit von 1,6nS zeigte.

Nach Einsatz subtypspezifischer anti-VDAC Antiseren wiesen immunhistochemische Experimente auf das Vorhandensein von VDAC1 und 2 im Ooplasma porciner Oozyten sowie in den sie umgebenden Follikelzellen, ohne sichtbare Veränderung der Lokalisation während der Follikulogenese, hin. Untersuchungen zur subzellulären Lokalisation von VDAC Protein in porcinen Oozyten wurden mittels konfokaler Laser-Mikroskopie durchgeführt. Eine homogen punktförmige Fluoreszenz an der Peripherie nicht permeabilisierter porciner

Oozyten im GV-Stadium nach Verwendung von Anti-VDAC1 Antikörpern legte den Schluss nahe, dass sich VDAC1 in der Plasmamembran befinden könnte. Permeabilisierte Oozyten, die mit Anti-VDAC1 und Anti-VDAC3 Antikörpern inkubiert wurden, wiesen ein klares punktförmiges Fluoreszenzmuster, insbesondere in der kortikale Region der Oozyten im GV- und MII-Stadium, auf. Immunfärbungen mit Anti-VDAC2 Antikörpern zeigten ringartige Strukturen, konzentriert in der kortikalen Region, einiger aber nicht aller untersuchten porcinen Oozyten im GV-Stadium.

Auch in immunbiochemischen Experimenten (SDS-PAGE und Immunoblot) wurden VDAC1 und VDAC2 Proteine in porcinen GV- und MII-Oozyten nachgewiesen. Dabei wurde eine Veränderung in der Immunreaktivität beobachtet und gleichzeitig erfolgte ein Shift einer Proteinbande von 30kDa in Oozyten im GV-Stadium zu 50kDa in Oozyten im MII-Stadium nach Einsatz von Anti-VDAC2 Antikörper. Durch die MALDI-TOF Massenspektrometrie und PMF-Analyse wurde das Vorhandensein von VDAC2 in porcinen Oozyten im GV-Stadium bestätigt.

In Experimenten zur funktionellen Relevanz von VDAC in Säugetiereizellen, wurden aus porcinen Spermatozoen aufgereinigte VDAC-Proteine in maturierte porcine und bovine Oozyten injiziert (intraooplasmatische Injektion). Die Ergebnisse dieser Untersuchungen zeigten, dass keine Eizell-Aktivierung ausgelöst bzw. eine Veränderung der Kalziumoszillationen beobachtet werden konnte.

Schließlich wurde durch die Inkubation von maturierten bovinen Oozyten mit Anti-VDAC1 Antikörpern eine signifikante Verzögerung von physiologischen Maturierungsvorgängen erreicht. Das lässt den Schluss zu, dass VDAC1 in diesem Prozess involviert sein könnte und durch die Antikörper zumindest partiell funktionell blockiert wurde.

Die Ergebnisse dieser Arbeit zeigen erstmals konkrete biochemische Charakteristika sowie eine spezifische Lokalisation von VDAC Subtypen in porcinen und bovinen Oozyten und geben erste Hinweise auf eine mögliche Funktion von VDAC1 während der Maturation in bovinen Oozyten.

7 Bibliography

Abrecht H, Wattiez R, Ruyschaert JM, and Homble F (2000) Purification and characterization of two voltage-dependent anion channel isoforms from plant seeds. *Plant Physiol*, 124, 1181-1190.

Adams V, Griffin L, Towbin J, Gelb B, Worley K, and McCabe ER (1991) Porin interaction with hexokinase and glycerol kinase: metabolic microcompartmentation at the outer mitochondrial membrane. *Biochem Med Metab Biol*, 45, 271-291.

Aires V, Wunsch A, Schneider X, Hinsch E, and Hinsch KD (2003) Localisation of porin subtypes in bovine spermatozoa. *Vet Med Austria*, 1, 90.

Aljamal JA, Genchi G, De P, V, Stefanizzi L, De Santis A, Benz R, and Palmieri F (1993) Purification and Characterization of Porin from Corn (*Zea mays* L.) Mitochondria. *Plant Physiol*, 102, 615-621.

Amano T, Mori T, and Watanabe T (2004) Activation and development of porcine oocytes matured *in vitro* following injection of inositol 1,4,5-trisphosphate. *Anim Reprod Sci*, 80, 101-112.

Anflous K, Armstrong DD, and Craigen WJ (2001) Altered mitochondrial sensitivity for ADP and maintenance of creatine-stimulated respiration in oxidative striated muscles from VDAC1-deficient mice. *J Biol Chem*, 276, 1954-1960.

Babel D, Walter G, Gotz H, Thinner FP, Jurgens L, Konig U, and Hilschmann N (1991) Studies on human porin. VI. Production and characterization of eight monoclonal mouse antibodies against the human VDAC "Porin 31HL" and their application for histotopological studies in human skeletal muscle. *Biol Chem Hoppe Seyler*, 372, 1027-1034.

Baccetti B, Pallini V, and Burrini AG (1973) The accessory fibers of the sperm tail. I. Structure and chemical composition of the bull "coarse fibers". *J Submicr Cytol*, 5, 237-256.

Barnouin K (2004) Two-dimensional gel electrophoresis for analysis of protein complexes. *Methods Mol Biol*, 261, 479-498.

Bathori G, Fonyo A, and Ligeti E (1995) Trace amounts of Triton X-100 modify the inhibitor sensitivity of the mitochondrial porin. *Biochim Biophys Acta*, 1234, 249-254.

Bathori G, Parolini I, Tombola F, Szabo I, Messina A, Oliva M, De Pinto V, Lisanti M, Sargiacomo M, and Zoratti M (1999) Porin is present in the plasma membrane where it is concentrated in caveolae and caveolae-related domains. *J Biol Chem*, 274, 29607-29612.

Bedford SJ, Kurokawa M, Hinrichs K, and Fissore RA (2003) Intracellular calcium oscillations and activation in horse oocytes injected with stallion sperm extracts or spermatozoa. *Reproduction*, 126, 489-499.

Ben Yosef D and Shalgi R (2001) Oocyte activation: lessons from human infertility. *Trends Mol Med*, 7, 163-169.

Benz R (1985) Porin from bacterial and mitochondrial outer membranes. *CRC Crit Rev Biochem*, 19, 145-190.

Benz R (1990) Biophysical properties of porin pores from mitochondrial outer membrane of eukaryotic cells. *Experientia*, 46, 131-137.

Benz R (1994) Permeation of hydrophilic solutes through mitochondrial outer membranes: review on mitochondrial porins. *Biochim Biophys Acta*, 1197, 167-196.

Benz R, Janko K, and Lauger P (1979) Ionic selectivity of pores formed by the matrix protein (porin) of *Escherichia coli*. *Biochim Biophys Acta*, 551, 238-247.

Benz R, Janko K, Boos W, and Lauger P (1978) Formation of large, ion-permeable membrane channels by the matrix protein (porin) of *Escherichia coli*. *Biochim Biophys Acta*, 511, 305-319.

Berkane E, Orlik F, Charbit A, Danelon C, Fournier D, Benz R, and Winterhalter M (2005) Nanopores: maltoporin channel as a sensor for maltodextrin and lambda-phage. *J Nanobiotechnology*, 3, 3.

Bernardi P, Petronilli V, Di Lisa F, and Forte M (2001) A mitochondrial perspective on cell death. *Trends Biochem Sci*, 26, 112-117.

Beutner G, Ruck A, Riede B, and Brdiczka D (1998) Complexes between porin, hexokinase, mitochondrial creatine kinase and adenylate translocator display properties of the permeability

transition pore. Implication for regulation of permeability transition by the kinases. *Biochim Biophys Acta*, 1368, 7-18.

Bilodeau-Goeseels S and Schultz GA (1997) Changes in the relative abundance of various housekeeping gene transcripts in *in vitro*-produced early bovine embryos. *Mol Reprod Dev*, 47, 413-420.

Blachly-Dyson E and Forte M (2001) VDAC channels. *IUBMB Life*, 52, 113-118.

Blachly-Dyson E, Zambronicz EB, Yu WH, Adams V, McCabe ER, Adelman J, Colombini M, and Forte M (1993) Cloning and functional expression in yeast of two human isoforms of the outer mitochondrial membrane channel, the voltage-dependent anion channel. *J Biol Chem*, 268, 1835-1841.

Bogner K, Hinsch KD, Nayudu P, Konrad L, Cassara C, and Hinsch E (2004) Localization and synthesis of zona pellucida proteins in the marmoset monkey (*Callithrix jacchus*) ovary. *Mol Hum Reprod*, 10, 481-488.

Bradley FM, Meth BM, and Bellve AR (1981) Structural proteins of the mouse spermatozoan tail: an electrophoretic analysis. *Biol Reprod*, 24, 691-701.

Buhler S, Michels J, Wendt S, Ruck A, Brdiczka D, Welte W, and Przybylski M (1998) Mass spectrometric mapping of ion channel proteins (porins) and identification of their supramolecular membrane assembly. *Proteins, Suppl* 2, 63-73.

Bustin SA (2000) Absolute quantification of mRNA using real-time reverse transcription polymerase chain reaction assays. *J Mol Endocrinol*, 25, 169-193.

Bustin SA, Benes V, Nolan T, and Pfaffl MW (2005) Quantitative real-time RT-PCR--a perspective. *J Mol Endocrinol*, 34, 597-601.

Bustin SA and Nolan T (2004) Pitfalls of quantitative real-time reverse-transcription polymerase chain reaction. *J Biomol Tech*, 15, 155-166.

Carroll J (2001) The initiation and regulation of Ca^{2+} signalling at fertilization in mammals. *Semin Cell Dev Biol*, 12, 37-43.

Casadio R, Jacoboni I, Messina A, and De P, V (2002) A 3D model of the voltage-dependent anion channel (VDAC). FEBS Lett, 520, 1-7.

Cheng EH, Sheiko TV, Fisher JK, Craigen WJ, and Korsmeyer SJ (2003) VDAC2 inhibits BAK activation and mitochondrial apoptosis. Science, 301, 513-517.

Choi JY, Lee EY, Cheong HT, Yoon BK, Bae DS, and Choi DS (2004) Effects of activation timing on the fertilization rate and early embryo development in porcine ROSI procedure. J Assist Reprod Genet, 21, 329-334.

Colombini M (2004) VDAC: the channel at the interface between mitochondria and the cytosol. Mol Cell Biochem, 256-257, 107-115.

Colombini M, Yeung CL, Tung J, and Konig T (1987) The mitochondrial outer membrane channel, VDAC, is regulated by a synthetic polyanion. Biochim Biophys Acta, 905, 279-286.

Cox LJ, Larman MG, Saunders CM, Hashimoto K, Swann K, and Lai FA (2002) Sperm phospholipase C zeta from humans and cynomolgus monkeys triggers Ca^{2+} oscillations, activation and development of mouse oocytes. Reproduction, 124, 611-623.

Cran DG (1985) Qualitative and quantitative structural changes during pig oocyte maturation. J Reprod Fertil, 74, 237-245.

Crompton M, Barksby E, Johnson N, and Capano M (2002) Mitochondrial intermembrane junctional complexes and their involvement in cell death. Biochimie, 84, 143-152.

De Pinto V, Benz R, Caggese C, and Palmieri F (1989) Characterization of the mitochondrial porin from *Drosophila melanogaster*. Biochim Biophys Acta, 987, 1-7.

De Pinto V, Messina A, Accardi R, Aiello R, Guarino F, Tomasello MF, Tommasino M, Tasco G, Casadio R, Benz R et al (2003) New functions of an old protein: the eukaryotic porin or voltage dependent anion selective channel (VDAC). Ital J Biochem, 52, 17-24.

De Pinto V, Prezioso G, and Palmieri F (1987a) A simple and rapid method for the purification of the mitochondrial porin from mammalian tissues. Biochim Biophys Acta, 905, 499-502.

De Pinto V, Ludwig O, Krause J, Benz R, and Palmieri F (1987b) Porin pores of mitochondrial outer membranes from high and low eukaryotic cells: biochemical and biophysical characterization. *Biochim Biophys Acta*, 894, 109-119.

De Sousa PA, Westhusin ME, and Watson AJ (1998) Analysis of variation in relative mRNA abundance for specific gene transcripts in single bovine oocytes and early embryos. *Mol Reprod Dev*, 49, 119-130.

Dellmann D and Eurell J (1998) *Textbook of Veterinary Histology*. 5th ed. edn, Williams & Wilkins, Baltimore, Maryland.

Dermietzel R, Hwang TK, Buettner R, Hofer A, Dotzler E, Kremer M, Deutzmann R, Thinnies FP, Fishman GI, and Spray DC (1994) Cloning and *in situ* localization of a brain-derived porin that constitutes a large-conductance anion channel in astrocytic plasma membranes. *Proc Natl Acad Sci U S A*, 91, 499-503.

Devroey P and Van Steirteghem A (2004) A review of ten years experience of ICSI. *Hum Reprod Update*, 10, 19-28.

Distler AM, Kerner J, Peterman SM, and Hoppel CL (2006) A targeted proteomic approach for the analysis of rat liver mitochondrial outer membrane proteins with extensive sequence coverage. *Anal Biochem*, 356, 18-29.

Dozortsev D, Rybouchkin A, De Sutter P, Qian C, and Dhont M (1995) Human oocyte activation following intracytoplasmic injection: the role of the sperm cell. *Hum Reprod*, 10, 403-407.

Ducibella T, Kurasawa S, Rangarajan S, Kopf GS, and Schultz RM (1990) Precocious loss of cortical granules during mouse oocyte meiotic maturation and correlation with an egg-induced modification of the zona pellucida. *Dev Biol*, 137, 46-55.

Dumollard R, Duchen M, and Sardet C (2006) Calcium signals and mitochondria at fertilisation. *Semin Cell Dev Biol*, 17, 314-323.

Eckert J and Niemann H (1996) Effects of platelet-derived growth factor (PDGF) on the *in vitro* production of bovine embryos in protein-free media. *Theriogenology*, 46, 307-320.

Eddy EM and O'Brien D. (1994) The Spermatozoon. In Knobil E and Neill JD (eds) The Physiology of Reproduction. Raven Press, New York, pp. 29-77.

Fan HY and Sun QY (2004) Involvement of mitogen-activated protein kinase cascade during oocyte maturation and fertilization in mammals. Biol Reprod, 70, 535-547.

Fawcett DW (1975) The mammalian spermatozoon. Dev Biol, 44, 394-436.

Fiek C, Benz R, Roos N, and Brdiczka D (1982) Evidence for identity between the hexokinase-binding protein and the mitochondrial porin in the outer membrane of rat liver mitochondria. Biochim Biophys Acta, 688, 429-440.

Fissore RA, Dobrinsky JR, Balise JJ, Duby RT, and Robl JM (1992) Patterns of intracellular Ca^{2+} concentrations in fertilized bovine eggs. Biol Reprod, 47, 960-969.

Freitag H, Neupert W, and Benz R (1982) Purification and characterisation of a pore protein of the outer mitochondrial membrane from *Neurospora crassa*. Eur J Biochem, 123, 629-636.

Galli C, Vassiliev I, Lagutina I, Galli A, and Lazzari G (2003) Bovine embryo development following ICSI: effect of activation, sperm capacitation and pre-treatment with dithiothreitol. Theriogenology, 60, 1467-1480.

Gilbert SF (2000) Developmental Biology. 6th ed. edn, Sinauer Associates, Inc., Sunderland, Massachusetts.

Gincel D, Silberberg SD, and Shoshan-Barmatz V (2000) Modulation of the Voltage-Dependent Anion Channel (VDAC) by Glutamate1. J Bioenerg Biomembr, 32, 571-583.

Gincel D, Vardi N, and Shoshan-Barmatz V (2002) Retinal voltage-dependent anion channel: characterization and cellular localization. Invest Ophthalmol Vis Sci, 43, 2097-2104.

Gincel D, Zaid H, and Shoshan-Barmatz V (2001) Calcium binding and translocation by the voltage-dependent anion channel: a possible regulatory mechanism in mitochondrial function. Biochem J, 358, 147-155.

Guarino F, Specchia V, Zapparoli G, Messina A, Aiello R, Bozzetti MP, and De P, V (2006) Expression and localization in spermatozoa of the mitochondrial porin isoform 2 in *Drosophila melanogaster*. *Biochem Biophys Res Commun*, 346, 665-670.

Guibert B, Dermietzel R, and Siemen D (1998) Large conductance channel in plasma membranes of astrocytic cells is functionally related to mitochondrial VDAC-channels. *Int J Biochem Cell Biol*, 30, 379-391.

Ha H, Hajek P, Bedwell DM, and Burrows PD (1993) A mitochondrial porin cDNA predicts the existence of multiple human porins. *J Biol Chem*, 268, 12143-12149.

Hajnoczky G, Csordas G, and Yi M (2002) Old players in a new role: mitochondria-associated membranes, VDAC, and ryanodine receptors as contributors to calcium signal propagation from endoplasmic reticulum to the mitochondria. *Cell Calcium*, 32, 363-377.

Heins L, Mentzel H, Schmid A, Benz R, and Schmitz UK (1994) Biochemical, molecular, and functional characterization of porin isoforms from potato mitochondria. *J Biol Chem*, 269, 26402-26410.

Hellman U, Wernstedt C, Genez J, and Heldin CH (1995) Improvement of an "In-Gel" digestion procedure for the micropreparation of internal protein fragments for amino acid sequencing. *Anal Biochem*, 224, 451-455.

Heyers S, Sousa M, Cangir O, Schmoll F, Schellander K, van d, V, and Montag M (2000) Activation of mouse oocytes requires multiple sperm factors but not sperm PLCgamma1. *Mol Cell Endocrinol*, 166, 51-57.

Hinsch E, Boehm JG, Groeger S, Mueller-Schloesser F, and Hinsch KD (2003) Identification of cytokeratins in bovine sperm outer dense fibre fractions. *Reprod Domest Anim*, 38, 155-160.

Hinsch KD, Asmarinah, Hinsch E, and Konrad L (2001) VDAC2 (porin-2) expression pattern and localization in the bovine testis. *Biochim Biophys Acta*, 1518, 329-333.

Hinsch KD, De Pinto V, Aires VA, Schneider X, Messina A, and Hinsch E (2004) Voltage-dependent anion-selective channels VDAC2 and VDAC3 are abundant proteins in bovine outer dense fibers, a cytoskeletal component of the sperm flagellum. *J Biol Chem*, 279, 15281-15288.

Homa ST (1988) Effects of cyclic AMP on the spontaneous meiotic maturation of cumulus-free bovine oocytes cultured in chemically defined medium. *J Exp Zool*, 248, 222-231.

Homa ST, Carroll J, and Swann K (1993) The role of calcium in mammalian oocyte maturation and egg activation. *Hum Reprod*, 8, 1274-1281.

Inaba K (2003) Molecular architecture of the sperm flagella: molecules for motility and signaling. *Zoolog Sci*, 20, 1043-1056.

Jeong YJ, Choi HW, Shin HS, Cui XS, Kim NH, Gerton GL, and Jun JH (2005) Optimization of real time RT-PCR methods for the analysis of gene expression in mouse eggs and preimplantation embryos. *Mol Reprod Dev*, 71, 284-289.

Johnson MH and Everitt B (1995) *Essential Reproduction*. Fourth ed. edn, Blackwell Science, USA.

Junankar PR, Dulhunty AF, Curtis SM, Pace SM, and Thinnes FP (1995) Porin-type 1 proteins in sarcoplasmic reticulum and plasmalemma of striated muscle fibres. *J Muscle Res Cell Motil*, 16, 595-610.

Jurgens L, Kleineke J, Brdiczka D, Thinnes FP, and Hilschmann N (1995) Localization of type-1 porin channel (VDAC) in the sarcoplasmatic reticulum. *Biol Chem Hoppe Seyler*, 376, 685-689.

Kaufman ML and Homa ST (1993) Defining a role for calcium in the resumption and progression of meiosis in the pig oocyte. *J Exp Zool*, 265, 69-76.

Kim NH, Cho SK, Choi SH, Kim EY, Park SP, and Lim JH (2000) The distribution and requirements of microtubules and microfilaments in bovine oocytes during *in vitro* maturation. *Zygote*, 8, 25-32.

Kimura Y and Yanagimachi R (1995) Intracytoplasmic sperm injection in the mouse. *Biol Reprod*, 52, 709-720.

Kimura Y, Yanagimachi R, Kuretake S, Bortkiewicz H, Perry AC, and Yanagimachi H (1998) Analysis of mouse oocyte activation suggests the involvement of sperm perinuclear material. *Biol Reprod*, 58, 1407-1415.

Kline D and Kline JT (1992) Repetitive calcium transients and the role of calcium in exocytosis and cell cycle activation in the mouse egg. *Dev Biol*, 149, 80-89.

Knijn HM, Wrenzycki C, Hendriksen PJ, Vos PL, Herrmann D, van der Weijden GC, Niemann H, and Dieleman SJ (2002) Effects of oocyte maturation regimen on the relative abundance of gene transcripts in bovine blastocysts derived *in vitro* or *in vivo*. *Reproduction*, 124, 365-375.

Krimmer T, Rapaport D, Ryan MT, Meisinger C, Kassenbrock CK, Blachly-Dyson E, Forte M, Douglas MG, Neupert W, Nargang FE et al (2001) Biogenesis of porin of the outer mitochondrial membrane involves an import pathway via receptors and the general import pore of the TOM complex. *J Cell Biol*, 152, 289-300.

Kusano H, Shimizu S, Koya RC, Fujita H, Kamada S, Kuzumaki N, and Tsujimoto Y (2000) Human gelsolin prevents apoptosis by inhibiting apoptotic mitochondrial changes via closing VDAC. *Oncogene*, 19, 4807-4814.

Laemmli UK (1970) Cleavage of structural proteins during assembly of the head of bacteriophage T4. *Nature*, 227, 680-685.

Le M, V, Troppmair J, Benz R, and Rapp UR (2002) Negative regulation of mitochondrial VDAC channels by C-Raf kinase. *BMC Cell Biol*, 3, 14.

Lechniak D (2002) Quantitative aspect of gene expression analysis in mammalian oocytes and embryos. *Reprod Biol*, 2, 229-241.

Lehmann T, Volkl A, and Fahimi HD (1995) The importance of tissue fixation for light microscopic immunohistochemical localization of peroxisomal proteins: the superiority of Carnoy's fixative over Baker's formalin and Bouin's solution. *Histochem Cell Biol*, 103, 187-195.

Lemasters JJ and Holmuhamedov E (2006) Voltage-dependent anion channel (VDAC) as mitochondrial governor--thinking outside the box. *Biochim Biophys Acta*, 1762, 181-190.

Leterrier JF, Rusakov DA, Nelson BD, and Linden M (1994) Interactions between brain mitochondria and cytoskeleton: evidence for specialized outer membrane domains involved in the association of cytoskeleton-associated proteins to mitochondria *in situ* and *in vitro*. *Microsc Res Tech*, 27, 233-261.

Lewis TM, Roberts ML, and Bretag AH (1994) Immunolabelling for VDAC, the mitochondrial voltage-dependent anion channel, on sarcoplasmic reticulum from amphibian skeletal muscle. *Neurosci Lett*, 181, 83-86.

-
- Liberatori S, Canas B, Tani C, Bini L, Buonocore G, Godovac-Zimmermann J, Mishra OP, Delivoria-Papadopoulos M, Bracci R, and Pallini V (2004) Proteomic approach to the identification of voltage-dependent anion channel protein isoforms in guinea pig brain synaptosomes. *Proteomics*, 4, 1335-1340.
- Linden M, Gellerfors P, and Nelson BD (1982a) Pore protein and the hexokinase-binding protein from the outer membrane of rat liver mitochondria are identical. *FEBS Lett*, 141, 189-192.
- Linden M, Gellerfors P, and Nelson BD (1982b) Purification of a protein having pore forming activity from the rat liver mitochondrial outer membrane. *Biochem J*, 208, 77-82.
- Linden M and Karlsson G (1996) Identification of porin as a binding site for MAP2. *Biochem Biophys Res Commun*, 218, 833-836.
- Lisanti MP, Scherer PE, Vidugiriene J, Tang Z, Hermanowski-Vosatka A, Tu YH, Cook RF, and Sargiacomo M (1994) Characterization of caveolin-rich membrane domains isolated from an endothelial-rich source: implications for human disease. *J Cell Biol*, 126, 111-126.
- Liu L, Ju JC, and Yang X (1998) Differential inactivation of maturation-promoting factor and mitogen-activated protein kinase following parthenogenetic activation of bovine oocytes. *Biol Reprod*, 59, 537-545.
- Liu L and Yang X (1999) Interplay of maturation-promoting factor and mitogen-activated protein kinase inactivation during metaphase-to-interphase transition of activated bovine oocytes. *Biol Reprod*, 61, 1-7.
- Liu W and Saint DA (2002) A new quantitative method of real time reverse transcription polymerase chain reaction assay based on simulation of polymerase chain reaction kinetics. *Anal Biochem*, 302, 52-59.
- Long CR, Dobrinsky JR, and Johnson LA (1999) *In vitro* production of pig embryos: comparisons of culture media and boars. *Theriogenology*, 51, 1375-1390.
- Ludwig O, Krause J, Hay R, and Benz R (1988) Purification and characterization of the pore forming protein of yeast mitochondrial outer membrane. *Eur Biophys J*, 15, 269-276.
-

-
- Machatkova M, Krausova K, Jokesova E, and Tomanek M (2004) Developmental competence of bovine oocytes: effects of follicle size and the phase of follicular wave on *in vitro* embryo production. *Theriogenology*, 61, 329-335.
- Malcuit C, Kurokawa M, and Fissore RA (2006a) Calcium oscillations and mammalian egg activation. *J Cell Physiol*, 206, 565-573.
- Malcuit C, Maserati M, Takahashi Y, Page R, and Fissore RA (2006b) Intracytoplasmic sperm injection in the bovine induces abnormal $[Ca^{2+}]_i$ responses and oocyte activation. *Reprod Fertil Dev*, 18, 39-51.
- McEnery MW, Snowman AM, Trifiletti RR, and Snyder SH (1992) Isolation of the mitochondrial benzodiazepine receptor: association with the voltage-dependent anion channel and the adenine nucleotide carrier. *Proc Natl Acad Sci U S A*, 89, 3170-3174.
- McGraw S, Robert C, Massicotte L, and Sirard MA (2003) Quantification of histone acetyltransferase and histone deacetylase transcripts during early bovine embryo development. *Biol Reprod*, 68, 383-389.
- Meinecke B and Meinecke-Tillmann S (1979) Effects of gonadotropins on oocyte maturation and progesterone production by porcine ovarian follicles cultured *in vitro*. *Theriogenology*, 11, 351-365.
- Meinecke B and Meinecke-Tillmann S (1993) Effects of alpha-amanitin on nuclear maturation of porcine oocytes *in vitro*. *J Reprod Fertil*, 98, 195-201.
- Mihara K and Sato R (1985) Molecular cloning and sequencing of cDNA for yeast porin, an outer mitochondrial membrane protein: a search for targeting signal in the primary structure. *EMBO J*, 4, 769-774.
- Moor RM, Mattioli M, Ding J, and Nagai T (1990) Maturation of pig oocytes *in vivo* and *in vitro*. *J Reprod Fertil Suppl*, 40, 197-210.
- Mourot M, Dufort I, Gravel C, Algriany O, Dieleman S, and Sirard MA (2006) The influence of follicle size, FSH-enriched maturation medium, and early cleavage on bovine oocyte maternal mRNA levels. *Mol Reprod Dev*, 73, 1367-1379.
-

Okada SF, O'Neal WK, Huang P, Nicholas RA, Ostrowski LE, Craigen WJ, Lazarowski ER, and Boucher RC (2004) Voltage-dependent anion channel-1 (VDAC-1) contributes to ATP release and cell volume regulation in murine cells. *J Gen Physiol*, 124, 513-526.

Palermo GD, Schlegel PN, Colombero LT, Zaninovic N, Moy F, and Rosenwaks Z (1996) Aggressive sperm immobilization prior to intracytoplasmic sperm injection with immature spermatozoa improves fertilization and pregnancy rates. *Hum Reprod*, 11, 1023-1029.

Petr J, Rozinek J, Jilek F, and Urbankova D (2000) Activation of porcine oocytes using cyclopiazonic acid, an inhibitor of calcium-dependent ATPases. *J Exp Zool*, 287, 304-315.

Petters RM and Wells KD (1993) Culture of pig embryos. *J Reprod Fertil Suppl*, 48, 61-73.

Pfaffl MW, Horgan GW, and Dempfle L (2002) Relative expression software tool (REST) for group-wise comparison and statistical analysis of relative expression results in real-time PCR. *Nucleic Acids Res*, 30, e36.

Rabilloud T (2002) Two-dimensional gel electrophoresis in proteomics: old, old fashioned, but it still climbs up the mountains. *Proteomics*, 2, 3-10.

Rahmani Z, Maunoury C, and Siddiqui A (1998) Isolation of a novel human voltage-dependent anion channel gene. *Eur J Hum Genet*, 6, 337-340.

Ramakers C, Ruijter JM, Deprez RH, and Moorman AF (2003) Assumption-free analysis of quantitative real-time polymerase chain reaction (PCR) data. *Neurosci Lett*, 339, 62-66.

Rapizzi E, Pinton P, Szabadkai G, Wieckowski MR, Vandecasteele G, Baird G, Tuft RA, Fogarty KE, and Rizzuto R (2002) Recombinant expression of the voltage-dependent anion channel enhances the transfer of Ca^{2+} microdomains to mitochondria. *J Cell Biol*, 159, 613-624.

Rath D, Long CR, Dobrinsky JR, Welch GR, Schreier LL, and Johnson LA (1999) *In vitro* production of sexed embryos for gender preselection: high-speed sorting of X-chromosome-bearing sperm to produce pigs after embryo transfer. *J Anim Sci*, 77, 3346-3352.

Raz T and Shalgi R (1998) Early events in mammalian egg activation. *Hum Reprod*, 13 Suppl 4, 133-145.

Razani B, Woodman SE, and Lisanti MP (2002) Caveolae: from cell biology to animal physiology. *Pharmacol Rev*, 54, 431-467.

Reymann S, Florke H, Heiden M, Jakob C, Stadtmüller U, Steinacker P, Lalk VE, Pardowitz I, and Thinner FP (1995) Further evidence for multitopological localization of mammalian porin (VDAC) in the plasmalemma forming part of a chloride channel complex affected in cystic fibrosis and encephalomyopathy. *Biochem Mol Med*, 54, 75-87.

Reymann S, Haase W, Krick W, Burckhardt G, and Thinner FP (1998) Endosomes: another extra-mitochondrial location of type-1 porin/voltage-dependent anion-selective channels. *Pflügers Arch*, 436, 478-480.

Reymann S, Kiafard Z, Rohm B, Strutz N, Hesse D, Kratzin HD, Zimmermann B, Thinner FP, and Hilschmann N (1999) Purification procedure and monoclonal antibodies: two instruments for research on vertebrate porins. *Anal Biochem*, 274, 289-295.

Rice A, Parrington J, Jones KT, and Swann K (2000) Mammalian sperm contain a Ca^{2+} -sensitive phospholipase C activity that can generate $\text{InsP}(3)$ from $\text{PIP}(2)$ associated with intracellular organelles. *Dev Biol*, 228, 125-135.

Robert C, McGraw S, Massicotte L, Pravetoni M, Gandolfi F, and Sirard MA (2002) Quantification of housekeeping transcript levels during the development of bovine preimplantation embryos. *Biol Reprod*, 67, 1465-1472.

Roman I, Figys J, Steurs G, and Zizi M (2006) Direct measurement of VDAC-actin interaction by surface plasmon resonance. *Biochim Biophys Acta*, 1758, 479-486.

Rostovtseva T and Colombini M (1996) ATP flux is controlled by a voltage-gated channel from the mitochondrial outer membrane. *J Biol Chem*, 271, 28006-28008.

Sabirov RZ, Sheiko T, Liu H, Deng D, Okada Y, and Craigen WJ (2006) Genetic demonstration that the plasma membrane maxianion channel and voltage-dependent anion channels are unrelated proteins. *J Biol Chem*, 281, 1897-1904.

Saling PM, Sowinski J, and Storey BT (1979) An ultrastructural study of epididymal mouse spermatozoa binding to zonae pellucidae *in vitro*: sequential relationship to the acrosome reaction. *J Cell Biol*, 83, 229-238.

Sampson MJ, Decker WK, Beaudet AL, Ruitenbeek W, Armstrong D, Hicks MJ, and Craigen WJ (2001) Immotile sperm and infertility in mice lacking mitochondrial voltage-dependent anion channel type 3. *J Biol Chem*, 276, 39206-39212.

Sampson MJ, Lovell RS, and Craigen WJ (1996) Isolation, characterization, and mapping of two mouse mitochondrial voltage-dependent anion channel isoforms. *Genomics*, 33, 283-288.

Sampson MJ, Lovell RS, and Craigen WJ (1997) The murine voltage-dependent anion channel gene family. Conserved structure and function. *J Biol Chem*, 272, 18966-18973.

Sathananthan AH, Selvaraj K, Girijashankar ML, Ganesh V, Selvaraj P, and Trounson AO (2006) From oogonia to mature oocytes: inactivation of the maternal centrosome in humans. *Microsc Res Tech*, 69, 396-407.

Sato K, Sato M, Audhya A, Oegema K, Schweinsberg P, and Grant BD (2006) Dynamic regulation of caveolin-1 trafficking in the germ line and embryo of *Caenorhabditis elegans*. *Mol Biol Cell*, 17, 3085-3094.

Saunders CM, Larman MG, Parrington J, Cox LJ, Royse J, Blayney LM, Swann K, and Lai FA (2002) PLC zeta: a sperm-specific trigger of Ca^{2+} oscillations in eggs and embryo development. *Development*, 129, 3533-3544.

Schein SJ, Colombini M, and Finkelstein A (1976) Reconstitution in planar lipid bilayers of a voltage-dependent anion-selective channel obtained from paramecium mitochondria. *J Membr Biol*, 30, 99-120.

Schwarzer C, Barnikol-Watanabe S, Thinnies FP, and Hilschmann N (2002) Voltage-dependent anion-selective channel (VDAC) interacts with the dynein light chain Tctex1 and the heat-shock protein PBP74. *Int J Biochem Cell Biol*, 34, 1059-1070.

Schwarzer C, Becker S, Awni LA, Cole T, Merker R, Barnikol-Watanabe S, Thinnies FP, and Hilschmann N (2000) Human voltage-dependent anion-selective channel expressed in the plasmalemma of *Xenopus laevis* oocytes. *Int J Biochem Cell Biol*, 32, 1075-1084.

Shafir I, Feng W, and Shoshan-Barmatz V (1998) Dicyclohexylcarbodiimide interaction with the voltage-dependent anion channel from sarcoplasmic reticulum. *Eur J Biochem*, 253, 627-636.

Shimizu S, Matsuoka Y, Shinohara Y, Yoneda Y, and Tsujimoto Y (2001) Essential role of voltage-dependent anion channel in various forms of apoptosis in mammalian cells. *J Cell Biol*, 152, 237-250.

Shinohara Y, Ishida T, Hino M, Yamazaki N, Baba Y, and Terada H (2000) Characterization of porin isoforms expressed in tumor cells. *Eur J Biochem*, 267, 6067-6073.

Shoshan-Barmatz V and Gincel D (2003) The voltage-dependent anion channel: characterization, modulation, and role in mitochondrial function in cell life and death. *Cell Biochem Biophys*, 39, 279-292.

Shoshan-Barmatz V, Hadad N, Feng W, Shafir I, Orr I, Varsanyi M, and Heilmeyer LM (1996) VDAC/porin is present in sarcoplasmic reticulum from skeletal muscle. *FEBS Lett*, 386, 205-210.

Shoshan-Barmatz V and Israelson A (2005) The voltage-dependent anion channel in endoplasmic/sarcoplasmic reticulum: characterization, modulation and possible function. *J Membr Biol*, 204, 57-66.

Shoshan-Barmatz V, Israelson A, Brdiczka D, and Sheu SS (2006) The voltage-dependent anion channel (VDAC): function in intracellular signalling, cell life and cell death. *Curr Pharm Des*, 12, 2249-2270.

Simerly C, Nowak G, de Lanerolle P, and Schatten G (1998) Differential expression and functions of cortical myosin IIA and IIB isotypes during meiotic maturation, fertilization, and mitosis in mouse oocytes and embryos. *Mol Biol Cell*, 9, 2509-2525.

Steinacker P, Awni LA, Becker S, Cole T, Reymann S, Hesse D, Kratzin HD, Morris-Wortmann C, Schwarzer C, Thinner FP et al (2000) The plasma membrane of *Xenopus laevis* oocytes contains voltage-dependent anion-selective porin channels. *Int J Biochem Cell Biol*, 32, 225-234.

Stricker SA, Swann K, Jones KT, and Fissore RA (2000) Injections of porcine sperm extracts trigger fertilization-like calcium oscillations in oocytes of a marine worm. *Exp Cell Res*, 257, 341-347.

Sun FZ, Bradshaw JP, Galli C, and Moor RM (1994) Changes in intracellular calcium concentration in bovine oocytes following penetration by spermatozoa. *J Reprod Fertil*, 101, 713-719.

Sun QY, Wu GM, Lai L, Park KW, Cabot R, Cheong HT, Day BN, Prather RS, and Schatten H (2001) Translocation of active mitochondria during pig oocyte maturation, fertilization and early embryo development *in vitro*. *Reproduction*, 122, 155-163.

Swann K (1994) Ca^{2+} oscillations and sensitization of Ca^{2+} release in unfertilized mouse eggs injected with a sperm factor. *Cell Calcium*, 15, 331-339.

Swann K and Parrington J (1999) Mechanism of Ca^{2+} release at fertilization in mammals. *J Exp Zool*, 285, 267-275.

Thinnes FP (1992) Evidence for extra-mitochondrial localization of the VDAC/porin channel in eucaryotic cells. *J Bioenerg Biomembr*, 24, 71-75.

Thinnes FP, Gotz H, Kayser H, Benz R, Schmidt WE, Kratzin HD, and Hilschmann N (1989) Identification of human porins. I. Purification of a porin from human B-lymphocytes (Porin 31HL) and the topochemical proof of its expression on the plasmalemma of the progenitor cell. *Biol Chem Hoppe Seyler*, 370, 1253-1264.

Thinnes FP, Hellmann KP, Hellmann T, Merker R, Brockhaus-Pruchniewicz U, Schwarzer C, Walter G, Gotz H, and Hilschmann N (2000a) Studies on human porin XXII: cell membrane integrated human porin channels are involved in regulatory volume decrease (RVD) of HeLa cells. *Mol Genet Metab*, 69, 331-337.

Thinnes FP, Hellmann KP, Hellmann T, Merker R, Schwarzer C, Walter G, Gotz H, and Hilschmann N (2000b) Studies on human porin XXI: gadolinium opens Up cell membrane standing porin channels making way for the osmolytes chloride or taurine-A putative approach to activate the alternate chloride channel in cystic fibrosis. *Mol Genet Metab*, 69, 240-251.

Tosti E (2006) Calcium ion currents mediating oocyte maturation events. *Reprod Biol Endocrinol*, 4, 26.

Van Blerkom J (1991) Microtubule mediation of cytoplasmic and nuclear maturation during the early stages of resumed meiosis in cultured mouse oocytes. *Proc Natl Acad Sci U S A*, 88, 5031-5035.

Wang WH, Abeydeera LR, Prather RS, and Day BN (2000) Polymerization of nonfilamentous actin into microfilaments is an important process for porcine oocyte maturation and early embryo development. *Biol Reprod*, 62, 1177-1183.

Wang WH, Machaty Z, Abeydeera LR, Prather RS, and Day BN (1998) Parthenogenetic activation of pig oocytes with calcium ionophore and the block to sperm penetration after activation. *Biol Reprod*, 58, 1357-1366.

Wassarman PM (2002) Sperm receptors and fertilization in mammals. *Mt Sinai J Med*, 69, 148-155.

Watson R, Anthony F, Pickett M, Lambden P, Masson GM, and Thomas EJ (1992) Reverse transcription with nested polymerase chain reaction shows expression of basic fibroblast growth factor transcripts in human granulosa and cumulus cells from *in vitro* fertilisation patients. *Biochem Biophys Res Commun*, 187, 1227-1231.

Weeber EJ, Levy M, Sampson MJ, Anflous K, Armstrong DL, Brown SE, Sweatt JD, and Craigen WJ (2002) The role of mitochondrial porins and the permeability transition pore in learning and synaptic plasticity. *J Biol Chem*, 277, 18891-18897.

Winer J, Jung CK, Shackel I, and Williams PM (1999) Development and validation of real-time quantitative reverse transcriptase-polymerase chain reaction for monitoring gene expression in cardiac myocytes *in vitro*. *Anal Biochem*, 270, 41-49.

Winkelbach H, Walter G, Morys-Wortmann C, Paetzold G, Hesse D, Zimmermann B, Florke H, Reymann S, Stadtmuller U, Thinnies FP et al (1994) Studies on human porin. XII. Eight monoclonal mouse anti-"porin 31HL" antibodies discriminate type 1 and type 2 mammalian porin channels/VDACs in western blotting and enzyme-linked immunosorbent assays. *Biochem Med Metab Biol*, 52, 120-127.

Wu H, He CL, and Fissore RA (1997) Injection of a porcine sperm factor triggers calcium oscillations in mouse oocytes and bovine eggs. *Mol Reprod Dev*, 46, 176-189.

Wu S, Sampson MJ, Decker WK, and Craigen WJ (1999) Each mammalian mitochondrial outer membrane porin protein is dispensable: effects on cellular respiration. *Biochim Biophys Acta*, 1452, 68-78.

Xu X, Decker W, Sampson MJ, Craigen WJ, and Colombini M (1999) Mouse VDAC isoforms expressed in yeast: channel properties and their roles in mitochondrial outer membrane permeability. *J Membr Biol*, 170, 89-102.

-
- Xu X, Forbes JG, and Colombini M (2001) Actin modulates the gating of *Neurospora crassa* VDAC. *J Membr Biol*, 180, 73-81.
- Xu Z, Kopf GS, and Schultz RM (1994) Involvement of inositol 1,4,5-trisphosphate-mediated Ca^{2+} release in early and late events of mouse egg activation. *Development*, 120, 1851-1859.
- Yanagida K, Katayose H, Hirata S, Yazawa H, Hayashi S, and Sato A (2001) Influence of sperm immobilization on onset of Ca^{2+} oscillations after ICSI. *Hum Reprod*, 16, 148-152.
- Yanagimachi R (1994) Mammalian Fertilization. In Knobil E and Neill JD (eds) *The Physiology of Reproduction*. Raven Press, Ltd., New York, pp. 189-317.
- Yoneda A, Kashima M, Yoshida S, Terada K, Nakagawa S, Sakamoto A, Hayakawa K, Suzuki K, Ueda J, and Watanabe T (2006) Molecular cloning, testicular postnatal expression, and oocyte-activating potential of porcine phospholipase C zeta. *Reproduction*, 132, 393-401.
- Yu WH, Wolfgang W, and Forte M (1995) Subcellular localization of human voltage-dependent anion channel isoforms. *J Biol Chem*, 270, 13998-14006.
- Zalk R, Israelson A, Garty ES, Azoulay-Zohar H, and Shoshan-Barmatz V (2005) Oligomeric states of the voltage-dependent anion channel and cytochrome c release from mitochondria. *Biochem J*, 386, 73-83.
-

“I declare that I have completed this dissertation single-handedly without the unauthorized help of a second party and only with the assistance acknowledged therein. I have appropriately acknowledged and referenced all text passages that are derived literally from or are based on the content of published or unpublished work of others, and all information that relates to verbal communications. I have abided by the principles of good scientific conduct laid down in the charter of the Justus Liebig University of Giessen in carrying out the investigations described in the dissertation.”

María Carolina Cassará

8 Acknowledgements

During the preparation of this thesis a large group of people and organizations have been extremely helpful to my development. Their personal effort I highly appreciate.

First, I am deeply grateful for the guidance and support of my advisors, Prof. Dr. K-D Hinsch and Prof. Dr. E. Hinsch. Special thanks to “Frau Hinsch” not only for her professional help and careful examination of this thesis but also for her constant “mother-like” care.

Thanks to Prof. Dr. Baniahmad for giving me his scientific support by reviewing my thesis. Thanks to the members of the PhD committee and organizing team for their work and effort on the next scientific generations.

I wish to acknowledge the various research groups that opened their doors to share their knowledge and gave me their support during my PhD studies. I appreciate the help and collaboration from Prof. Dr. Meinecke, Prof. Dr. Meinecke-Tillmann and their fantastic working environment. Thanks to Prof. Dr. Benz and his team for their introduction into, for me, a totally new subject. I also like to thank Dr. Montag and working group; he kindly helped me with the calcium oscillation experiments and was open to questions and discussions. Last but not least, I would like to thank Prof. Dr. Niemann, Dr. Wrenzycki and the FAL team for their valuable help with the IVM functional experiments and their friendly welcome.

I appreciate the intellectual contribution made by my colleagues from the “Cell-Cell Interaction in reproduction” graduate program. Especial thanks to Mariuzs and Henry, for their help on ISH and *in situ* RT-PCR.

Many thanks, to my first colleagues and then good friends from the lab (Doro, Vivi, Yvonne, Simone, Xenia and Katja). You made everyday easier and funnier. You were the best master mix made from science, talks, laughs, good and bad moments and lots of coffees.

Thanks to my friends, from near and far away, you shared many great times with me and helped during the hard parts. Great thanks to Tim for our usual “Biologist” talks and for taking the time to read this thesis and providing me with useful comments.

Stefan my deepest thanks, for your scientific support, for the great time in the lab, for your friendship and mainly for our lovely life together.

Above all, special thanks to my family, their daily support, patience and love made every step and decision easy to make.

This research was supported by the German Research Foundation (DFG) under the project GK533. Their support is gratefully acknowledged.

9 Curriculum Vitae

Name	Cassara, María Carolina
-------------	-------------------------

Date of birth	October 18, 1977
----------------------	------------------

Place of birth	Buenos Aires, Argentina
-----------------------	-------------------------

Marital status	Single
-----------------------	--------

Nationality	Argentinean / Italian
--------------------	-----------------------

2003-2006	PhD and DFG-Graduate program student “Cell-cell interaction in Reproduction” Justus Liebig University Giessen, Germany. Thesis “Characterization of Voltage Dependent Anion Channel (VDAC) subtypes in mammalian follicles and potential physiological relevance”
------------------	--

2001-2003	Master in molecular biology and genetic engineering. Favaloro University. Bs.As., Argentina. Thesis (2004) “Expression and localisation of Zona pellucida mRNA in bovine ovaries”
------------------	--

1996-2001	Diploma in Biological Science CAECE University. Bs. As., Argentina. Thesis (2001). “Hormonal induction of the spermiation in the pejerrey <i>Odontesthes bonariensis</i> “
------------------	---
